DIGITAL SOIL BOUNDARY DETECTION USING QUANTITATIVE HYDROLOGIC REMOTE SENSING

by
Emily M. Engle

Submitted in Partial Fulfillment
of the Requirements for the

Masters of Science in Geology

New Mexico Institute of Mining and Technology
Department of Earth and Environmental Science

Socorro, New Mexico

May, 2009

ABSTRACT

Creating accurate, small scale soil maps in remote areas is a very time consuming and expensive process. Traditional methods of soil mapping involve spending considerable amounts of time in the field, often verifying boundaries identified from aerial photographs and validating the boundaries with point observations in soil pits. Remote sensing techniques can provide data that is spatially and spectrally contiguous and has been used successfully to conduct landuse and landcover surveys as well as to obtain surface information about soils and soil properties. The remote sensing algorithms used for digital soil mapping typically input digital values and derive parameters such as root zone soil moisture that provide information about the land surface. The objective of this study is to use quantitative hydrological parameters such as root zone soil moisture for the identification of soil boundaries. The root zone soil moisture is derived using the Surface Energy Balance Algorithm for Land (SEBAL) model, which allows us to investigate the soil conditions of the root zone. No other study has used this technique.

We will test the hypothesis that the use of remotely sensed root zone soil moisture obtained through SEBAL will reveal subsurface trends that can identify soil map boundaries that do not have a strong surface expression. By using the split moving window technique on a principle component analysis on raw digital values of each day, a stack of all days and a stack of all root zone soil moisture images we believe that we can enhance spatial trends and reduce temporal trends. While a composite of both the root

zone soil moisture and a principle component analysis of each day will reveal information not seen in a single image, we hypothesize that the root zone soil moisture will be more useful in identifying spatial trends. Our new approach will be tested in semi-arid desert and riparian areas located in the Middle Rio Grande Valley of New Mexico.

Using the efficiency and failure rates we determined that the daily root zone soil moisture and the daily digital value PCAs performed equally well. By compiling multiple images from different days we were able to detect trends that would not be seen in a single image. The results of the comparison between the overall root zone soil moisture and digital value PCAs reveal that both provide valuable data under different conditions

ACKNOWLEDGEMENTS

I would like to thank my funding agencies, the Department of Defense and the Sevilleta National Wildlife Refuge Summer Fellowship. I would also like to thank my research committee, consisting of Dr. Jan Hendricks, Dr. Bruce Harrison and Dr. Brian Borchers for all of their support. Without their assistance, this project would never have reached fruition. I received further assistance from Sung-ho Hong, Alex Rinehart and Colin Cikoski, for which I am also very grateful. I would like to thank Dr. Fred Phillips and Dr. Bruce Harrison for further monetary support in their labs. I would also like to thank Dr. Jim McCord and everyone at the Socorro AMEC office for helping me get my career in environmental consulting off the ground and supporting me as I finished my research.

I am very appreciative for all the encouragement along the way that I received from Marty Frisbee, my parents, Garey and Maris Engle, my sisters and brother and my entire extended family. Without them and all my friends at New Mexico Tech (who are too numerous to name!), I would not have been able to complete this endeavor. In particular, I would like to thank Shasta Marrero, Shannon Williams and Megan Curry for their comments and help on my defense presentation.

I would like to dedicate this thesis to both of my grandfathers, Edmund Beard Anderson and Clifton Greene Engle, who were not able to be here to see me finish but who were hopefully watching.

TABLE OF CONTENTS

PAGE

LIST OF TABLES

Table Page

LIST OF FIGURES

Figure Page

This thesis is accepted on behalf of the
Faculty of the Institute by the following committee:

J B Harrison
Advisor

Brian Borchers

H Hendrickx

6-10-2009
Date

I release this document to the New Mexico Institute of Mining and Technology.

Emily Hefe
Student's Signature

6-17-2009
Date

INTRODUCTION

The soil landscape is complex and highly variable, reflecting the complex interactions of geomorphological and pedogenic processes. There are two conceptual models that describe the extremes of the soil landscape: 1) the soil landscape consists of a series of individual particulate units (Arnold, 1983; King, 1983; Heuvelink and Webster, 2001) and 2) the soil landscape is continuous and all boundaries are gradational (Knox, 1967). Examples of each of these conceptual models occur along with the range between these extremes in most soil landscapes.

These different conceptual models affect how soil maps are produced and can be dependent on the scale at which the map is produced. Very fine scale maps used in intensive agricultural areas are usually produced through detailed grid sampling using a soil auger. For larger scale maps the map units are identified from aerial photography and proxy data identified by the state factor equations (Jenny, 1941), such as slope, aspect, landforms and vegetation. The soil map units are then checked and validated. It is interesting to note, however, in a study on the identification of boundaries using aerial photographs, Bie and Beckett (1973) determined that different mappers would place boundaries in very different locations. It is logistically impossible to develop detailed soil maps of rangelands although there is an increasing demand for this information from land managers and researchers. Remote sensing can provide a means by which this task can be completed.

The US Department of Agriculture developed the soil taxonomic classification system to classify soils (Soil Survey Staff, 1999). Taxonomic units are different from mapping units, which are an identifiable part of the landscape (Soil Survey Staff, 1999). Mapping units often contain of two or more taxonomic units, creating soil associations (units in which the different soils can be resolved on a map at the 1:24,000 scale) and complexes (units in which different soils cannot be resolved at the 1:24,000 scale). Critics of the soil taxonomy believe that it is too quantitative and relies on laboratory data so much as to be too time consuming to be useful (Schaetzl and Anderson, 2000).

New techniques have advanced the field of soil mapping, particularly in remote areas. These latest methods utilize GIS and remote sensing to assist in the creation of soil maps, termed digital soil mapping. Digital soil mapping is the advancement of statistical or numerical methods that can show relationships between soil properties and environmental variables (Bui, 2007). These relationships can then be applied to a soil database and used to create a map (Scull et al., 2003). Remotely sensed data are often used for digital soil mapping because they allows quick data collection that is spatially and spectrally contiguous (Kruse et al., 1996). It has been used successfully in the past to carry out numerous landuse and landcover surveys. The Landsat Multispectral Scanner (MSS) and Thematic Mapper (TM) have been used with positive results to map land cover, soils, terrains and man-made features such as dams and urban areas (Baban and Yusof, 2001). The use of the India Remote Sensing satellite Linear Imaging Self-scanning Sensor (IRS-1B LISS-II) can provide details about soil classes that are often not found on existing soils map that were produced by reconnaissance and semi-detailed intensities (Karale et al., 1991). In the Ismalia Province in Egypt, the thermal bands of

the Landsat TM have been used to successfully discriminate gypsiferous and saline soils (Goossens and Van Ranst, 1998). Airborne gamma-ray imagery has been used to detect the mineral composition of a soil. It can also measure the amounts of potassium, uranium and thorium which indicate rock composition and the type of weathering taking place (Wilford and Minty, 2007). The HyMap airborne imaging spectrometer is a hyperspectral sensor that collects data in the visible and near-infrared range. It can be used to create combinations of bands that discriminate soils of different color, and identify carbonate and clay features (Madiera Netto et al., 2007). Cole and Boettinger (2007) performed both unsupervised and supervised classifications on Landsat data and compared the results to soils, landscapes and vegetation types found in the field. An unsupervised classification is a process that will divide the landscape into a user specified number of classes. A supervised classification requires the identification of training sites of user specified landcover types. The process will then divide the landscape accordingly. They came to two conclusions: 1) the unsupervised classification proved useful in separating the landscape into classes but these classes do not have any readily interpretable meaning and 2) the supervised classification closely matched the polygons along the border of the survey area but the ability to classify soils accurately decreased as distance from the border increased (Cole and Boettinger, 2007). These types of surveys and methods have one facet in common: all use raw digital values from remotely sensed imagery from a single day. However, this raw data is only from the top one to two centimeters of the surface. More information could be gained by reaching further into the soil. Each study has identified one or two soil properties at the most: gypsiferous and saline soils, mineral composition, rock composition, or weathering type among others.

While all these properties are useful, no single study has gained enough to produce a soil map without further information.

A new approach to soil mapping is needed to fill the growing demand for small scale maps. The methodology developed here focuses on identifying temporal responses of the soil landscape to changing environmental conditions using root zone soil moisture and digital values from Landsat data. In order to do this, images from multiple days are used, as opposed to most previous studies that use only a single image. Also, more insight is gained into the subsurface by incorporating Landsat imagery that has been processed through the Surface Energy Balance Algorithm for Land (SEBAL) model. SEBAL is a remote sensing flux algorithm that solves the surface energy balance on an instantaneous time scale for every pixel of a satellite image. The method is based on the computation of evapotranspiration and root zone soil moisture from the multispectral satellite data (Bastiaanssen et al., 1998; (Bastiaanssen, 2000); Hendrickx and Hong, 2005). While the bands of the Landsat 5 and 7 penetrate up to 10cm into the subsurface, the root zone soil moisture data reflects moisture conditions throughout the entire rooting depth (Table 1). Another advantage to using the SEBAL model is that the resulting data is an assessment of a physical variable unlike other methodologies which use the digital values. With the SEBAL dataset, we are directly monitoring the landscape response to environmental change.

On even very large scale maps, so generalization of boundary placement is necessary because it is not possible to map every soil type. A soil mapper will place the boundary between two map units where the rate of change is greatest. This placement is only an estimate (Campbell, 1977). Womble (1951) developed a method for datasets of

	Penetration Depth (cm)
Landsat Bands 1-5 & 7	0.1
Landsat Band 6	10
Root zone soil moisture	Up to 500 for trees

Table 1: Penetration depth of Landsat bands and root zone soil moisture

gene frequencies that measure continuous variables with the goal of finding zones of abrupt change in a dataset. Graphing this function can identify areas of rapid change, which is what soil mappers are looking for in the field. This type of analysis works particularly well with gridded data and its effectiveness is dependent mostly on the data resolution (Fortin, 1997). Webster (1973) proposed an alternative method called the split moving window technique to automatically detect boundaries using multivariate data along a one dimensional transect. This method can detect a maximum difference between groups of pixels, which indicates the presence of a boundary (Webster, 1978). Hendrickx et al. (1986) points out that while this procedure is quantitative, the interpretation of what qualifies a meaningful peak is still partially subjective. This aspect is examined here by varying the critical peak height, which is the value that a peak must exceed in order to be considered a boundary. Also, by varying the window size the method can be modified for each field area: a large window will result in fewer but larger peaks while a smaller window will result in numerous, smaller peaks. The ability to adjust the size of the window allows the split moving window technique to be customized to fit any needs.

Traditionally, soil mappers acknowledge that variation exists in each map unit but this is only described qualitatively (Heuvelink and Webster, 2001). Our research focuses on quantitatively detecting boundaries so to reduce this variability. The ability to detect boundaries will depend on the boundary type. Cutler (1977) recognized three types of boundaries: 1) boundary intergrades, 2) sharp boundaries, and 3) gradational changes (Figure 1). The first and third types of boundaries tend to occur in a continuous landscape while the second occurs in a particulate landscape. Burrough et al (1997)

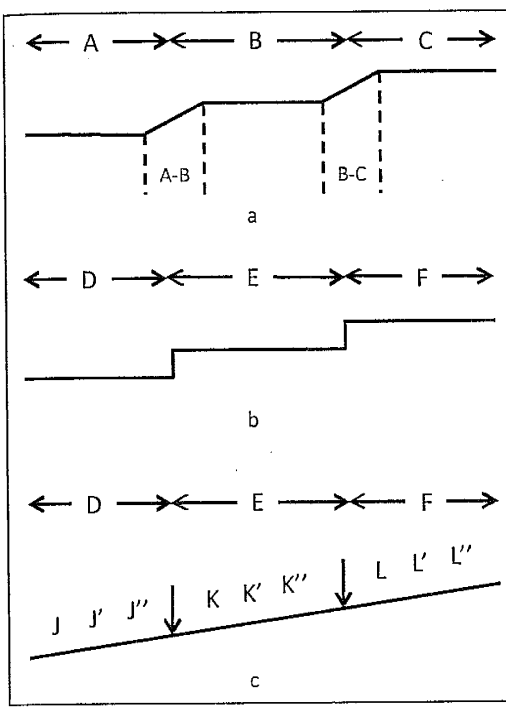

a) Boundary intergrades A-B, B-C between normal mapping units, A, B, C. This is the most common kind of boundary between soils.

b) Sharp boundaries, without intergrades, between discrete mapping units, D, E, F as on terraces in a river valley

c) Gradational change, as on parts of Canterbury Plains between mapping units J, K, L. The boundaries are arbitrary and divide a continuum J, J', J'', K, K', K'', L, L', L''.

Figure 1: Soil boundary types, after Cutler, 1977

termed the sharp boundaries 'primary boundaries,' and defined them as boundaries which are clear and abrupt. Burrough et al also defined 'secondary boundaries' as boundaries which reflect interpreted and interpolated differences between soils. However, each of these boundary types are drawn the same on soil maps. Other studies (Greve and Greve, 2004) have come to similar conclusions. They classified map unit delineation into three divisions during a field mapping exercise: abrupt, intermediate and gradual. Gile (1975a) determined that several types of boundaries caused by differences in soil ages would not have surface expression, such as cases where there was deposition against older materials at the same elevation and when channels are backfilled to the level of the surrounding landscapes. Transitional boundaries were also identified by Giles (1975b). Examples of this include changes from Argid soils to Orthid soils caused by fan-piedmont dissection and the associated slow soil truncation which can transition over a few meters. Another approach is 'continuous classification, in which a soil can be a member of multiple classes instead of only one (Burrough, 1989; De Gruijter et al., 1997; Heuvelink and Webster, 2001). This is applied to soil mapping by gradually transitioning from one soil type to another. The boundary then represents a gradual decrease and increase in the membership.

The goal of this study is to investigate the use of remotely sensed data over multiple days in identifying soil and landscape boundaries. We will use the Landsat digital values and root zone soil moisture and determine if one variable proves more efficient. The boundary type (sharp boundary, intergrade boundary, gradational boundary, etc) can be determined from the range and percentage of days over which each boundary occurs.

STUDY AREA

Two field areas were used in this study: the Sevilleta National Wildlife Refuge and the Hilton Ranch (Figure 2). These areas where chosen in part because the soils had been previously mapped by the Natural Resources Conservation Service (NRCS) and the landforms had been mapped. These soil and landform boundaries are used to evaluate the efficiency of our methodology. The two study areas also cover different ecotones. The Sevilleta covers the typical semi-arid environment while the Hilton Ranch encompasses a riverine environment which transitions into the surrounding semi-arid desert.

Sevilleta National Wildlife Refuge

The Sevilleta National Wildlife Refuge (NWR) is located in central New Mexico and covers an area of approximately 1,000 km^2 (Figure 2). It is also a Long-Term Ecological Research (LTER) site which sustains a wide range of research topics including vegetation dynamics, organism populations, climate variability and soil development. This area was chosen as a LTER site because four major ecosystems occur in a relatively small area. These ecosystems are the Chihuhuan desert, Great Plains grasslands, Colorado Plateau shrub-steppe and conifer woodlands. Landforms include alluvial fans, pediments and terraces of various ages and active channels. In this study, we focused on the northwestern quadrant of the refuge, which contains the Chihuhuan desert, Colorado Plateau shrub-steppes and conifer woodlands. The NRCS mapped the

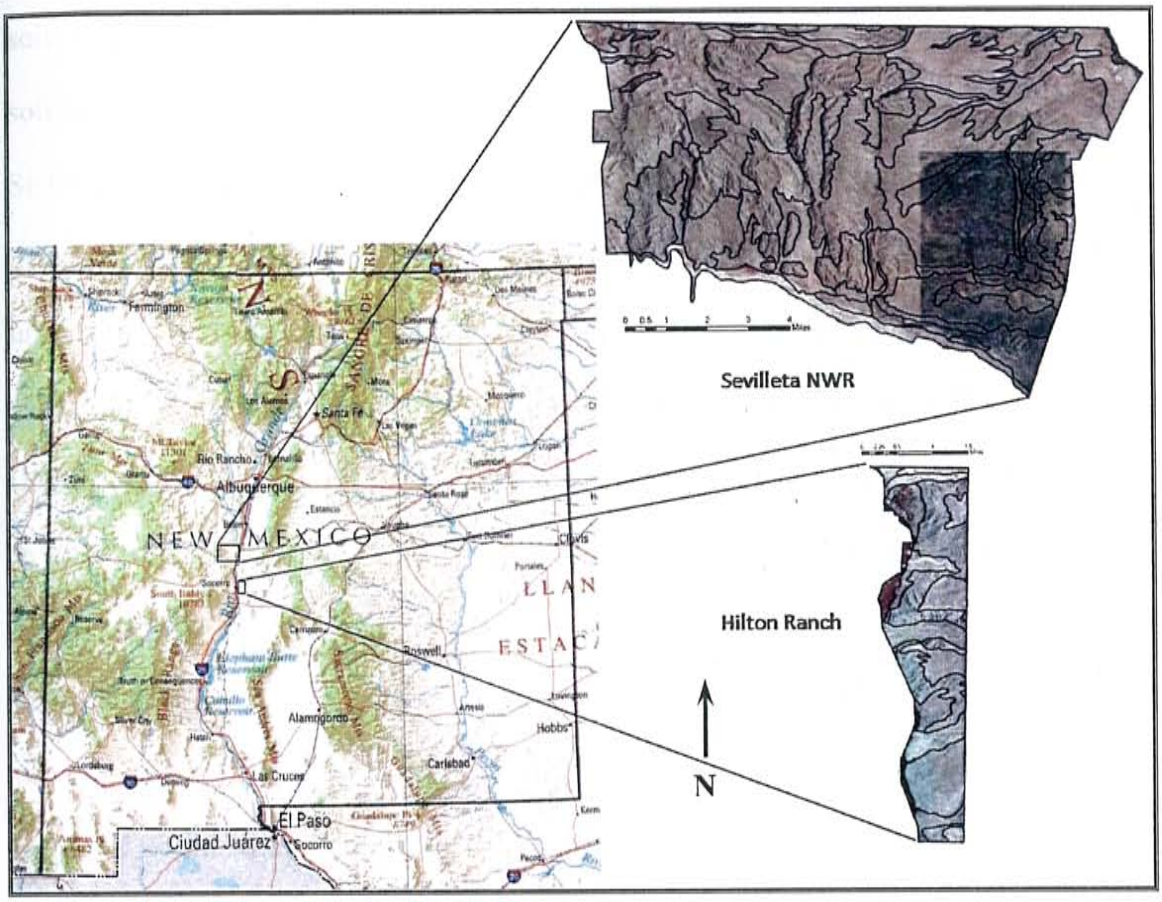

Figure 2: Location of Sevilleta National Wildlife Refuge and Hilton Ranch

soils this area in 1984 at a scale of 1:48,000 and 1:24,000 (Figure 3). There are seventeen soil associations and complexes that range from shallow rocky soils on the slopes of the Sierra Ladrone Mountains to soils on the floodplains of the Rio Grande that are about 1.8 m deep (Soil Survey Staff, 1984). This area was mapped broadly: none of these soil map units contain only one soil taxonomic unit. Climatic data averaged from 1989 to 2005 show that the area receives about 22.4 cm of precipitation per year (http://sev.lternet.edu) (Figure 4). Approximately 45% of precipitation falls as rain during the monsoon season from July to September while the rest results from frontal storms occurring in the winter. The average air temperature is 14.4 °C; the maximum and minimum temperatures are 41.4 and -16.9 °C. The average daily temperature fluctuation is 12.1 °C. The average wind speed is 2.9 m/s (http://sev.lternet.edu). Vegetation at the Sevilleta includes: juniper, creosote, mesquite, cholla, prickly pear and grasses.

Hilton Ranch

The Hilton Ranch is located on the east side of the Rio Grande, opposite of the town of Socorro, NM (Figure 2). The range of landforms is similar to those of the Sevilleta, however; due to its proximity to the Rio Grande more riparian vegetation is present along with floodplains (Figure 3). There are six soil complexes and associations present in this area (Soil Survey Staff, 1984). The Hilton Ranch receives on average 26.0 cm of precipitation per year (http://www.noaa.gov) (Figure 5). The range of temperature is also similar to that of the Sevilleta. Vegetation includes: juniper, creosote, mesquite, grasses, cottonwood and salt cedar.

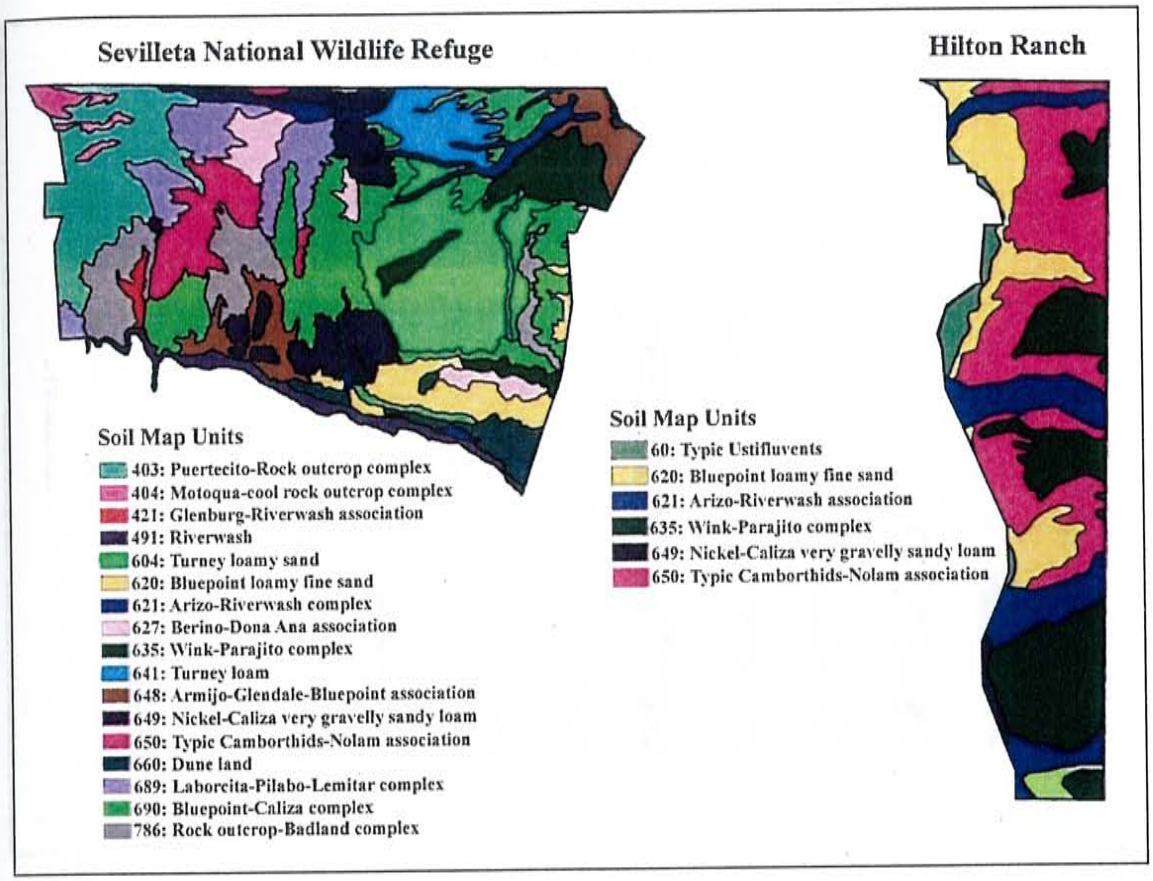

Figure 3: NRCS soil map of the Sevilleta NWR and Hilton Ranch, after Soil Survey Staff, 1984

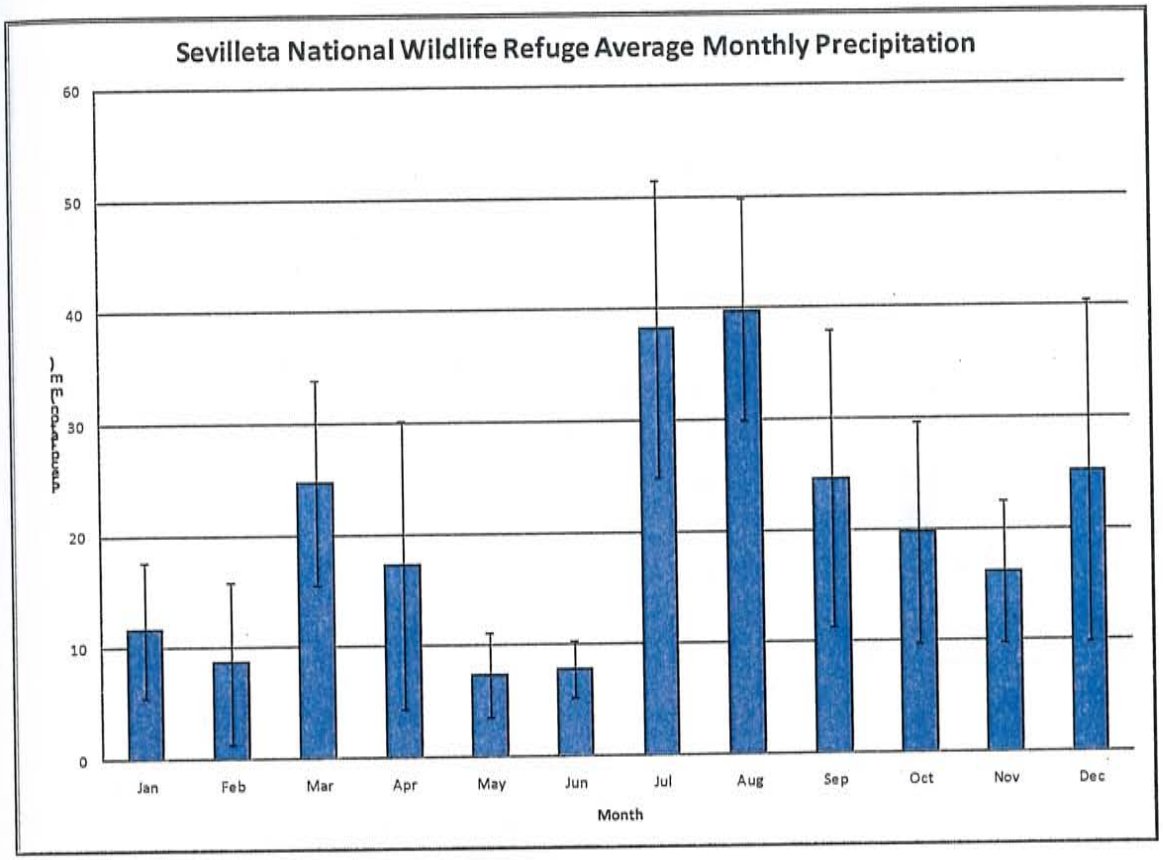

Figure 4: Sevilleta NWR average monthly precipitation, error bars show standard deviation. Source: Sevilleta LTER database

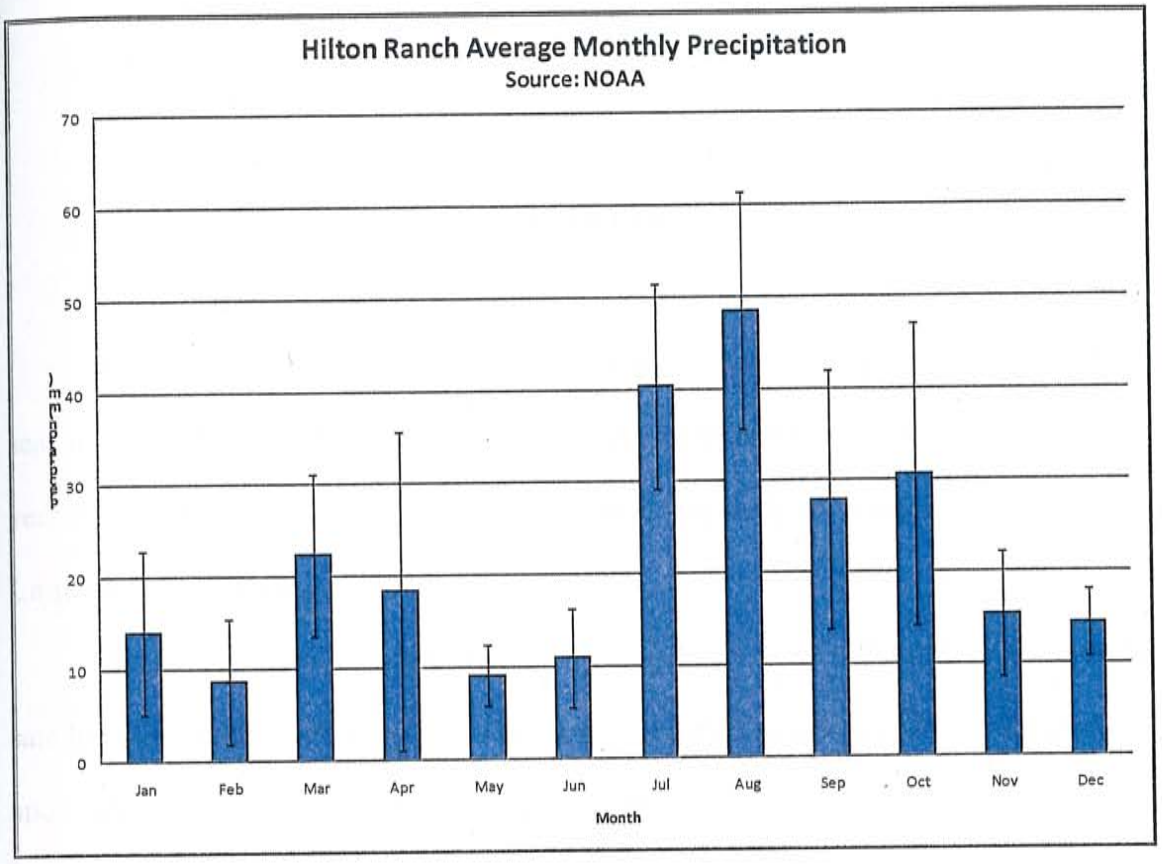

Figure 5: Hilton Ranch average monthly precipitation, error bars show standard deviation
Source: NOAA database

METHODS

For this project we are using twenty Landsat images, all taken during the growing season from April to October (Table 2). Monthly precipitation was during the month and year of each image in order to determine the antecedent moisture conditions.

Landsat 5 and 7 Images

All images for this study came from the Landsat 5 and 7 (Table 2). The Landsat 5 satellite was launched on March 1, 1984. It was designed as a backup for the Landsat 4 and is identical in its specifications. The main instruments on board are the Thematic Mapper (TM) and Multispectral Scanner (MSS). The Thematic Mapper senses data in seven bands, with the sixth band sensing infrared radiation. Bands 1-5 and 7 have a resolution of 30 m^2 and band 6 has a resolution of 120 m^2. The Landsat 7 satellite was launched by NASA on April 15, 1999 and is operated by NOAA and USGS. The main instrument on board Landsat 7 is the Enhanced Thematic Mapper Plus (ETM+). The ETM+ is very similar to the TM on board the Landsat 5 satellite because it senses the visible, near infrared and mid-infrared channels. However, the EMT+ improves resolution of the thermal channel from 120 m^2 to 60 m^2 and has an additional 15 m^2 panchromatic channel. Both are polar, sun-synchronous satellites with an orbit of 16 days. The swath width, defined as the width of the image on each pass, is 185 km (Campbell, 2007).

Landsat coverage information

Date	Start Time	Path Number	Row Number	Satellite	Study Area
4/7/2000	2000:098:17:31:05.1178404	33	36	Landsat 7	Hilton, Sevilleta
5/6/2002	2002:126:17:33:41.1955229	34	36	Landsat 7	Hilton, Sevilleta
5/9/2000	2000:130:17:30:47.1290071	33	36	Landsat 7	Hilton, Sevilleta
5/12/2004	2004:133:17:19:09.02194	33	36	Landsat 5	Hilton
5/22/2005	2005:142:17:32:11.82375	34	36	Landsat 7	Hilton, Sevilleta
5/28/2004	2004:149:17:19:35.41369	33	36	Landsat 5	Hilton
5/31/2002	2002:151:17:27:40.7146875	33	37	Landsat 7	Hilton, Sevilleta
6/4/2001	2001:155:17:34:30.9953451	34	36	Landsat 7	Hilton, Sevilleta
6/13/2004	2004:165:17:20:03.30106	33	36	Landsat 5	Hilton
6/16/2002	2002:167:17:27:10.5069375	33	36	Landsat 7	Hilton, Sevilleta
7/2/2005	2005:183:17:26:17.49113	33	36	Landsat 5	Hilton
7/6/2004	2004:188:17:26:55.63275	34	36	Landsat 5	Hilton, Sevilleta
7/28/2000	2000:210:17:29:51.5247857	33	36	Landsat 7	Hilton, Sevilleta
7/31/2004	2004:213:17:21:20.99275	33	36	Landsat 5	Hilton
8/3/2005	2005:215:17:26:37.89150	33	36	Landsat 5	Hilton, Sevilleta
8/19/2002	2002:231:17:26:48.3184374	33	36	Landsat 7	Hilton, Sevilleta
9/14/2000	2000:258:17:29:16.2793605	33	36	Landsat 7	Hilton, Sevilleta
9/17/2004	2004:261:17:22:33.85738	33	36	Landsat 5	Hilton
9/30/2000	2000:274:17:29:06.6599898	33	36	Landsat 7	Hilton, Sevilleta
10/14/1999	1999:287:17:31:39.2421053	33	36	Landsat 7	Hilton, Sevilleta

Table 2: Landsat 5 and 7 path and row numbers of images used

Surface Energy Balance Algorithm for Land (SEBAL)

Fourteen images were created to represent the Sevilleta and twenty were created for the Hilton Ranch. These images were collected from 1999 to 2005 and each has different antecedent moisture conditions. The moisture conditions range from images that were taken during months with no precipitation to months with significant precipitation. Each image was processed through the SEBAL model by New Mexico Tech Postdoc Sung-ho Hong and Professor Jan Hendrickx. SEBAL is a remote sensing flux algorithm that solves the surface energy balance on an instantaneous time scale for every pixel of a satellite image. The method is based on the computation of evapotranspiration and root zone soil moisture. It considers a user defined wet and dry pixel to assume the sensible heat flux is zero and the latent heat flux is zero, respectively. The radiation balance can then be solved for each pixel in the entire image relative to those two points (Bastiaanssen et al., 1998; (Bastiaanssen, 2000); Hendrickx and Hong, 2005).

Landform Map

A landform map of the Sevilleta NWR was created at a scale of 1:24,000 by New Mexico Tech Ph.D. student Alex Reinhart (Figure 6). It was created by identifying geomorphologic features identified in orthophotos, 5 m and 10 m contour maps, USGS map of Quaternary faults and hillshade maps. Landform boundaries were initially delineated at the 1:24,000 scale while confirmation and exact placement was completed electronically at the 1:10,000 scale. The identification of the landforms was based on topography, vegetation, surface color, soil texture and the surrounding features.

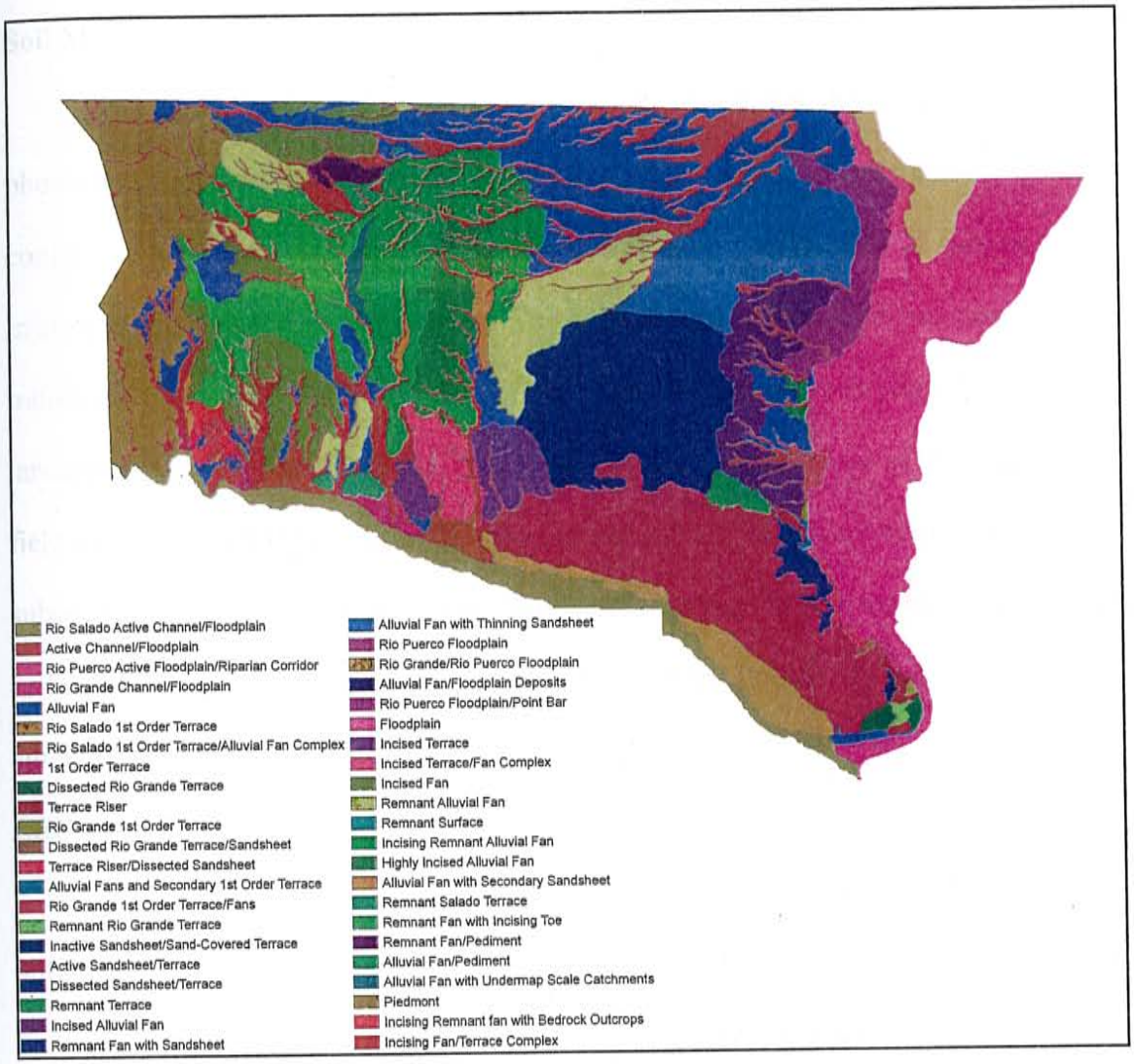

Figure 6: Landform map of the Sevilleta NWR

Soil Map

The digital NRCS soil maps were revised after examining the landscape in aerial photos and digital orthophoto quarter quads (DOQQs). The digital soil maps did not conform to landform boundaries. For example, soil complexes that should only be found in arroyos often extended up hillslopes. This is most likely due to digitizing errors when transferring the paper copies to digital format. The NRCS maps were corrected to the landscape using the ArcGIS Spatial Adjustment Editor. The positions of the edges of the field area were pinned by creating identity links to prevent movement during the subsequent realignment. Displacement links were then used to shift the boundaries of the soil map units so that they were aligned with the landform boundaries and in better agreement with the printed version of the soil map.

ERDAS Imagine Processing

ERDAS Imagine was used extensively to process the data in this study. It was utilized to generate three of the four main datasets that were used for analyses in testing our methodology. For each of the subsequent process descriptions, the Sevilleta LTER and the Hilton Ranch were completed separately. It was used to complete a principle component analysis on the digital values from all bands from each day of Landsat coverage (Figure 7). This dataset is called the daily digital value principle component (daily DV PCA). Principle component analysis (PCA) is a statistical method used to reduce high volumes of data. It is very useful for datasets of high dimensions, such as the Landsat images composed of seven bands, because it can rank and reduce critical components of variation (Figure 8) (Smith, 2002). The PCA will shift the axes of the image (in the case of a Landsat image this is seven dimensions) so that each axes covers

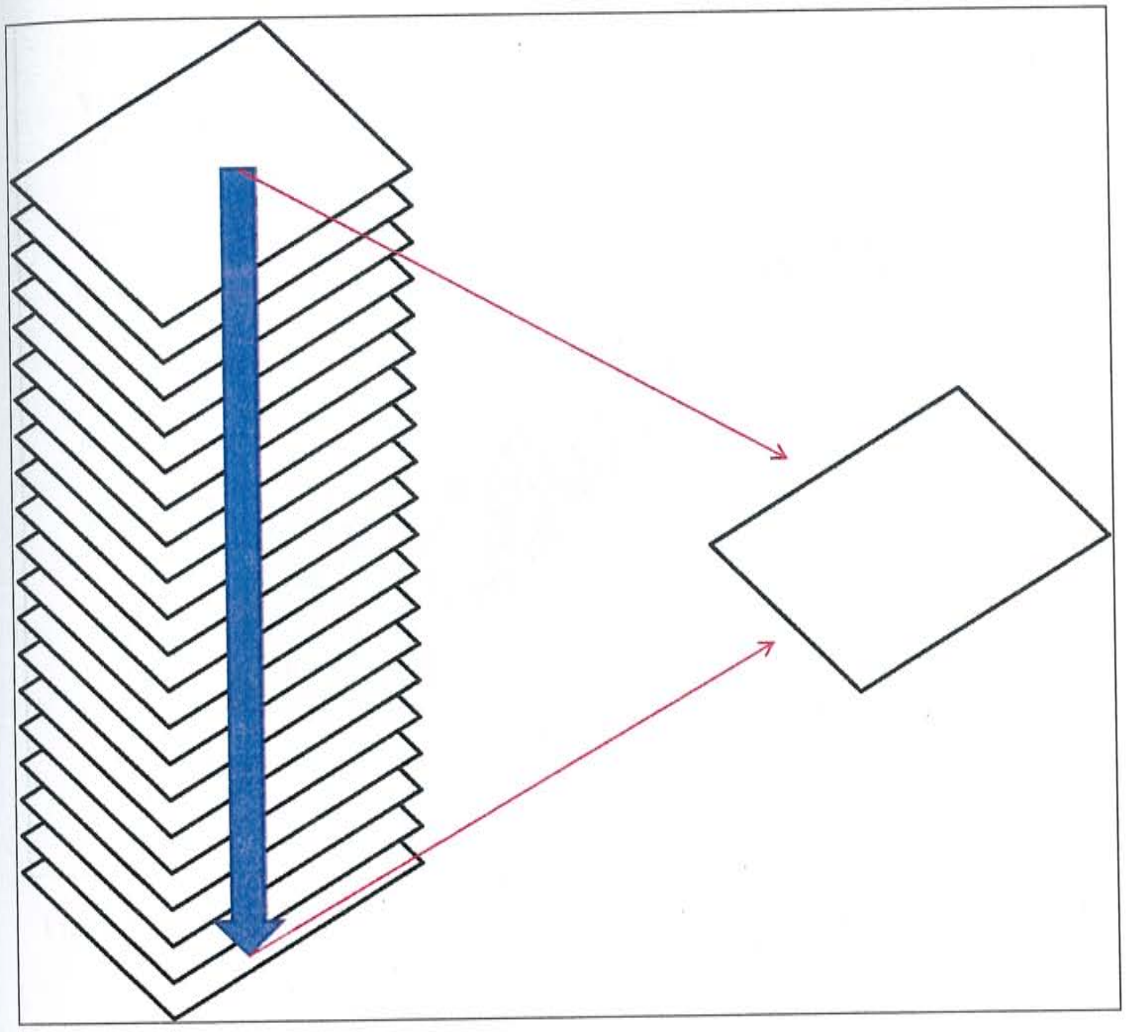

Figure 7: A single image with 280 bands is created by a stacking 20 separate images using ERDAS Imagine

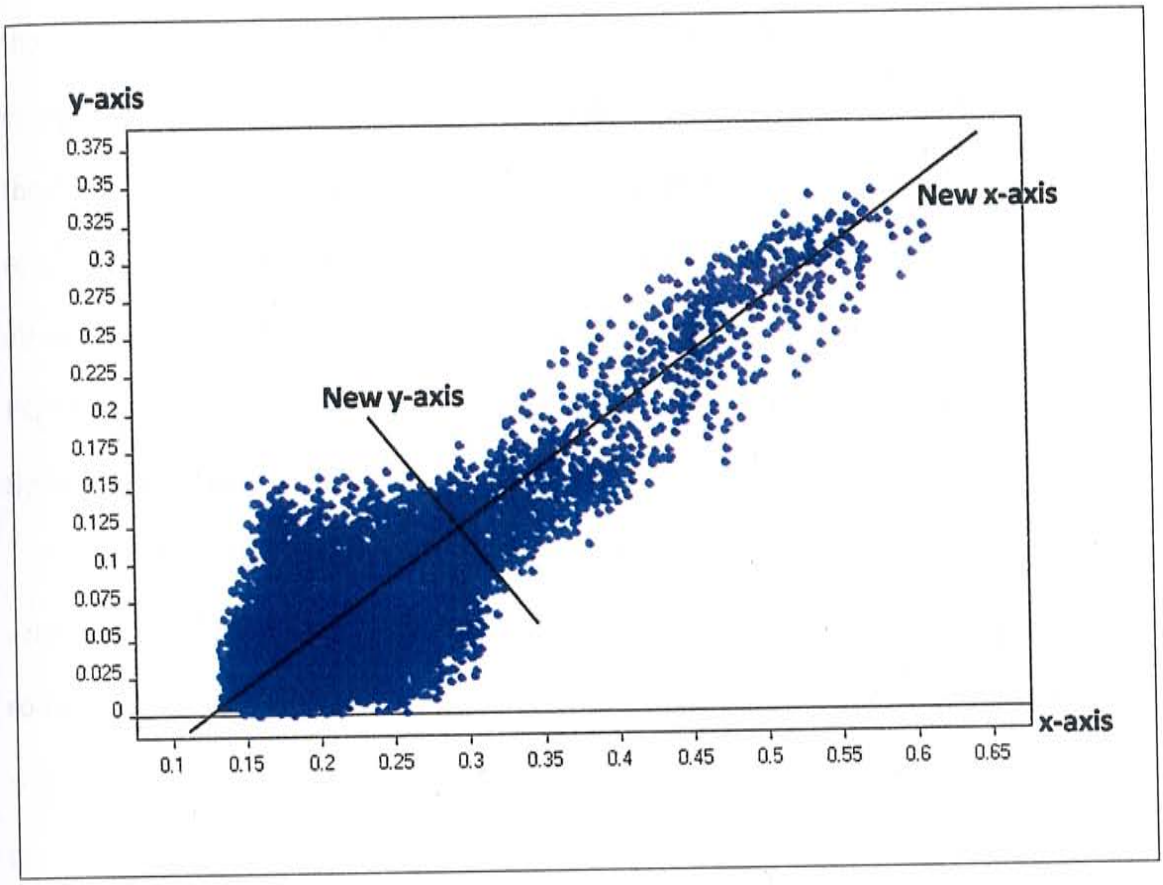

Figure 8: Performing a principle component analysis will shift the axis so that they will explain the maximum amount of variability

the maximum amount of variability. The result is an image that contains a number of components that is equal to the number of bands in the original image. In this study, only the first component is used because it contains at least 70% of the variability of the original image. A PCA was also performed on a stack of all bands' digital values from all days (overall DV PCA) as well as a stack of all root zone soil moisture (overall RZSM PCA). In each case the first principle component is used in the subsequent methodology.

Split Moving Window Analysis

Sixteen transects were selected for further analysis (Figure 9). They were selected in both field areas to fully test our methodology. The transects were positioned so that they crossed landform and soil map boundaries. Transects, such as transect 1, were also placed between landform and soil map boundaries to test how the methodology performed when the boundaries were not as strong or stable.

A t-value is calculated using the split moving window technique to detect boundaries along transects. The t-test, resulting in the t-value, is used to determine if the adjacent pixels are statistically different. This is calculated using the mean and the standard deviation of each window. The split moving window technique examines two adjacent groups of pixels along a transect consisting of n positions; the two windows are then compared using the t-value. Where the t-value reaches a maximum it is assumed that a boundary is located at that position (Figure 10) (Hendrickx et al., 1986; Webster, 1978; Wierenga et al., 1987). Four different critical t-values, 6, 8, 10 and 12 were tested. For each critical t-value, all boundaries that met or exceed it were compiled in a graph

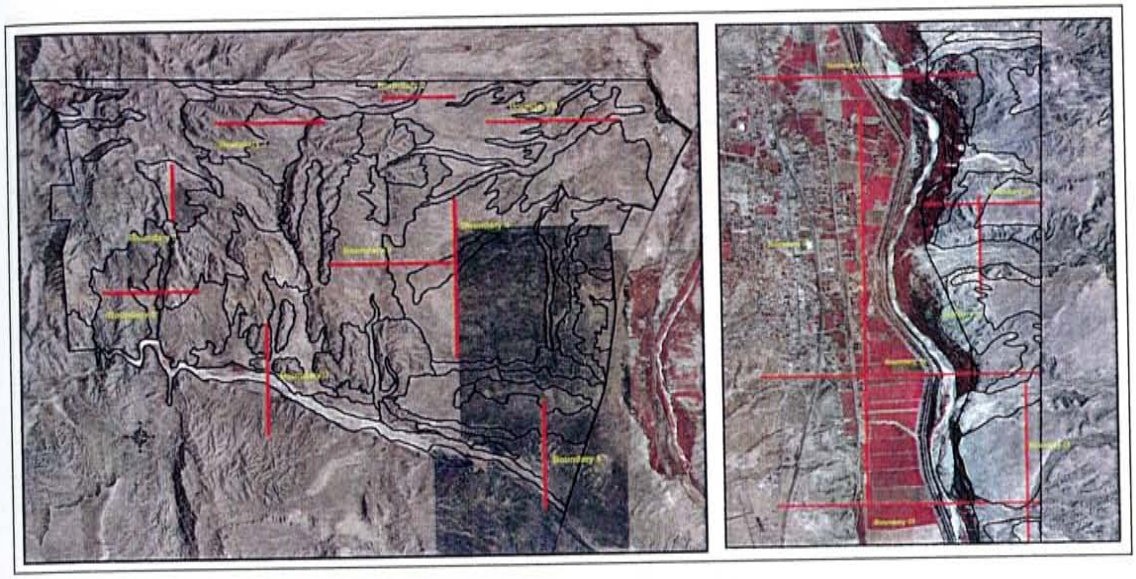

Figure 9: Location of sixteen transects used in split moving window analysis

0.0279	0.0385	0.0349	0.0319	0.0284	0.0449	0.0437	0.0540	0.0524	0.0399	0.0374	0.0380	0.0369	0.0435	0.0424	0.0373
0.0279	0.0385	0.0349	0.0319	0.0284	0.0449	0.0437	0.0540	0.0524	0.0399	0.0374	0.0380	0.0369	0.0435	0.0424	0.0373
0.0279	0.0385	0.0349	0.0319	0.0284	0.0449	0.0437	0.0540	0.0524	0.0399	0.0374	0.0380	0.0369	0.0435	0.0424	0.0373
0.0279	0.0385	0.0349	0.0319	0.0284	0.0449	0.0437	0.0540	0.0524	0.0399	0.0374	0.0380	0.0369	0.0435	0.0424	0.0373

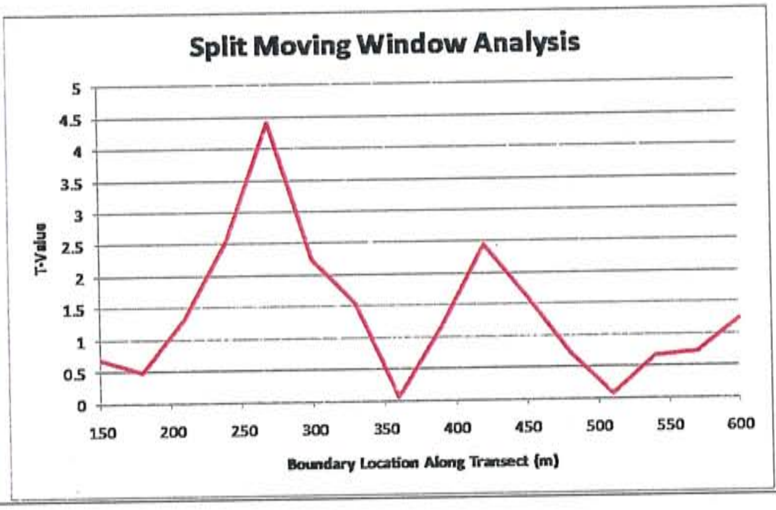

Figure 10: The split moving window technique compares adjacent windows of n positions using the t-value. The t-value is best illustrated using graphs such as these with the absolute value of the t-value on the y-axis and the location on the x-axis.

(Figure 11), along with the location (in meters) of the boundary and the difference in averages across the two windows (Figure 12). This process was completed for each dataset.

The window size across the boundary can be varied and we tested window sizes of 3, 5, 8, 10, 15 and 20 to determine the effect of window size on the number of boundaries detected (Figure 13). It was determined that a window size of 5 was the most appropriate for our datasets. It is small enough to capture boundaries that occur over short distances or are close together but it is large enough to minimize noise. The window size is also affected by the georeferencing error which is about three pixels or 100 m.

While this approach provides a statistical probability that a boundary exists, there are some concerns about how it will perform for different boundary types other than sharp boundaries. The split moving window should work well for identifying hard boundaries such as landscape boundaries. Gradational boundaries will be harder to detect because they do not exhibit the sudden change in properties that will generate a large t-value in the split moving window analysis. Transitional boundaries will also be hard to detect. These are boundaries whose locations will shift based on antecedent conditions. The boundaries identified from the split moving window technique will be classified based on two variables: the percentage of days over which each boundary is present and the spatial range over which they occur. A classification scheme has been developed to describe each boundary (Table 3). We can also determine the efficiency and failure rate of our method at detecting previously identified soil map unit and landform boundaries (preexisting boundaries). The equations used are:

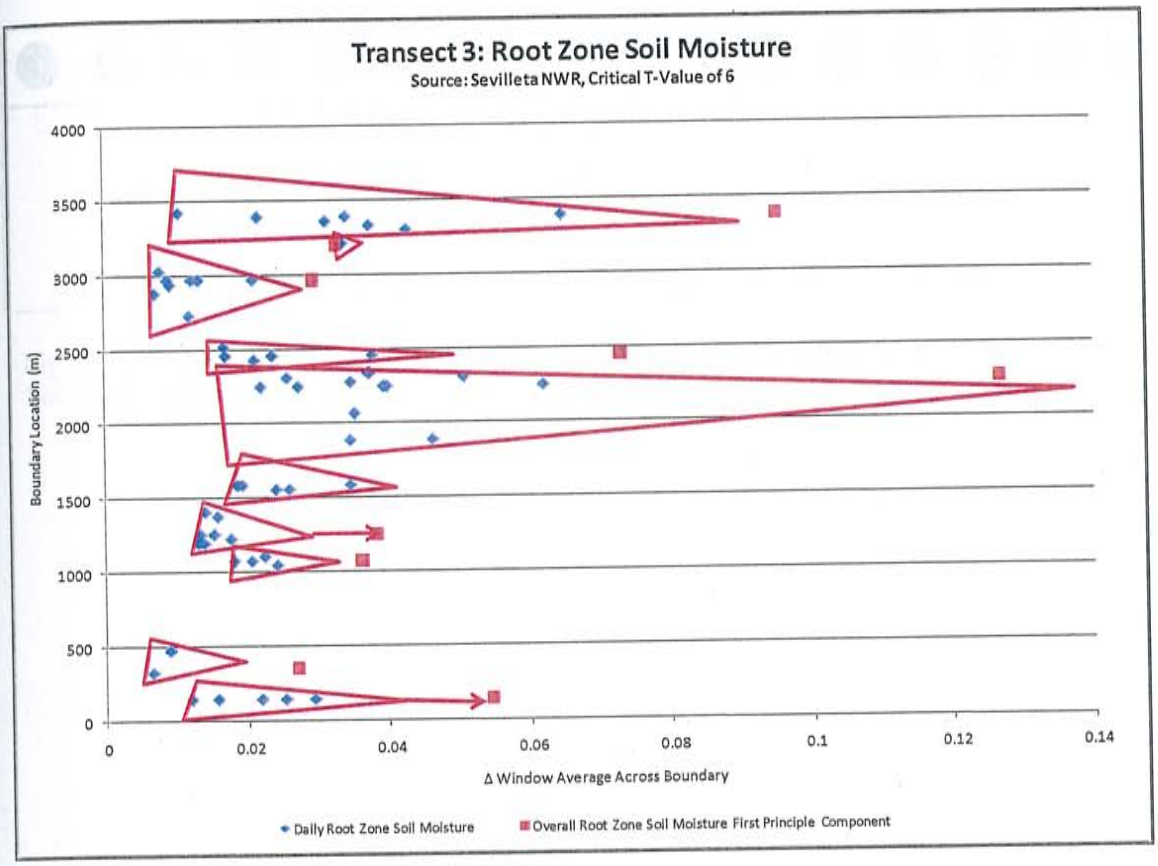

Figure 11: Plot of boundary location and difference in average across the boundary. These were used to delineate boundaries across each transect.

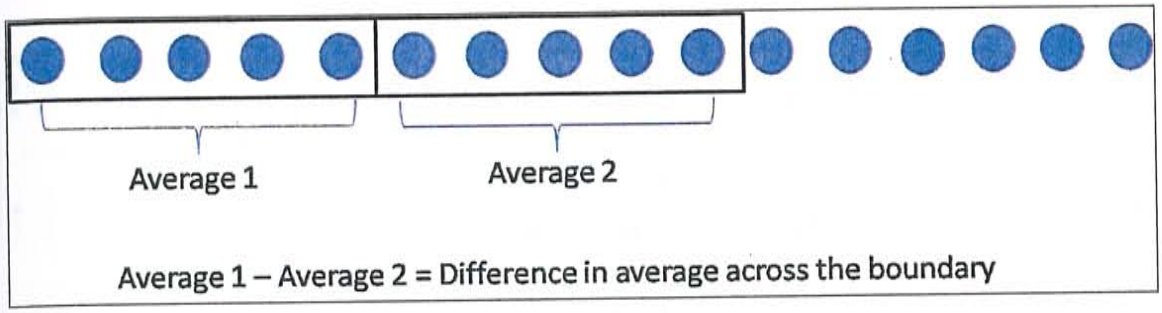

Figure 12: The difference in averages across a boundary can give information about the type of boundary. If the difference is high, it is likely that it is a stable boundary; if it is low it is more possible that it is only scatter.

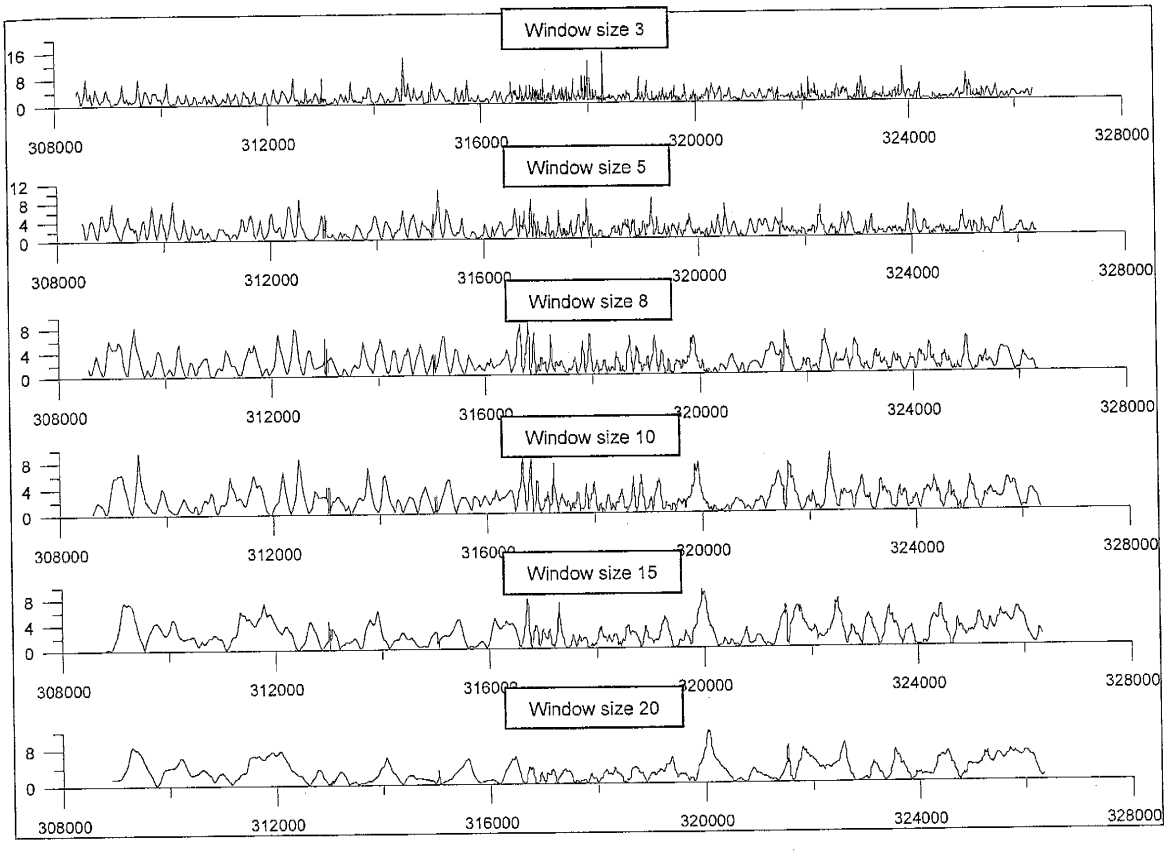

Figure 13: Different sizes of windows were tested to determine the most appropriate size for our methodology.

Boundary Classification

Percentage of days	Boundary strength	Range	Boundary type
0 - 30%	Strong	0 - 100 m	Stable
30 - 60%	Intermediate	100 -200 m	intermediate/stable
60 - 100%	Weak	200 - 300 m	intermediate/transitional
		300 - 400 m	Transitional

Table 3: Classification scheme of boundaries detected

Efficiency of detecting preexisting boundaries = Number of preexisting boundaries detected / Total number of preexisting boundaries * 100 (Eq. 1)

Failure rate = 100% - Efficiency (Eq. 2)

RESULTS

Root Zone Soil Moisture Overlay

A visual correlation was made when the SEBAL derived root zone soil moisture images were overlain with the NRCS soil map in the Sevilleta NWR and the Hilton Ranch. This was performed to determine if any initial correlations observed. An average root zone soil moisture map was created from all images available and was overlain with the soil map. Strong correlations were observed with some soil map unit boundaries (see red circles in Figure 14). The correlations often coincide with landform boundaries which have been used to define the soil map units. The circled areas are examples of landscape features that are strongly reflected in the root zone soil moisture images. While visual correlations were verified in this comparison, a more quantitative analysis is needed.

Split Moving Window Analysis

Two main criteria were used for identifying boundaries: the boundary location and the difference in the average value across each boundary. These two variables were used to create graphs that would delineate boundaries across each transect (Figure 11). Two graphs were generated for each transect. The first displayed the daily root zone soil moisture and the overall root zone soil moisture PCA. The other displayed the daily

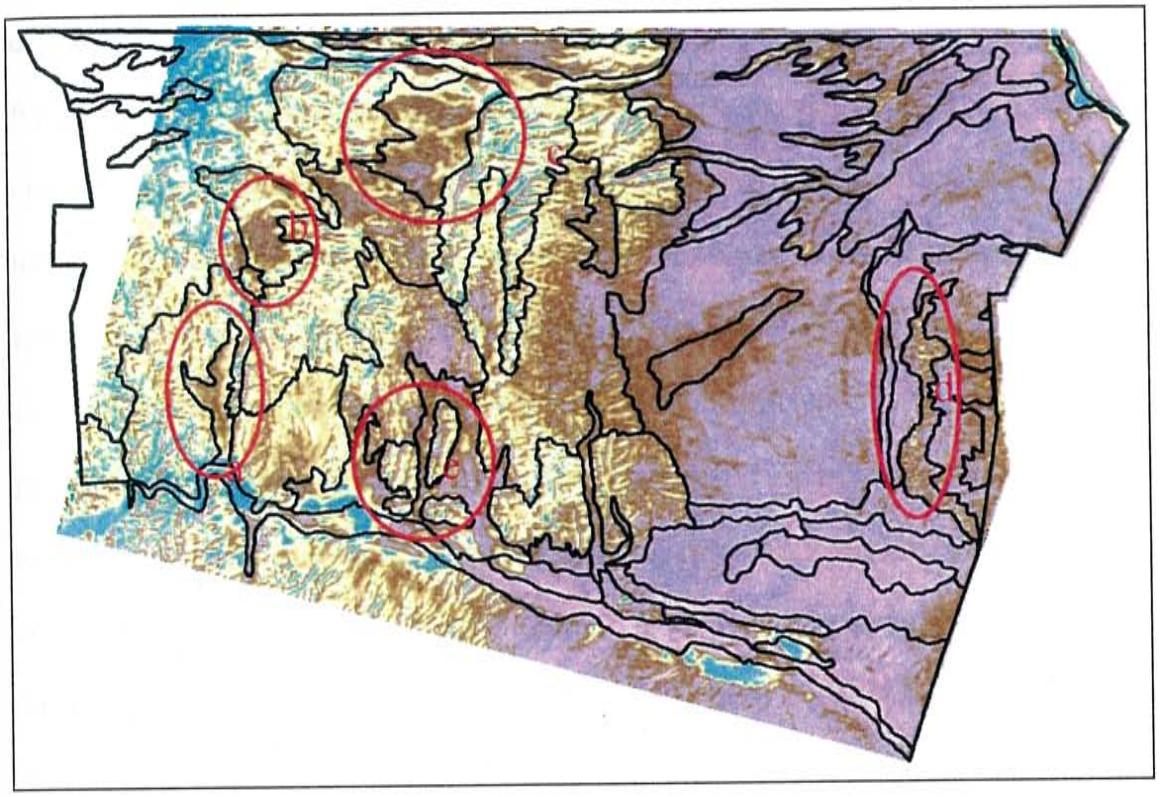

Figure 14: Average root zone soil moisture image overlain with NRCS soil map. Note circled areas where changes in soil moisture correlate well with soil map

digital value PCA and the overall digital value PCA. From these graphs, it was frequently noted that the data would cluster around a few locations (Figure 11). The clusters suggest that boundaries are present at those locations and are depicted by a triangle. A triangle was selected to represent the boundaries because there will be more scatter in the location of a boundary when the difference in the average (of each variable from each dataset) across the boundary is small. As the difference increases, the data points should converge on one location. The convergence of the data points is then recorded as the center of the boundary. Because of the nature of the dataset, each image contributes only one point to a single boundary. In order to correlate the boundaries detected by the split moving window with boundaries from the landform and soil maps, the boundary centers, strength and range were tabulated into summary tables (Table 4).

Split Moving Window T-Tests

Transect 3

Transect 3 is an example where our methodology worked very well. In the summary table, the first two rows, labeled 'landform map' and 'soil map,' contain the locations of boundaries in the respective maps. These locations are listed as meters along the transect (from left to right or from up to down). For each critical t-value, there are the four variables listed: the daily digital value principle component analysis (Daily DV PCA), overall digital value principle component analysis (Overall DV PCA), daily root zone soil moisture (Daily RZSM) and overall root zone soil moisture principle component analysis (Overall RZSM PCA). Beneath each variable are the range and percentage of days out of the total number of images each boundary was detected. It is expected that landform boundaries will tend to be stronger and have lower

B3

Landform Map Soil Map	Boundary Location (m)											
	30	120			1200 1230	1620 1560	2010 1950	2310 2310			3240 3240	3450
Daily DV PCA 6 percentage of days range (m)			510 7.14 0	1050 35.71 630		1600 64.29 60	1900 35.71 180	2275 92.86 120	2520 14.29 30	3000 50.00 270		3400 21.43 30
Overall DV PCA 6 T-Value			480 6.4			1590 8.8		2280 7.1	2520 7.3	3000 7.4		3390 9.3
Daily RZSM 6 percentage of days range (m)		125 35.71 0	400 14.29 150	1080 28.57 60	1250 50.00 150	1580 35.71 30		2200 92.86 450	2450 35.71 90	2925 57.14 300	3210 7.14 0	3325 50.00 120
Overall RZSM PCA 6 T-Value		150 7.5	360 6.4	1080 6.8	1260 7.3			2280 6.7	2460 6.1	2970 9.4	3210 7.7	3390 8.7
Daily DV PCA 8 percentage of days range (m)						1550 28.57 30		2250 42.86 330		3000 14.29 60		3360 7.14 0
Overall DV PCA 8 T-Value						1590 8.8						3390 9.3
Daily RZSM 8 percentage of days range (m)		150 7.14 0		1050 7.14 0		1500 28.57 180		2250 57.14 270		2950 28.57 90	3210 7.14 0	3300 21.43 90
Overall RZSM PCA 8 T-Value										2970 9.4		3390 8.7
Daily DV PCA 10 percentage of days range (m)						1590 21.43 30		2280 7.14 0		2970 7.14 0		
Overall DV PCA 10 T-Value												
Daily RZSM 10 percentage of days range (m)						1500 21.43 180		2280 7.14 0		2970 14.29 0		3400 21.43 210
Overall RZSM PCA 10 T-Value												
Daily DV PCA 12 percentage of days range (m)						1560 7.14 0						
Overall DV PCA 12 T-Value												
Daily RZSM 12 percentage of days range (m)						1560 7.14 0		2280 7.14 0		2970 14.29 0		3390 7.14 0
Overall RZSM PCA 12 T-Value												

Table 4: The summary table of transect 3 includes the locations of the soil and landform boundaries along the transect, the locations, percentage of days and range of boundaries detected by the daily digital values, overall digital value PCA, daily root zone soil moisture and overall root zone soil moisture PCA using a critical t-value of 6, 8, 10 and 12

ranges due to the fact that they are stable, permanent boundaries. Detected boundaries with lower percentages of occurrence and higher ranges are expected to be more gradational or transitional. These might only appear under the certain antecedent moisture conditions. Under other conditions, for example when the landscape is completely dry or saturated, these boundaries may not be detectable. These tables are represented graphically in

Figure 15 and Figure 16). In the daily data figure (

Figure 15), the northern boundary of the Rio Salado is clearly seen in all datasets while the southern boundary is not readily apparent. Some of the boundaries do correspond with landform and soil map boundaries. Other boundaries that do not correspond could either be false detections or transitional/gradational boundaries that were not detected during when the soil map was developed. The overall PCA data shows similar results (Figure 16). The northern boundary of the Rio Salado appears in only one dataset (overall digital value PCA). The third and fourth boundaries seen at 2280 and 2500 m in the daily data appear in the overall PCA data also. There are boundaries, mostly in the northern section of the transect, that do not correspond to preexisting boundaries. However, they are also identified in the daily data. The next step would be to validate these boundaries in the field to determine if they are real boundaries.

Transect 10

Transect 10 is an example of a transect crossing agricultural fields and the Rio Grande floodplain, which is the most complex soil landscape in both study areas (Figure 17). As a result, there are many boundaries detected in both the root zone soil moisture and the digital value PCA. Because the fields are often irrigated separately, the moisture content

in each field will be different so that the boundaries detected are the edges of the

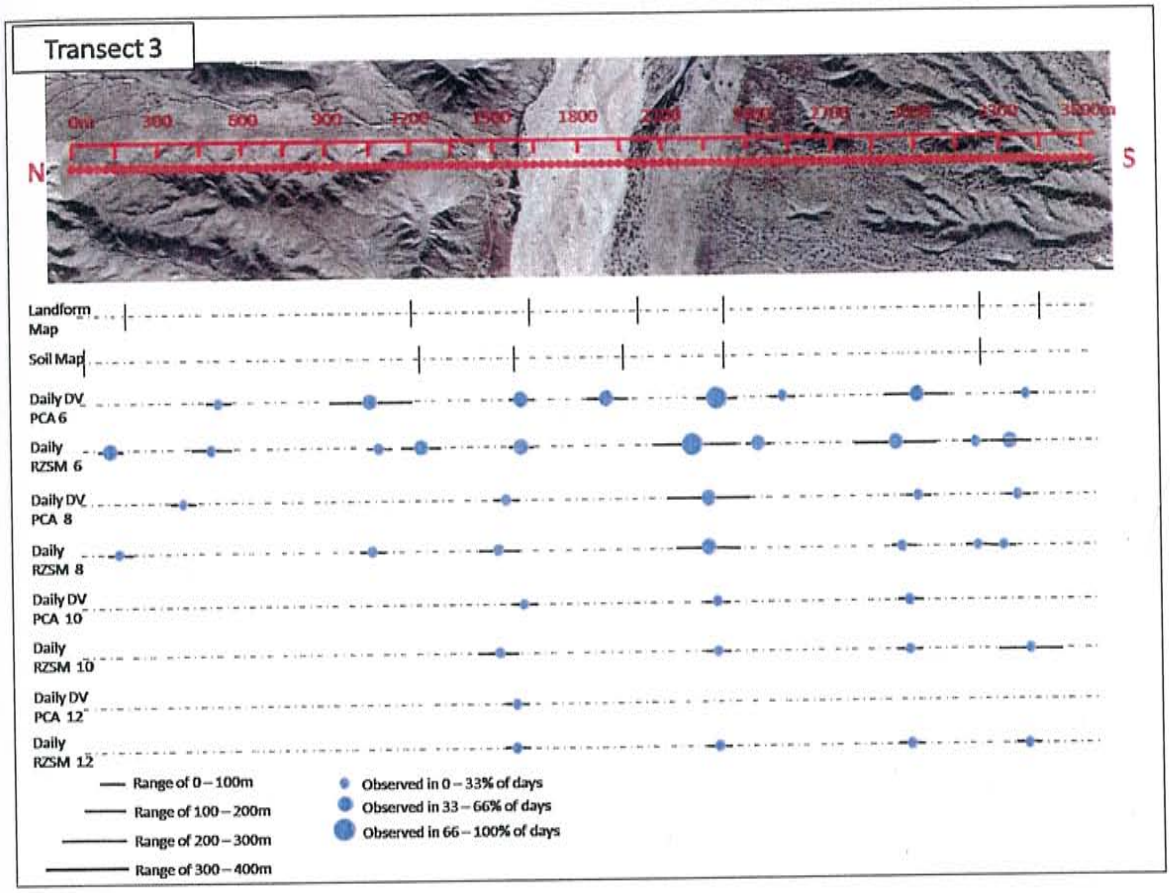

Figure 15: Graphical representation of daily root zone soil moisture and digital value PCA at critical t-values of 6, 8, 10 and 12 along transect 3. The size of the dot represents the percentage of days the boundary occurs in and the line represents the range over which it occurs.

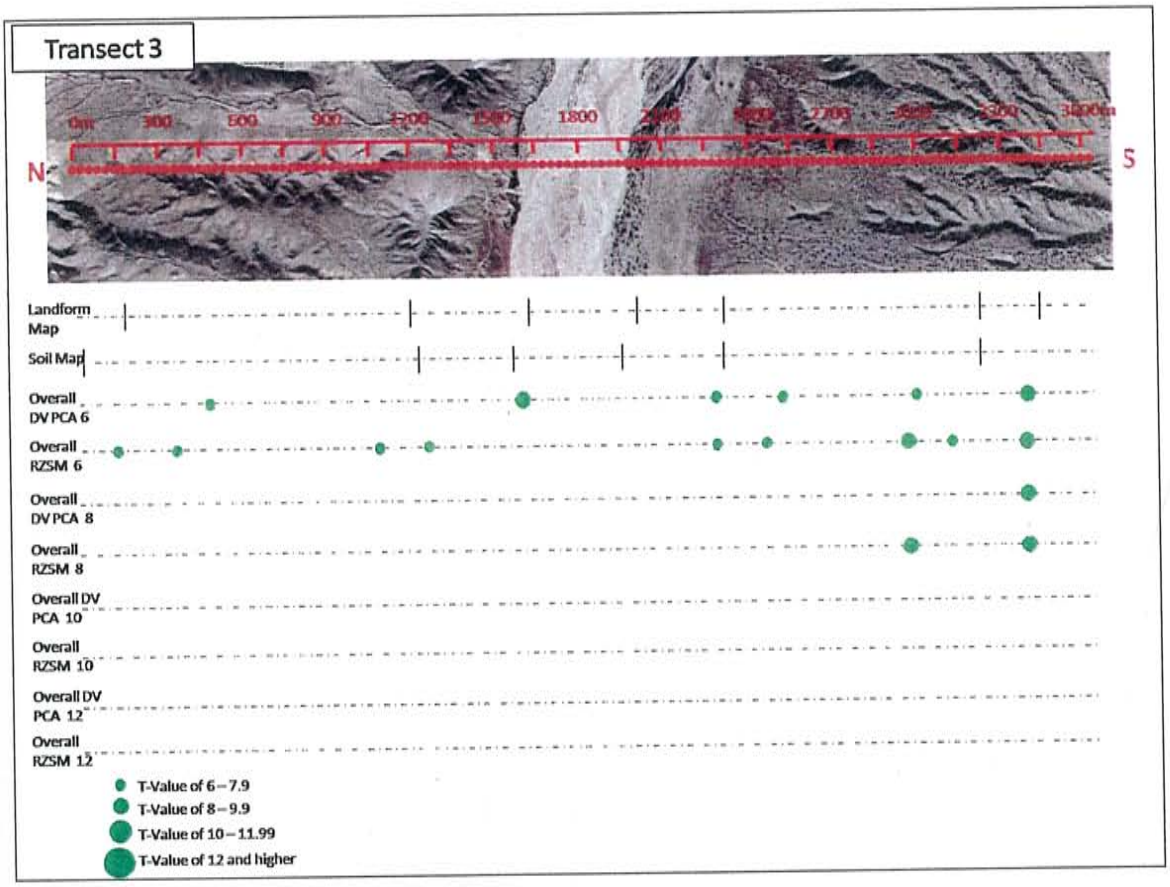

Figure 16: Graphical representation of overall root zone soil moisture and digital value PCA data at critical t-values of 6, 8, 10 and 12 along transect 3. The size of the dot represents the t-value of each boundary.

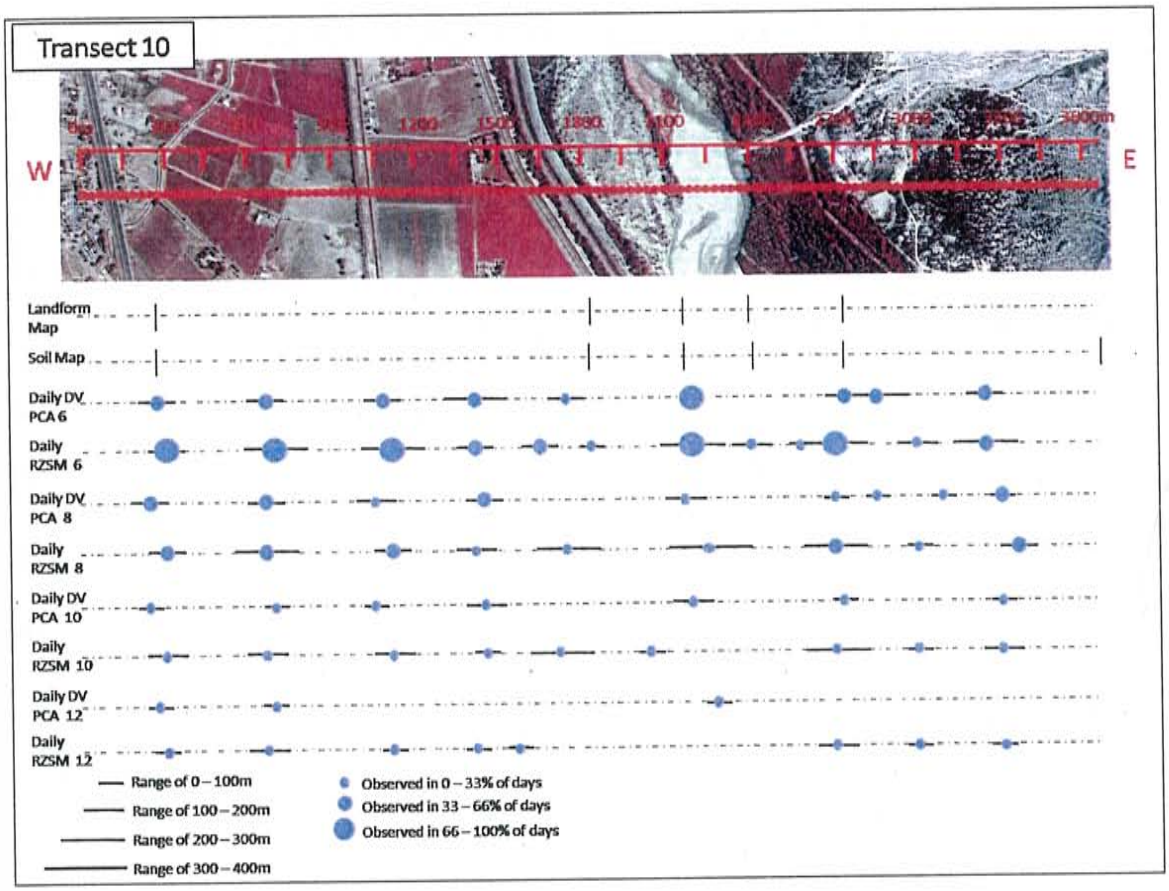

Figure 17: Graphical representation of daily root zone soil moisture and digital value PCA at critical t-values of 6, 8, 10 and 12 along transect 10. The size of the dot represents the percentage of days the boundary occurs in and the line represents the range over which it occurs.

field. Most of the boundaries detected have high t-values which attest to their strength. The start of the fields can be detected easily with this method due to the difference between the fields and the surrounding desert.

Transect 12

Sandsheets originate from rivers and arroyos and often move across the landscape. Transect 12 crosses one on the east side of the Rio Grande (Figure 18 and Figure 19). While there are several boundaries that correspond to landform boundaries, there is also a significant amount of scatter on the east side that does not conform to any visible surface features.

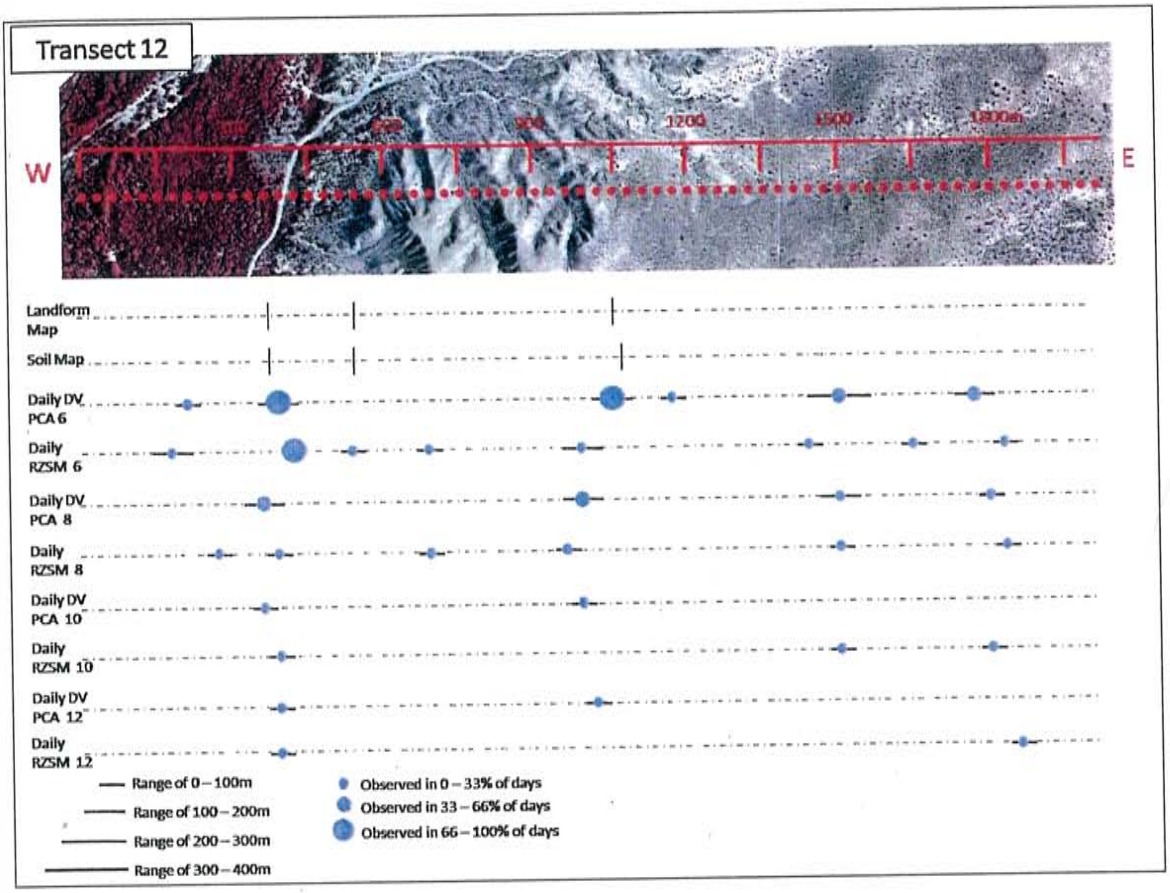

Figure 18: Graphical representation of daily root zone soil moisture and digital value PCA at critical t-values of 6, 8, 10 and 12 along transect 12. The size of the dot represents the percentage of days the boundary occurs in and the line represents the range over which it occurs. There is a significant amount of scatter on the east side of the transect where there are no visible surface correlations.

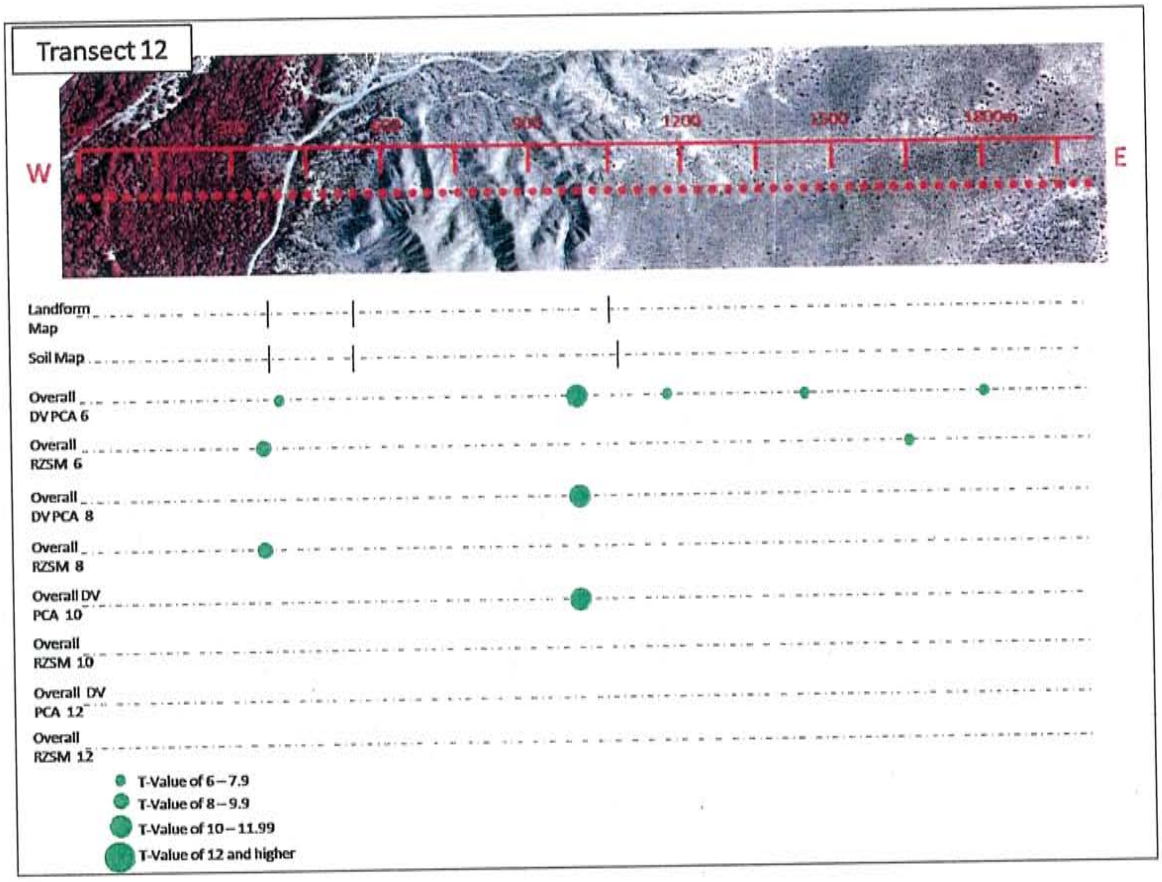

Figure 19: Graphical representation of overall root zone soil moisture and overall digital value PCA data at critical t-values of 6, 8, 10 and 12 along transect 12. The size of the dot represents the t-value of each boundary.

DISCUSSION

SEBAL and Digital Values

Along the on-dimensional transect, both the root zone soil moisture and daily PCA's were successful at detecting boundaries. There are some cases in which there are higher amounts of scatter seen in the root zone soil moisture and very little detected in the daily PCA. An example of this is seen in the second half of transect 4 (Figure 20 and Table 5). This suggests that the root zone soil moisture is detecting some change at depth that did not have a surficial expression. Because most of these images were taken during the growing season, the root zone moisture conditions vary not just from day to day but also spatially across the study areas. By combining multiple images we can reduce this effect while still incorporating a sequence of varying levels of soil moisture. In this way we are able to enhance the spatial trends while minimizing the temporal effects of localized precipitation.

While it was hypothesized that the image generated by the root zone soil moisture would identify more boundaries than the image generated by the daily PCA, this is not always the case. Valuable information can be gained from the root zone soil moisture; but under the certain environmental conditions valuable information can also be taken from the daily PCA. Tables of each transect were generated to quantify the efficiency of the detection of preexisting boundaries from the root zone soil moisture and the digital values. When all datasets are combined, daily and overall, the efficiency of the

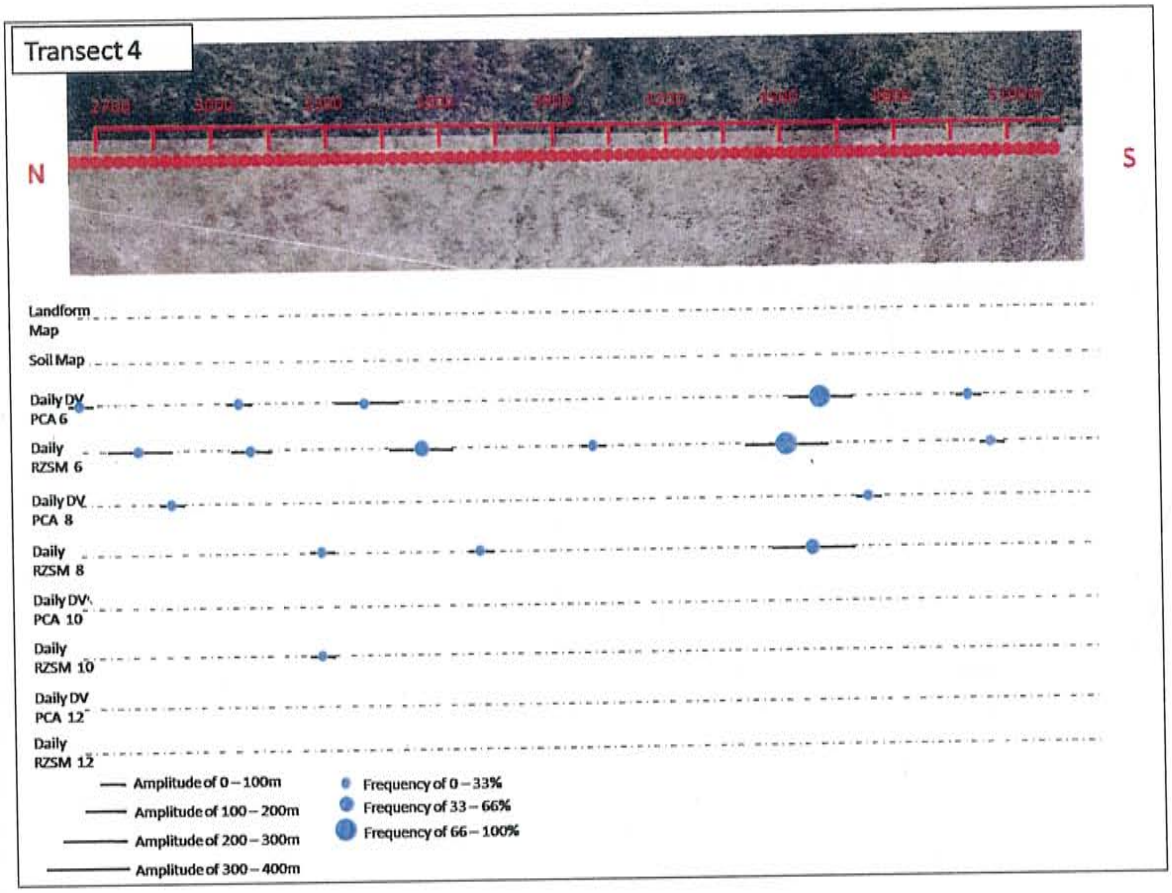

Figure 20: Graphical representation of daily root zone soil moisture and digital value PCA at critical t-values of 6, 8, 10 and 12 along the second half of transect 4 The size of the dot represents the percentage of days the boundary occurs in and the line represents the range over which it occurs. This illustrates how the root zone soil moisture often detects more scatter than the digital values

B4

Landform Map Soil Map	Boundary Location (m)												
	540		1380		1860		2490						
Daily DV PCA 6 percentage of days range (m)	300 14.29 0		1290 50 30	1650 28.5714 60		2100 35.7143 60	2340 7.14286 0	2640 7.14286 0	3060 7.14286 0	3400 21.4286 210			4600 100 270	4980 7.14286 0
Overall DV PCA 6 T-Value	300 6		1290 7.1	1680 9.1		2130 9.1						4500 7.7	4650 7.1	
Daily RZSM 6 percentage of days range (m)		700 14.2857 150	1300 42.8571 90	1700 35.7143 180		2050 21.4286 330		2800 28.5714 210	3100 21.4286 180	3550 35.7143 270	3990 7.14286 0	4500 92.8571 540		5040 7.14286 0
Overall RZSM PCA 6 T-Value			1290 7.4			2100 7.3				3270 7.1		4500 8	4680 7.2	
Daily DV PCA 8 percentage of days range (m)			1290 7.14286 0	1650 14.2857 30		2130 21.4286 30							4700 21.4286 60	
Overall DV PCA 8 T-Value				1680 9.1		2130 8.9								
Daily RZSM 8 percentage of days range (m)		810 7.14286 0	1350 7.14286 0	1750 21.4286 180				2880 7.14286 0	3270 7.14286 0	3690 7.14286 0		4550 28.5714 390		
Overall RZSM PCA 8 T-Value												4500 8		
Daily DV PCA 10 percentage of days range (m)				1650 7.14286 0										
Overall DV PCA 10 T-Value														
Daily RZSM 10 percentage of days range (m)				1770 7.14286 0					3270 7.14286 0					
Overall RZSM PCA 10 T-Value														
Daily DV PCA 12 percentage of days range (m)														
Overall DV PCA 12 T-Value														
Daily RZSM 12 percentage of days range (m)														
Overall RZSM PCA 12 T-Value														

Table 5: The summary table of transect 4 includes the locations of the soil and landform boundaries along the transect, the locations, percentage of days and range of boundaries detected by the daily digital values, overall digital value PCA, daily root zone soil moisture and overall root zone soil moisture PCA using a critical t-value of 6, 8, 10 and 12

methodology at detecting confirmed boundaries decreases as the t-value increases from 70.4% to 24.5% (Figure 20 and Table 6). This is expected because as the t-value increases the boundaries with lower differences across the windows will be filtered out, leaving only the strongest boundaries. The failure rate of detecting preexisting boundaries also increases as the critical t-value increases, from 29.6% to 75.5% (Table 6). The analysis of root zone soil moisture and digital values alone will reveal if any one of these datasets provide more information. The efficiency of the root zone soil moisture data ranges from 56.1% at a critical t-value of 6 to 16.3% at a critical t-value of 12, while the failure rate increases from 43.9% to 83.7% (Table 7 and Figure 22). The efficiency of the digital values ranges from 53.1% to 14.3% and the failure rate increases from 47.0% to 85.7% (Table 8 and Figure 23). The efficiency rates are lower for the overall root zone soil moisture PCA and the overall digital value PCA, which range 13.3% to 0% and 43.9% to 1.0%. (Table 9, Table 10, Figure 24 and Figure 25) The results of the efficiency and failure analysis are surprising: the raw daily Landsat digital value PCA is slightly better able to detect preexisting boundaries, while the overall digital value PCA is significantly better than the root zone soil moisture data. When detecting landform boundaries, the root zone soil moisture and the digital value have very similar efficiencies and failure rates in all critical t-values (Table 11, Figure 26, Figure 27, Figure 28 and Figure 29). When all data is combined the efficiency rates increase dramatically (Figure 30). At critical t-values of 6 and 8 the daily root zone soil moisture is able to detect soil boundaries better than the daily digital value PCA, while the overall data performs about the same at all critical t-values (Table 12, Figure 31, Figure 32, Figure 33, Figure 34).

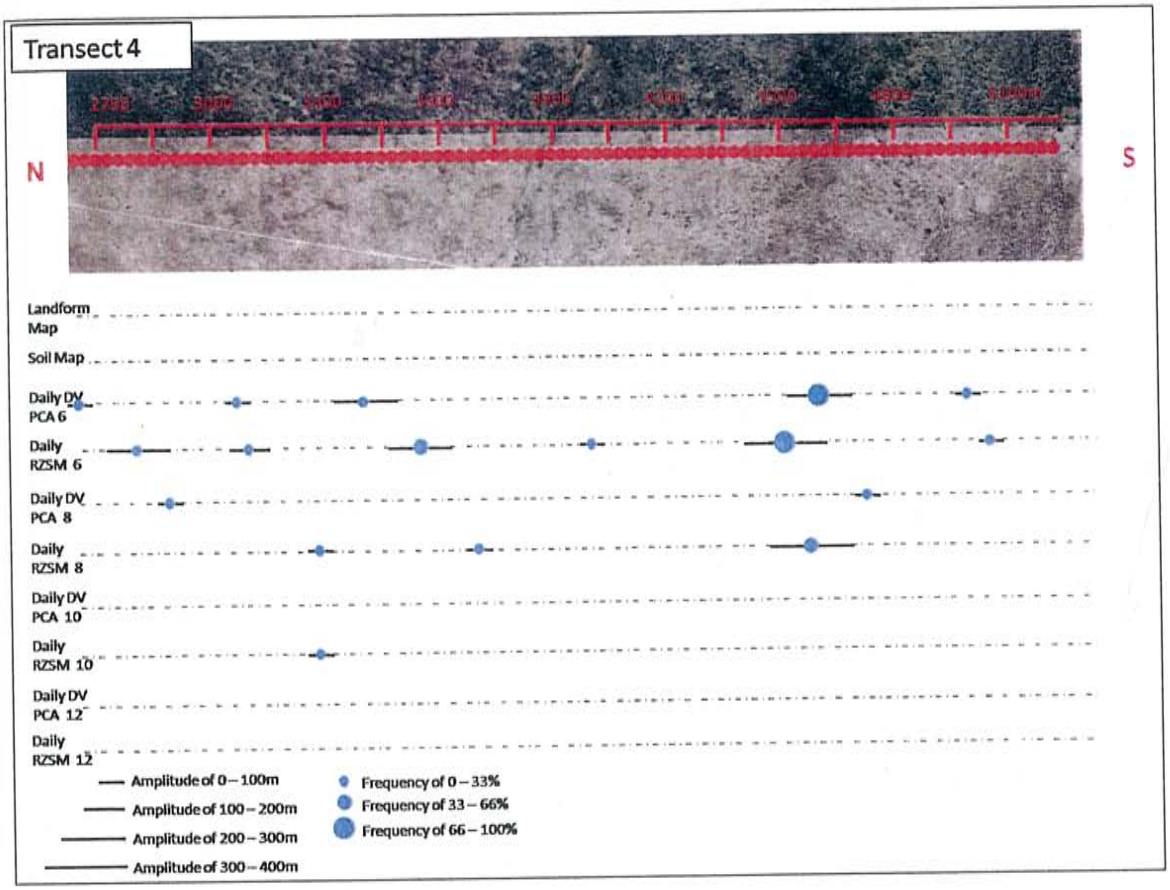

Figure 21: Graphical representation of daily root zone soil moisture and digital value PCA at critical t-values of 6, 8, 10 and 12 along the second half of transect 4 The size of the dot represents the percentage of days the boundary occurs in and the line represents the range over which it occurs. This illustrates how the root zone soil moisture often detects more scatter than the digital values

All Data

Critical T-Value 6

Transect	Total Number of Boundaries Detected	Total Number of Landform and Soil Boundaries	Total Landform and Soil Boundaries Detected	Number of Landform Boundaries	Number of Soil Boundaries	Detected Landform Boundaries	Detected Soil Boundaries	Detected Both Soil and Landform Boundaries?	Extra Boundaries	Non-Detected Landform or Soil Boundaries
1	5	7	3	7	0	3	0	0	2	4
2	9	5	4	4	2	3	2	1	5	1
3	11	8	7	7	6	7	5	5	4	1
4	13	4	3	2	2	2	1	0	10	1
5	12	5	5	3	4	3	4	2	7	0
6	9	12	7	12	4	7	2	2	2	5
7	13	7	5	7	2	5	2	2	8	2
8	13	7	6	7	3	6	2	2	7	1
9	11	7	7	6	2	6	2	1	4	0
10	13	6	5	5	6	5	5	5	8	1
11	6	11	6	7	8	5	5	4	0	5
12	9	3	3	3	3	3	3	3	6	0
14	9	10	5	6	10	4	5	4	4	5
15	8	6	3	5	4	3	2	2	5	3
Totals	141	98	69	81	56	62	40	33	72	29

Efficiency Rate 70.40816327 Failure Rate 29.59183673

Critical T-Value 8

Transect	Total Number of Boundaries	Total Number of Landform and Soil Boundaries	Total Landform and Soil Boundaries Detected	Number of Landform Boundaries	Number of Soil Boundaries	Detected Landform Boundaries	Detected Soil Boundaries	Detected Both Soil and Landform Boundaries?	Extra Boundaries	Non-Detected Landform or Soil Boundaries
1	2	7	2	7	0	2	0	0	0	5
2	7	5	3	4	2	2	1	0	4	2
3	7	8	5	7	6	5	3	3	2	3
4	9	4	1	2	2	1	0	0	8	3
5	10	5	5	3	4	3	4	2	5	0
6	5	12	4	12	4	4	2	2	1	8
7	10	7	5	7	2	5	2	2	5	2
8	12	7	7	7	3	7	3	3	5	0
9	7	7	5	6	2	4	2	1	2	2
10	10	6	4	5	6	4	4	4	6	2
11	5	11	5	7	8	4	4	3	0	6
12	6	3	2	3	3	2	2	2	4	1
14	9	10	5	6	10	4	5	4	4	5
15	8	6	4	5	4	3	3	2	4	2
Totals	107	98	57	81	56	50	35	28	50	41

Efficiency Rate 58.16326531 Failure Rate 41.83673469

Critical T-Value 10

Transect (Critical T-Value 10)	Total Number of Boundaries	Total Number of Landform and Soil Boundaries	Total Landform and Soil Boundaries Detected	Number of Landform Boundaries	Number of Soil Boundaries	Detected Landform Boundaries	Detected Soil Boundaries	Detected Both Soil and Landform Boundaries?	Extra Boundaries	Non-Detected Landform or Soil Boundaries
1	2	7	2	7	0	2	0	0	0	5
2	3	5	1	4	2	1	0	0	2	4
3	4	8	2	7	6	3	2	2	1	5
4	2	4	0	2	2	0	0	0	2	4
5	7	5	3	3	4	2	3	2	4	2
6	2	12	2	12	4	2	1	1	0	10
7	7	7	3	7	2	3	1	1	4	4
8	6	7	2	7	3	2	0	0	4	5
9	7	7	5	6	2	4	2	1	2	2
10	9	6	4	5	6	4	4	4	5	2
11	3	11	3	7	8	3	2	2	0	8
12	4	3	2	3	3	2	2	2	2	1
14	9	10	5	6	10	3	4	3	5	6
15	5	6	3	5	4	2	2	1	2	3
Totals	70	98	37	81	56	33	23	19	33	61

Efficiency Rate 37.75510204 Failure Rate 62.24489796

Critical T-Value 12

Transect (Critical T-Value 12)	Total Number of Boundaries	Total Number of Landform and Soil Boundaries	Total Landform and Soil Boundaries Detected	Number of Landform Boundaries	Number of Soil Boundaries	Detected Landform Boundaries	Detected Soil Boundaries	Detected Both Soil and Landform Boundaries?	Extra Boundaries	Non-Detected Landform or Soil Boundaries
1	1	7	1	7	0	1	0	0	0	6
2	1	5	0	4	2	0	0	0	1	5
3	4	8	3	7	6	3	2	2	1	5
4	0	4	0	2	2	0	0	0	0	4
5	3	5	2	3	4	2	2	2	1	3
6	1	12	1	12	4	1	0	0	0	11
7	4	7	3	7	2	3	1	1	1	4
8	5	7	2	7	3	2	0	0	3	5
9	2	7	2	6	2	2	1	1	0	5
10	9	6	3	5	6	3	3	3	6	3
11	0	11	0	7	8	0	0	0	0	11
12	3	3	2	3	3	2	2	2	1	1
14	7	10	3	6	10	2	3	2	4	7
15	4	6	2	5	4	2	1	1	2	4
Totals	44	98	24	81	56	23	15	14	20	74

Efficiency Rate 24.48979592 Failure Rate 75.51020408

Table 6: Efficiency and failure rate of both all data combined

Daily Root Zone Soil Moisture

Critical T-Value 6

Transect	Total Number of Boundaries Detected	Total Number of Landform and Soil Boundaries	Total Landform and Soil Boundaries Detected	Number of Landform Boundaries	Number of Soil Boundaries	Detected Landform Boundaries	Detected Soil Boundaries	Detected Both Soil and Landform Boundaries?	Extra Boundaries	Non-Detected Landform or Soil Boundaries
1	2	7	2	7	0	2	0	0	0	5
2	8	5	3	4	2	2	1	0	5	2
3	10	8	6	7	6	6	4	4	4	2
4	10	4	1	2	2	1	0	0	9	3
5	9	5	4	3	4	2	4	2	5	1
6	7	12	5	12	4	5	2	2	2	7
7	12	7	5	7	2	5	2	2	7	2
8	11	7	6	7	3	6	2	2	5	1
9	7	7	3	6	2	2	1	0	4	4
10	12	6	5	5	6	5	5	5	7	1
11	4	11	4	7	8	3	3	2	0	7
12	8	3	3	3	3	3	3	3	5	0
14	9	10	5	6	10	4	5	4	4	5
15	7	6	3	5	4	3	2	2	4	3
Totals	116	98	55	81	56	49	34	28	61	43
Efficiency Rate	56.12244898	Failure Rate	43.87755102							

Critical T-Value 8

Transect	Total Number of Boundaries Detected	Total Number of Landform and Soil Boundaries	Total Landform and Soil Boundaries Detected	Number of Landform Boundaries	Number of Soil Boundaries	Detected Landform Boundaries	Detected Soil Boundaries	Detected Both Soil and Landform Boundaries?	Extra Boundaries	Non-Detected Landform or Soil Boundaries
1	1	7	1	7	0	1	0	0	0	6
2	5	5	2	4	2	1	1	0	3	3
3	7	8	5	7	6	5	3	3	2	3
4	7	4	1	2	2	1	0	0	6	3
5	8	5	5	3	4	3	4	2	3	0
6	3	12	2	12	4	2	1	1	1	10
7	10	7	5	7	2	5	2	2	5	2
8	8	7	5	7	3	5	3	3	3	2
9	3	7	1	6	2	1	0	0	2	6
10	9	6	4	5	6	4	4	4	5	2
11	4	11	4	7	8	3	3	2	0	7
12	6	3	2	3	3	2	2	2	4	1
14	9	10	5	6	10	4	5	4	4	5
15	6	6	3	5	4	2	2	1	3	3
Totals	86	98	45	81	56	39	30	24	41	53
Efficiency Rate	45.91836735	Failure Rate	54.08163265							

Critical T-Value 10

Transect	Total Number of Boundaries Detected	Total Number of Landform and Soil Boundaries	Total Landform and Soil Boundaries Detected	Number of Landform Boundaries	Number of Soil Boundaries	Detected Landform Boundaries	Detected Soil Boundaries	Detected Both Soil and Landform Boundaries?	Extra Boundaries	Non-Detected Landform or Soil Boundaries
1	1	7	1	7	0	1	0	0	0	6
2	2	5	1	4	2	1	0	0	1	4
3	4	8	3	7	6	3	2	2	1	5
4	2	4	0	2	2	0	0	0	2	4
5	4	5	3	3	4	2	3	2	1	2
6	1	12	1	12	4	1	1	1	0	11
7	4	7	2	7	2	2	1	1	2	5
8	5	7	2	7	3	2	0	0	3	5
9	1	7	0	6	2	0	0	0	1	7
10	9	6	4	5	6	4	4	4	5	2
11	1	11	1	7	8	1	0	0	0	10
12	3	3	1	3	3	1	1	1	2	2
14	8	10	3	6	10	2	3	2	5	7
15	4	6	2	5	4	1	1	0	2	4
Totals	49	98	24	81	56	21	16	13	25	74
Efficiency Rate	24.48979592	Failure Rate	75.51020408							

Critical T-Value 12

Transect	Total Number of Boundaries Detected	Total Number of Landform and Soil Boundaries	Total Landform and Soil Boundaries Detected	Number of Landform Boundaries	Number of Soil Boundaries	Detected Landform Boundaries	Detected Soil Boundaries	Detected Both Soil and Landform Boundaries?	Extra Boundaries	Non-Detected Landform or Soil Boundaries
1	0	7	0	7	0	0	0	0	0	7
2	0	5	0	4	2	0	0	0	0	5
3	4	8	3	7	6	3	2	2	1	5
4	0	4	0	2	2	0	0	0	0	4
5	3	5	2	3	4	2	2	2	1	3
6	0	12	0	12	4	0	0	0	0	12
7	3	7	2	7	2	2	1	1	1	5
8	3	7	2	7	3	2	0	0	1	5
9	0	7	0	6	2	0	0	0	0	7
10	8	6	2	5	6	2	2	2	6	4
11	0	11	0	7	8	0	0	0	0	11
12	2	3	1	3	3	1	1	1	1	2
14	6	10	3	6	10	2	3	2	3	7
15	3	6	1	5	4	1	0	0	2	5
Totals	32	98	16	81	56	15	11	10	16	82
Efficiency Rate	16.32653061	Failure Rate	83.67346939							

Table 7: Efficiency and failure rates for daily root zone soil moisture

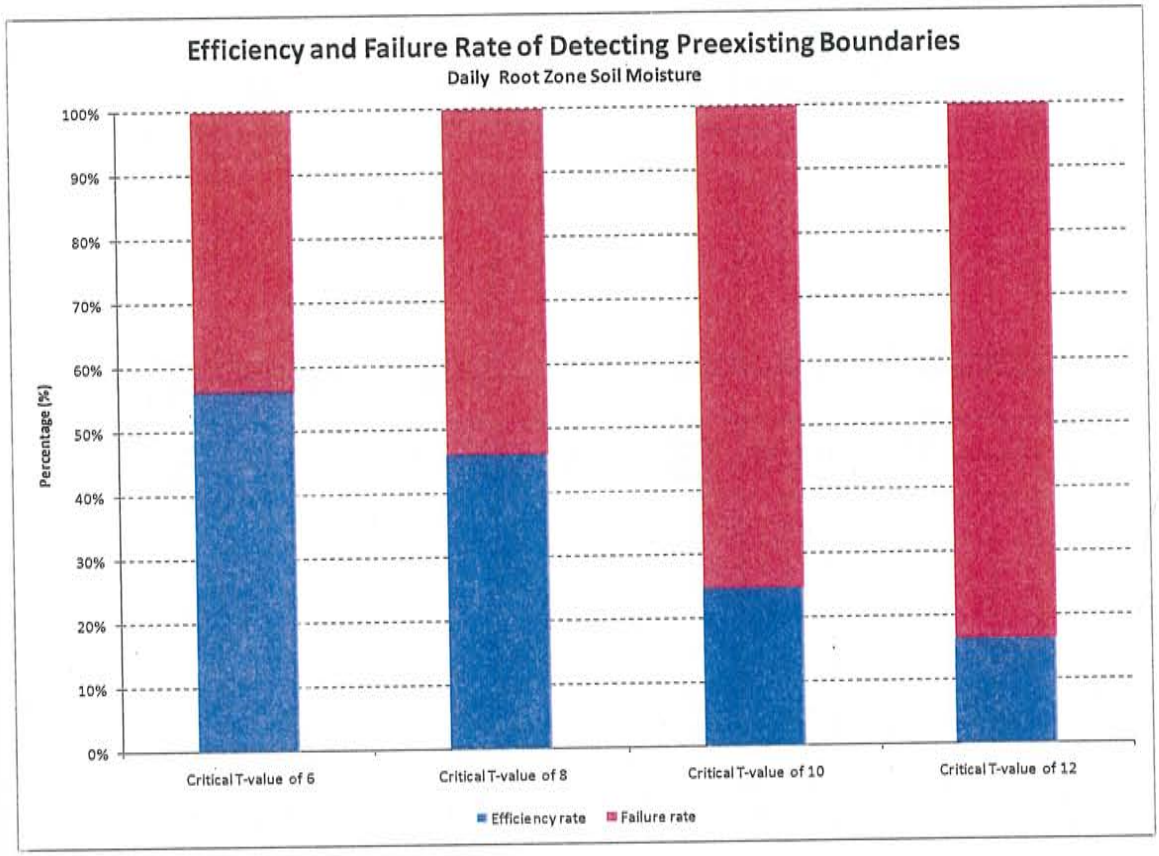

Figure 22: Efficiency and failure rates of the daily root zone soil moisture at critical t-values of 6, 8, 10 and 12

Daily Digital Values

Critical T-Value of 6

Transect	Total Number of Boundaries Detected	Total Number of Landform and Soil Boundaries	Total Landform and Soil Boundaries Detected	Number of Landform Boundaries	Number of Soil Boundaries	Detected Landform Boundaries	Detected Soil Boundaries	Detected Both Soil and Landform Boundaries?	Extra Boundaries	Non-Detected Landform or Soil Boundaries
1	4	7	2	7	0	2	0	0	2	5
2	6	5	3	4	2	2	2	1	3	2
3	8	8	4	7	6	4	3	3	4	4
4	10	4	3	2	2	2	1	0	7	1
5	10	5	4	3	4	3	3	2	6	1
6	7	12	6	12	4	6	2	2	1	6
7	7	7	5	7	2	5	2	2	2	2
8	12	7	6	7	3	6	2	2	6	1
9	9	7	5	6	2	4	2	1	4	2
10	9	6	4	5	6	4	4	4	5	2
11	4	11	4	7	8	4	3	3	0	7
12	6	3	2	3	3	2	2	2	4	1
14	6	10	2	6	10	2	2	2	4	8
15	5	6	2	5	4	2	1	1	3	4
Totals	103	98	52	81	56	48	29	25	51	46

Efficiency Rate 53.06122449 Failure Rate 46.93877551

Critical T-Value of 8

Transect	Total Number of Boundaries Detected	Total Number of Landform and Soil Boundaries	Total Landform and Soil Boundaries Detected	Number of Landform Boundaries	Number of Soil Boundaries	Detected Landform Boundaries	Detected Soil Boundaries	Detected Both Soil and Landform Boundaries?	Extra Boundaries	Non-Detected Landform or Soil Boundaries
1	1	7	1	7	0	1	0	0	0	6
2	3	5	2	4	2	1	1	0	1	3
3	4	8	3	7	6	3	2	2	1	5
4	4	4	1	2	2	1	0	0	3	3
5	8	5	3	3	4	3	2	2	5	2
6	4	12	4	12	4	4	2	2	0	8
7	6	7	3	7	2	3	1	1	3	4
8	8	7	5	7	3	5	1	1	3	2
9	6	7	5	6	2	4	2	1	1	2
10	9	6	3	5	6	3	3	3	6	3
11	3	11	3	7	8	2	2	1	0	8
12	4	3	2	3	3	2	2	2	2	1
14	7	10	4	6	10	3	4	3	3	6
15	5	6	2	5	4	2	1	1	3	4
Totals	72	98	41	81	56	37	23	19	31	57

Efficiency Rate 41.83673469 Failure Rate 58.16326531

Critical T-Value of 10

Transect	Total Number of Boundaries Detected	Total Number of Landform and Soil Boundaries	Total Landform and Soil Boundaries Detected	Number of Landform Boundaries	Number of Soil Boundaries	Detected Landform Boundaries	Detected Soil Boundaries	Detected Both Soil and Landform Boundaries?	Extra Boundaries	Non-Detected Landform or Soil Boundaries
1	1	7	1	7	0	1	0	0	0	6
2	1	5	0	4	2	0	0	0	1	5
3	3	8	2	7	6	2	2	2	1	6
4	1	4	0	2	2	0	0	0	1	4
5	5	5	1	3	4	1	1	1	4	4
6	1	12	1	12	4	1	0	0	0	11
7	5	7	2	7	2	2	1	1	3	5
8	4	7	2	7	3	2	0	0	2	5
9	5	7	4	6	2	4	1	1	1	3
10	7	6	3	5	6	3	3	3	4	3
11	3	11	3	7	8	3	2	2	0	8
12	2	3	2	3	3	2	2	2	0	1
14	4	10	2	6	10	1	2	1	2	8
15	2	6	1	5	4	1	1	1	1	5
Totals	44	98	24	81	56	23	15	14	20	46

Efficiency Rate 24.48979592 Failure Rate 46.93877551

Critical T-Value of 12

Transect	Total Number of Boundaries Detected	Total Number of Landform and Soil Boundaries	Total Landform and Soil Boundaries Detected	Number of Landform Boundaries	Number of Soil Boundaries	Detected Landform Boundaries	Detected Soil Boundaries	Detected Both Soil and Landform Boundaries?	Extra Boundaries	Non-Detected Landform or Soil Boundaries
1	1	7	1	7	0	1	0	0	0	6
2	1	5	0	4	2	0	0	0	1	5
3	1	8	1	7	6	1	1	1	0	7
4	0	4	0	2	2	0	0	0	0	4
5	1	5	1	3	4	1	1	1	0	4
6	0	12	0	12	4	0	0	0	0	12
7	1	7	1	7	2	1	0	0	0	6
8	4	7	2	7	3	2	0	0	2	5
9	2	7	2	6	2	2	1	1	0	5
10	3	6	2	5	6	2	2	2	1	4
11	0	11	0	7	8	0	0	0	0	11
12	2	3	2	3	3	2	2	2	0	1
14	3	10	1	6	10	0	1	0	2	9
15	1	6	1	5	4	1	1	1	0	5
Totals	20	98	14	81	56	13	9	8	6	84

Efficiency Rate 14.28571429 Failure Rate 85.71428571

Table 8: Efficiency and failure rates of daily digital values

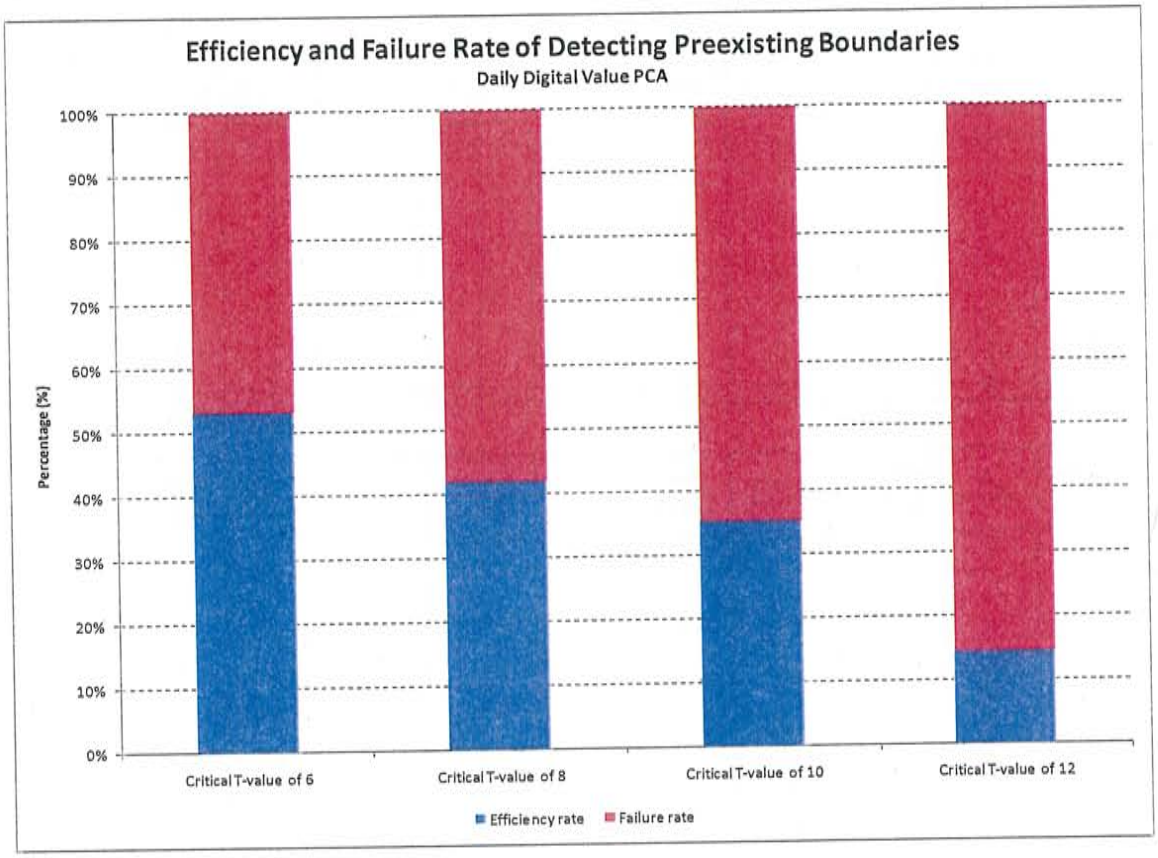

Figure 23: Failure rates of daily digital value PCA at critical t-values of 6, 8, 10, and 12

Overall Root Zone Soil Moisture

Critical T-Value of 6

Transect	Total Number of Boundaries Detected	Total Number of Landform and Soil Boundaries	Total Landform and Soil Boundaries Detected	Number of Landform Boundaries	Number of Soil Boundaries	Detected Landform Boundaries	Detected Soil Boundaries	Detected Both Soil and Landform Boundaries?	Extra Boundaries	Non-Detected Landform or Soil Boundaries
1	1	7	1	7	0	1	0	0	0	6
2	3	5	1	4	2	1	0	0	2	4
3	9	8	5	7	6	5	3	3	4	3
4	5	4	1	2	2	1	0	0	4	3
5	4	5	2	3	4	2	2	2	2	3
6	1	12	1	12	4	1	0	0	0	11
7	7	7	4	7	2	4	2	2	3	3
8	6	7	4	7	3	4	1	1	2	3
9	4	7	3	6	2	2	2	1	1	4
10	8	6	4	5	6	4	4	4	4	2
11	3	11	3	7	8	2	2	1	0	8
12	2	3	0	3	3	0	0	0	2	3
14	9	10	5	6	10	4	5	4	4	5
15	4	6	2	5	4	2	1	1	2	4
Totals	66	98	36	81	56	33	22	19	30	62

Efficiency Rate 36.73469388 Failure Rate 63.26530612

Critical T-Value of 8

Transect	Total Number of Boundaries Detected	Total Number of Landform and Soil Boundaries	Total Landform and Soil Boundaries Detected	Number of Landform Boundaries	Number of Soil Boundaries	Detected Landform Boundaries	Detected Soil Boundaries	Detected Both Soil and Landform Boundaries?	Extra Boundaries	Non-Detected Landform or Soil Boundaries
1	0	7	0	7	0	0	0	0	0	7
2	1	5	0	4	2	0	0	0	1	5
3	2	8	1	7	6	1	0	0	1	7
4	1	4	0	2	2	0	0	0	1	4
5	3	5	2	3	4	2	2	2	1	3
6	0	12	0	12	4	0	0	0	0	12
7	2	7	1	7	2	1	1	1	1	6
8	1	7	1	7	3	1	0	0	0	6
9	1	7	1	6	2	1	1	1	0	6
10	1	6	1	5	6	1	1	1	0	5
11	3	11	3	7	8	2	2	1	0	8
12	0	3	0	3	3	0	0	0	0	3
14	3	10	2	6	10	1	2	1	1	8
15	1	6	1	5	4	1	0	0	0	5
Totals	19	98	13	81	56	11	9	7	6	85

Efficiency Rate 13.26530612 Failure Rate 86.73469388

Critical T-Value of 10

Transect	Total Number of Boundaries Detected	Total Number of Landform and Soil Boundaries	Total Landform and Soil Boundaries Detected	Number of Landform Boundaries	Number of Soil Boundaries	Detected Landform Boundaries	Detected Soil Boundaries	Detected Both Soil and Landform Boundaries?	Extra Boundaries	Non-Detected Landform or Soil Boundaries
1	0	7	0	7	0	0	0	0	0	7
2	0	5	0	4	2	0	0	0	0	5
3	0	8	0	7	6	0	0	0	0	8
4	0	4	0	2	2	0	0	0	0	4
5	0	5	0	3	4	0	0	0	0	5
6	0	12	0	12	4	0	0	0	0	12
7	0	7	0	7	2	0	0	0	0	7
8	0	7	0	7	3	0	0	0	0	7
9	0	7	0	6	2	0	0	0	0	7
10	0	6	0	5	6	0	0	0	0	6
11	0	11	0	7	8	0	0	0	0	11
12	0	3	0	3	3	0	0	0	0	3
14	1	10	0	6	10	0	0	0	1	10
15	0	6	0	5	4	0	0	0	0	6
Totals	1	98	0	81	56	0	0	0	1	98

Efficiency Rate 0 Failure Rate 100

Critical T-Value of 12

Transect	Total Number of Boundaries Detected	Total Number of Landform and Soil Boundaries	Total Landform and Soil Boundaries Detected	Number of Landform Boundaries	Number of Soil Boundaries	Detected Landform Boundaries	Detected Soil Boundaries	Detected Both Soil and Landform Boundaries?	Extra Boundaries	Non-Detected Landform or Soil Boundaries
1	0	7	0	7	0	0	0	0	0	7
2	0	5	0	4	2	0	0	0	0	5
3	0	8	0	7	6	0	0	0	0	8
4	0	4	0	2	2	0	0	0	0	4
5	0	5	0	3	4	0	0	0	0	5
6	0	12	0	12	4	0	0	0	0	12
7	0	7	0	7	2	0	0	0	0	7
8	0	7	0	7	3	0	0	0	0	7
9	0	7	0	6	2	0	0	0	0	7
10	0	6	0	5	6	0	0	0	0	6
11	0	11	0	7	8	0	0	0	0	11
12	0	3	0	3	3	0	0	0	0	3
14	1	10	0	6	10	0	0	0	1	10
15	0	6	0	5	4	0	0	0	0	6
Totals	1	98	0	81	56	0	0	0	1	98

Efficiency Rate 0 Failure Rate 100

Table 9: Efficiency and failure rates of overall root zone soil moisture

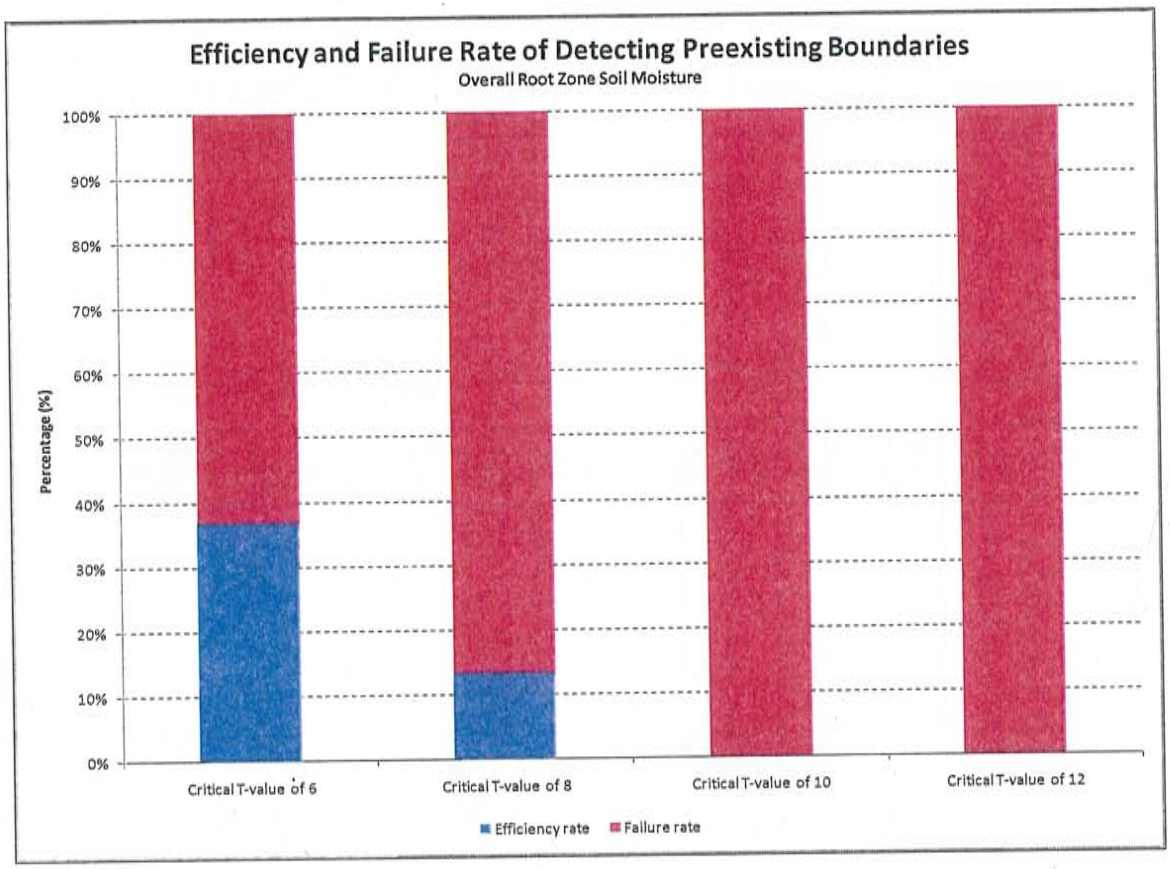

Figure 24: Efficiency and failure rates of the overall root zone soil moisture PCA at critical t-values of 6, 8, 10 and 12

Overall Digital Values

Critical T-Value of 6

Transect	Total Number of Boundaries Detected	Total Number of Landform and Soil Boundaries	Total Landform and Soil Boundaries Detected	Number of Landform Boundaries	Number of Soil Boundaries	Detected Landform Boundaries	Detected Soil Boundaries	Detected Both Soil and Landform Boundaries?	Extra Boundaries	Non-Detected Landform or Soil Boundaries
1	2	7	2	7	0	2	0	0	0	5
2	5	5	2	4	2	1	1	0	4	3
3	6	8	3	7	6	3	2	2	3	5
4	6	4	2	2	2	2	0	0	4	2
5	4	5	1	3	4	1	1	1	3	4
6	5	12	5	12	4	5	1	1	0	7
7	6	7	3	7	2	3	0	0	3	4
8	11	7	6	7	3	6	3	3	5	1
9	7	7	5	6	2	4	2	1	2	2
10	8	6	4	5	6	4	4	4	4	2
11	4	11	4	7	8	4	3	3	0	7
12	5	3	2	3	3	2	2	2	3	1
14	6	10	3	6	10	2	3	2	3	7
15	3	6	1	5	4	1	1	1	2	5
Totals	78	98	43	81	56	40	23	20	36	55

Efficiency Rate 43.87755102 Failure Rate 56.12244898

Critical T-Value of 8

Transect	Total Number of Boundaries Detected	Total Number of Landform and Soil Boundaries	Total Landform and Soil Boundaries Detected	Number of Landform Boundaries	Number of Soil Boundaries	Detected Landform Boundaries	Detected Soil Boundaries	Detected Both Soil and Landform Boundaries?	Extra Boundaries	Non-Detected Landform or Soil Boundaries
1	1	7	1	7	0	1	0	0	0	6
2	0	5	0	4	2	0	0	0	0	5
3	2	8	2	7	6	2	1	1	0	6
4	2	4	0	2	2	0	0	0	2	4
5	1	5	0	3	4	0	0	0	1	5
6	1	12	1	12	4	1	0	0	0	11
7	0	7	0	7	2	0	0	0	0	7
8	3	7	1	7	3	1	0	0	2	6
9	1	7	1	6	2	0	1	0	0	6
10	4	6	2	5	6	2	2	2	2	4
11	3	11	3	7	8	3	2	2	0	8
12	2	3	2	3	3	2	2	2	0	1
14	3	10	2	6	10	1	2	1	1	8
15	1	6	1	5	4	1	1	1	0	5
Totals	24	98	16	81	56	14	11	9	8	82

Efficiency Rate 16.32653061 Failure Rate 83.67346939

Critical T-Value of 10

Transect	Total Number of Boundaries Detected	Total Number of Landform and Soil Boundaries	Total Landform and Soil Boundaries Detected	Number of Landform Boundaries	Number of Soil Boundaries	Detected Landform Boundaries	Detected Soil Boundaries	Detected Both Soil and Landform Boundaries?	Extra Boundaries	Non-Detected Landform or Soil Boundaries
1	0	7	0	7	0	0	0	0	0	7
2	0	5	0	4	2	0	0	0	0	5
3	0	8	0	7	6	0	0	0	0	8
4	0	4	0	2	2	0	0	0	0	4
5	0	5	0	3	4	0	0	0	0	5
6	1	12	1	12	4	1	0	0	0	11
7	0	7	0	7	2	0	0	0	0	7
8	1	7	0	7	3	0	0	0	1	7
9	1	7	1	6	2	0	1	0	0	6
10	1	6	1	5	6	1	1	1	0	5
11	1	11	0	7	8	1	1	1	0	10
12	1	3	1	3	3	1	1	1	0	2
14	0	10	0	6	10	0	0	0	0	10
15	0	6	0	5	4	0	0	0	0	6
Totals	6	98	4	81	56	4	4	3	1	93

Efficiency Rate 4.081632653 Failure Rate 94.89795918

Critical T-Value of 12

Transect	Total Number of Boundaries Detected	Total Number of Landform and Soil Boundaries	Total Landform and Soil Boundaries Detected	Number of Landform Boundaries	Number of Soil Boundaries	Detected Landform Boundaries	Detected Soil Boundaries	Detected Both Soil and Landform Boundaries?	Extra Boundaries	Non-Detected Landform or Soil Boundaries
1	0	7	0	7	0	0	0	0	0	7
2	0	5	0	4	2	0	0	0	0	5
3	0	8	0	7	6	0	0	0	0	8
4	0	4	0	2	2	0	0	0	0	4
5	0	5	0	3	4	0	0	0	0	5
6	1	12	1	12	4	1	0	0	0	11
7	0	7	0	7	2	0	0	0	0	7
8	1	7	0	7	3	0	0	0	1	7
9	0	7	0	6	2	0	0	0	0	7
10	0	6	0	5	6	0	0	0	0	6
11	0	11	0	7	8	0	0	0	0	11
12	0	3	0	3	3	0	0	0	0	3
14	0	10	0	6	10	0	0	0	0	10
15	0	6	0	5	4	0	0	0	0	6
Totals	2	98	1	81	56	1	0	0	1	97

Efficiency Rate 1.020408163 Failure Rate 98.97959184

Table 10: Efficiency and failure rate of overall digital values

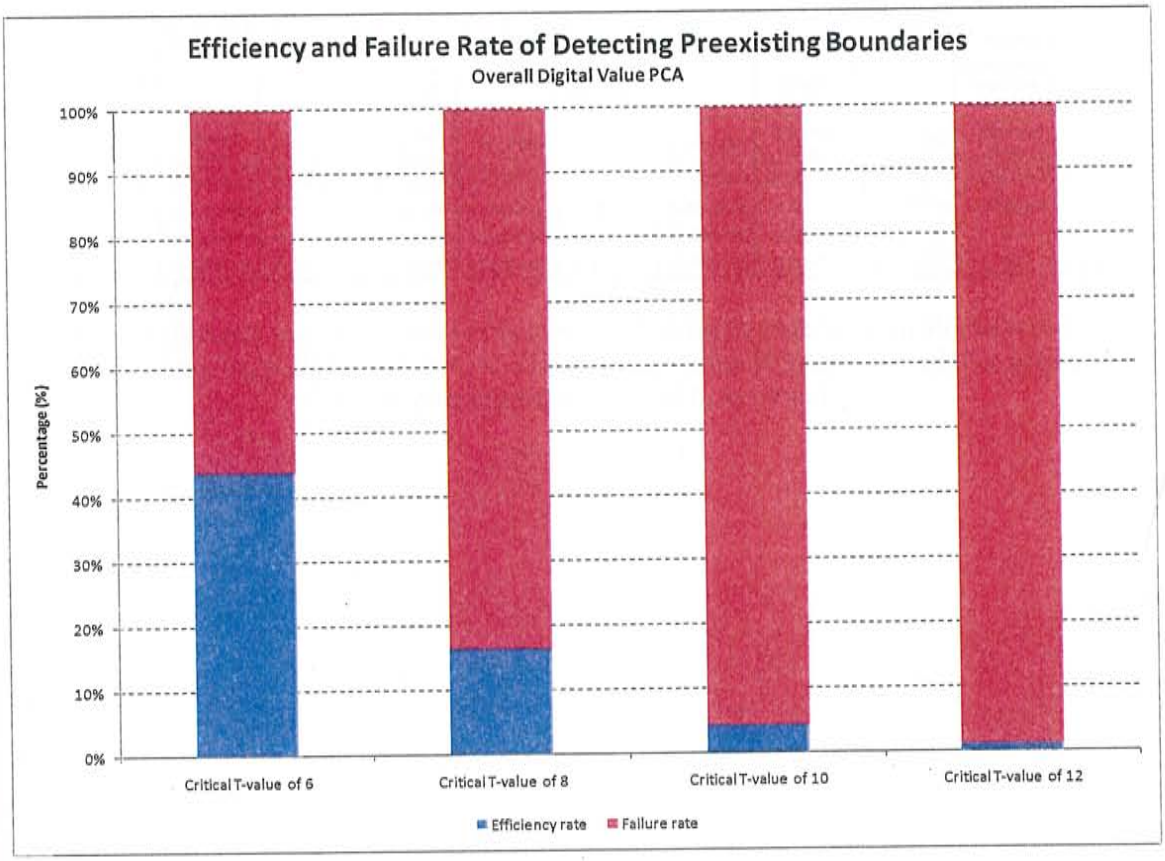

Figure 25: Efficiency and failure rates of the overall digital value PCA at critical t-values of 6, 8, 10 and 12

Efficiency and Failure Rate of Detecting Landform Boundaries

	All Data		Daily Root Zone Soil Moisture		Daily Digital Values		Overall Digital Values		Overall Root Zone Soil Moisture	
	Efficiency Rate	Failure Rate	Efficiency Rate	Failure Rate	Efficiency Rate	Failure Rate	Efficiency Rate	Failure Rate	Efficiency Rate	Failure Rate
Critical T-Value 6	76.54320988	23.45679012	60.49382716	39.50617284	59.25925926	40.74074074	49.38271605	50.61728395	40.74074074	59.25925926
Critical T-Value 8	61.72839506	38.27160494	48.14814815	51.85185185	45.67901235	54.32098765	17.28395062	82.71604938	13.58024691	86.41975309
Critical T-Value 10	40.74074074	59.25925926	25.92592593	74.07407407	28.39506173	71.60493827	4.938271605	95.0617284	0	100
Critical T-Value 12	28.39506173	71.60493827	18.51851852	81.48148148	16.04938272	83.95061728	1.234567901	98.7654321	0	100

Table 11: Efficiency and failure rates of detecting landform boundaries with all, daily root zone soil moisture, daily digital value PCA, overall digital value PCA and overall root zone soil moisture over critical t-values of 6, 8, 10 and 12

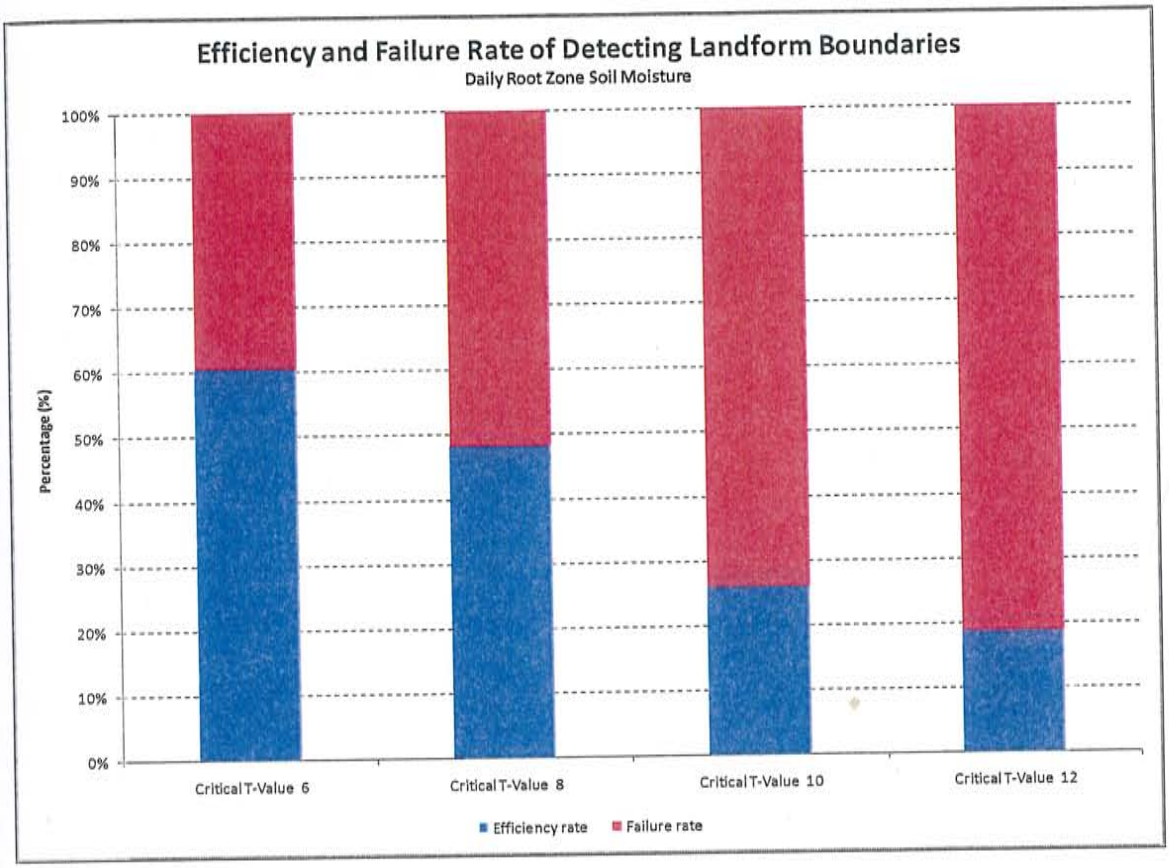

Figure 26: Efficiency and failure rates of detecting landform boundaries using the daily root zone soil moisture at critical t-values of 6, 8, 10 and 12

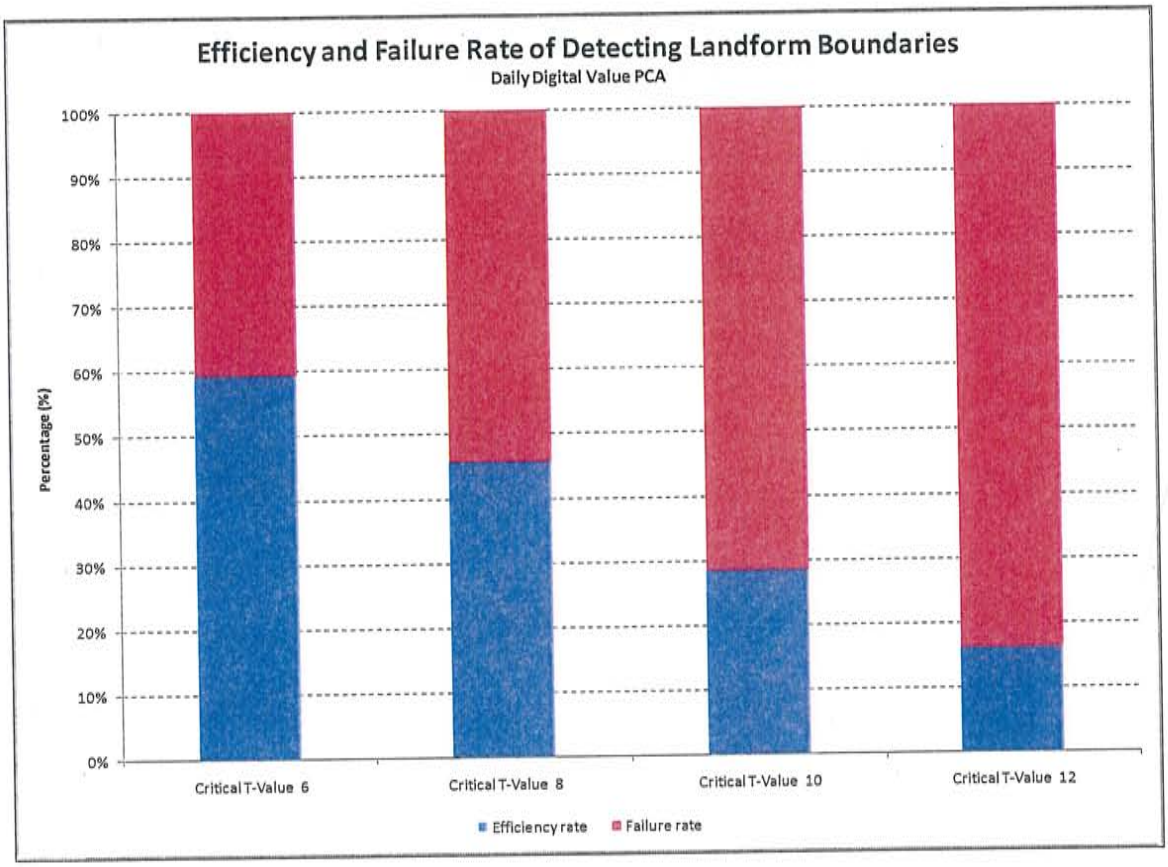

Figure 27: Efficiency and failure rate of detecting landform boundaries using the daily digital PCA at critical t-values of 6, 8, 10 and 12

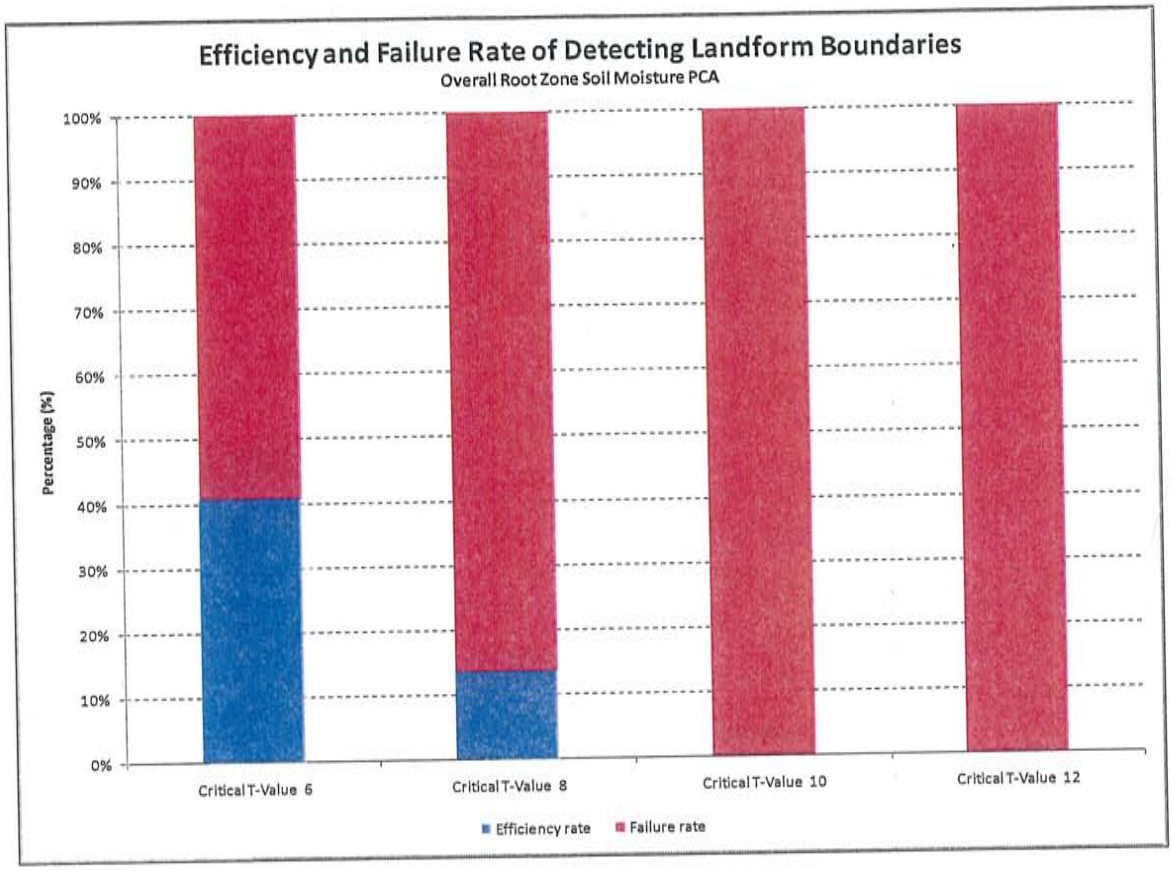

Figure 28: Efficiency and failure rates of detecting landform boundaries using the overall root zone soil moisture at critical t-values of 6, 8, 10 and 12

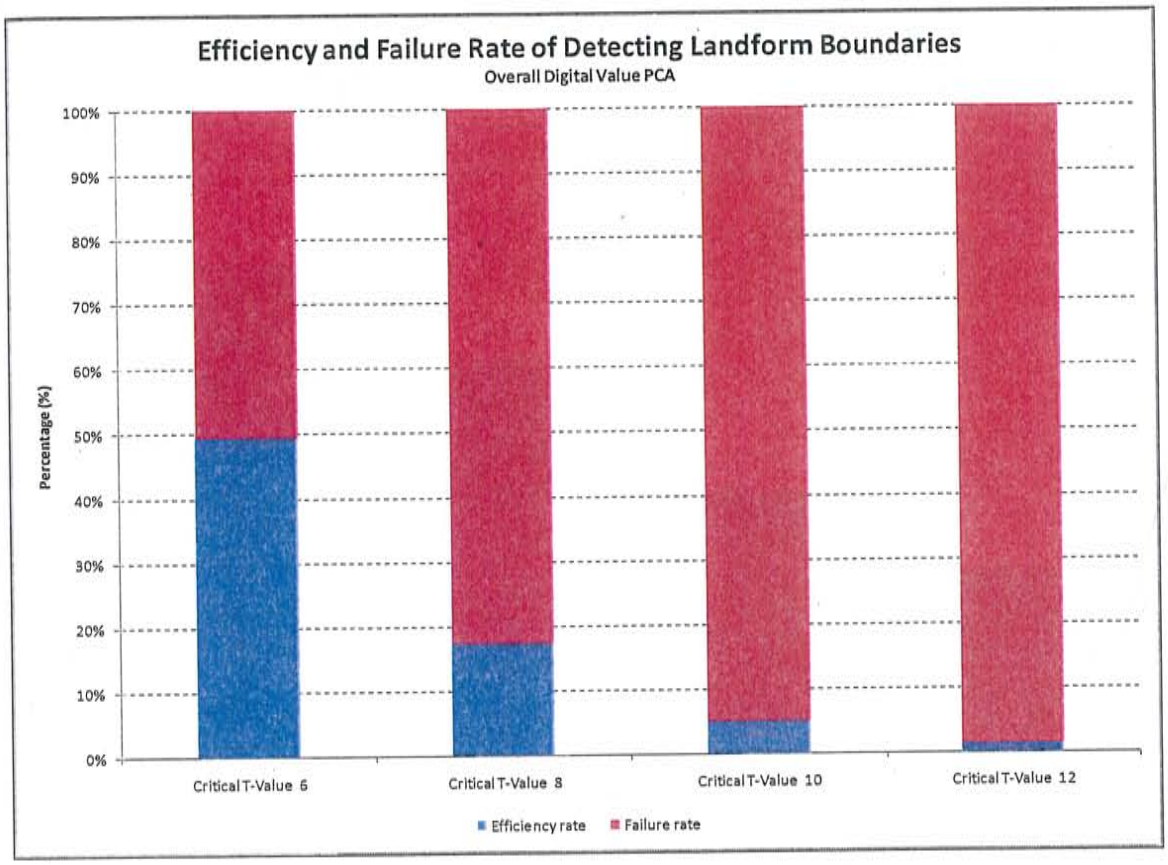

Figure 29: Efficiency and failure rates of detecting landform boundaries using the overall digital value PCA at critical t-values of 6, 8, 10 and 12

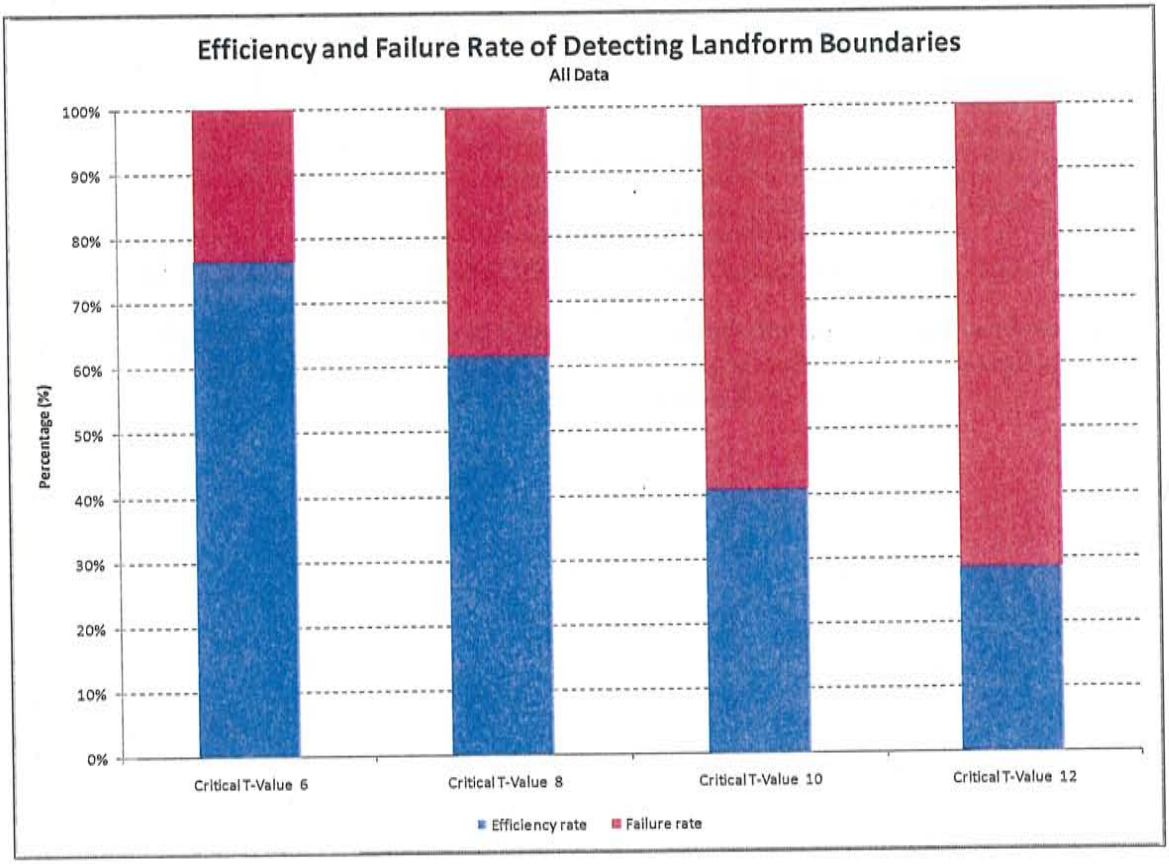

Figure 30: Efficiency and failure rates of detecting landform boundaries using all data combined at critical t-values of 6, 8, 10 and 12

Efficiency and Failure Rate of Detecting Soil Boundaries

	All Data		Daily Root Zone Soil Moisture		Daily Digital Values		Overall Digital Values		Overall Root Zone Soil Moisture	
	Efficiency Rate	Failure Rate	Efficiency Rate	Failure Rate	Efficiency Rate	Failure Rate	Efficiency Rate	Failure Rate	Efficiency Rate	Failure Rate
Critical T-Value 6	71.42857143	28.57142857	60.71428571	39.28571429	51.78571429	48.21428571	41.07142857	58.92857143	39.28571429	60.71428571
Critical T-Value 8	62.5	37.5	53.57142857	46.42857143	41.07142857	58.92857143	19.64285714	80.35714286	16.07142857	83.92857143
Critical T-Value 10	41.07142857	58.92857143	28.57142857	71.42857143	26.78571429	73.21428571	7.142857143	92.85714286	0	100
Critical T-Value 12	26.78571429	73.21428571	19.64285714	80.35714286	16.07142857	83.92857143	0	100	0	100

Table 12: Efficiency and failure rates of detecting soil boundaries using all data combined, daily root zone soil moisture, daily digital value PCA, overall digital value PCA and overall root zone soil moisture at critical t-values of 6, 8, 10 and 12

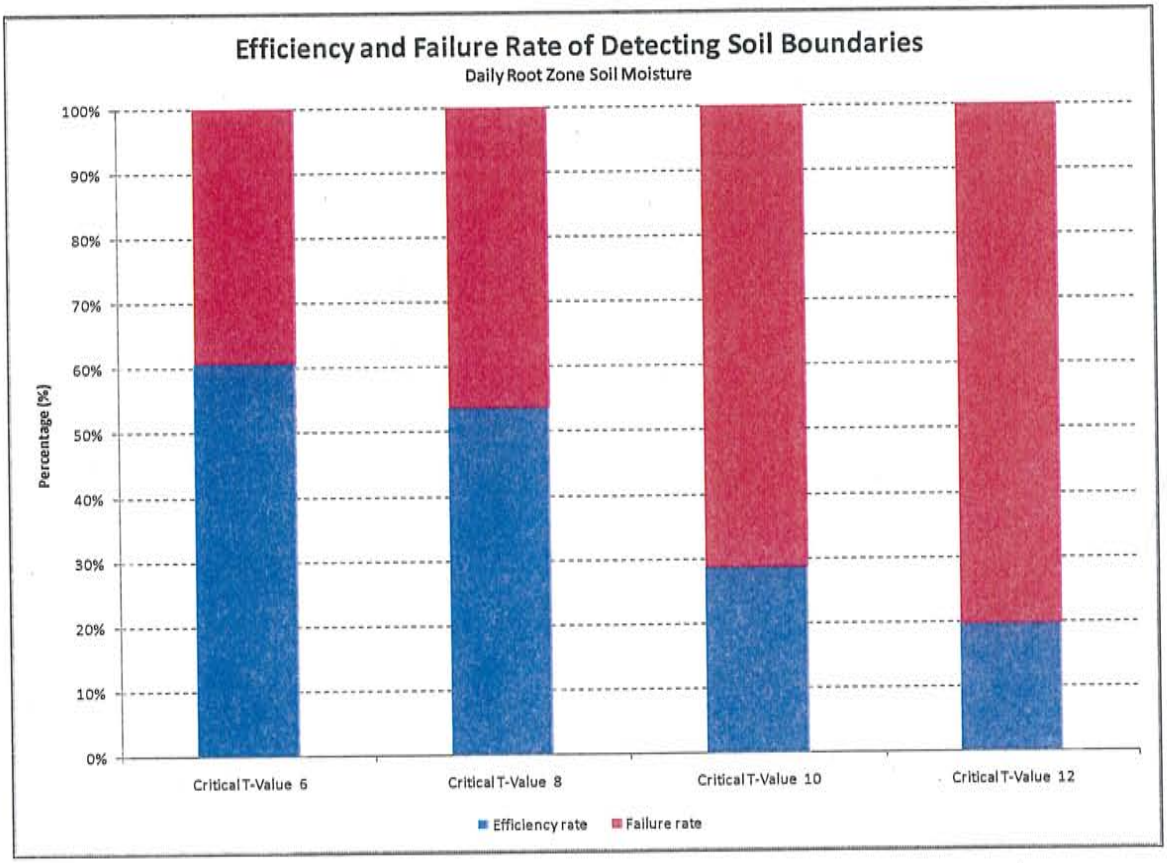

Figure 31: Efficiency and failure rates of detecting soil boundaries using the daily root zone soil moisture at critical t-values of 6, 8, 10 and 12

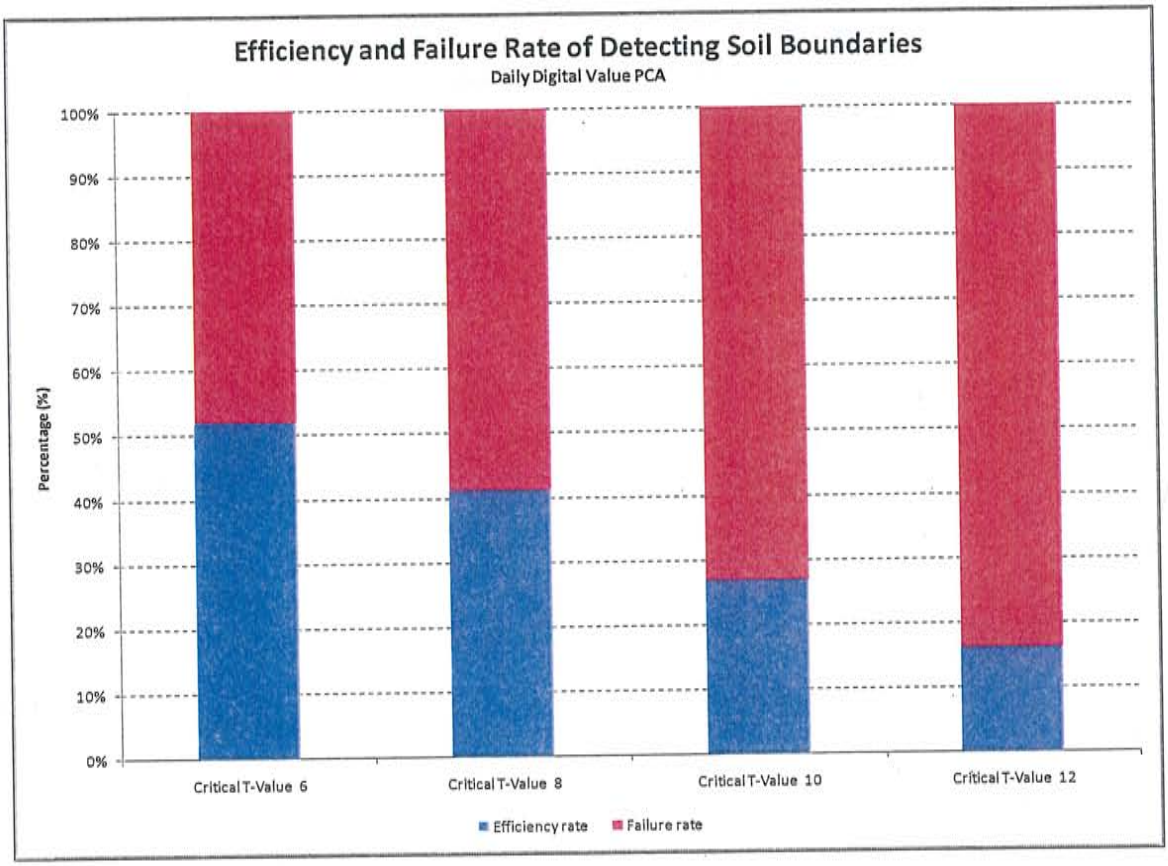

Figure 32: Efficiency and failure rates of detecting soil boundaries using the daily digital value PCA at critical t-values of 6, 8, 10 and 12

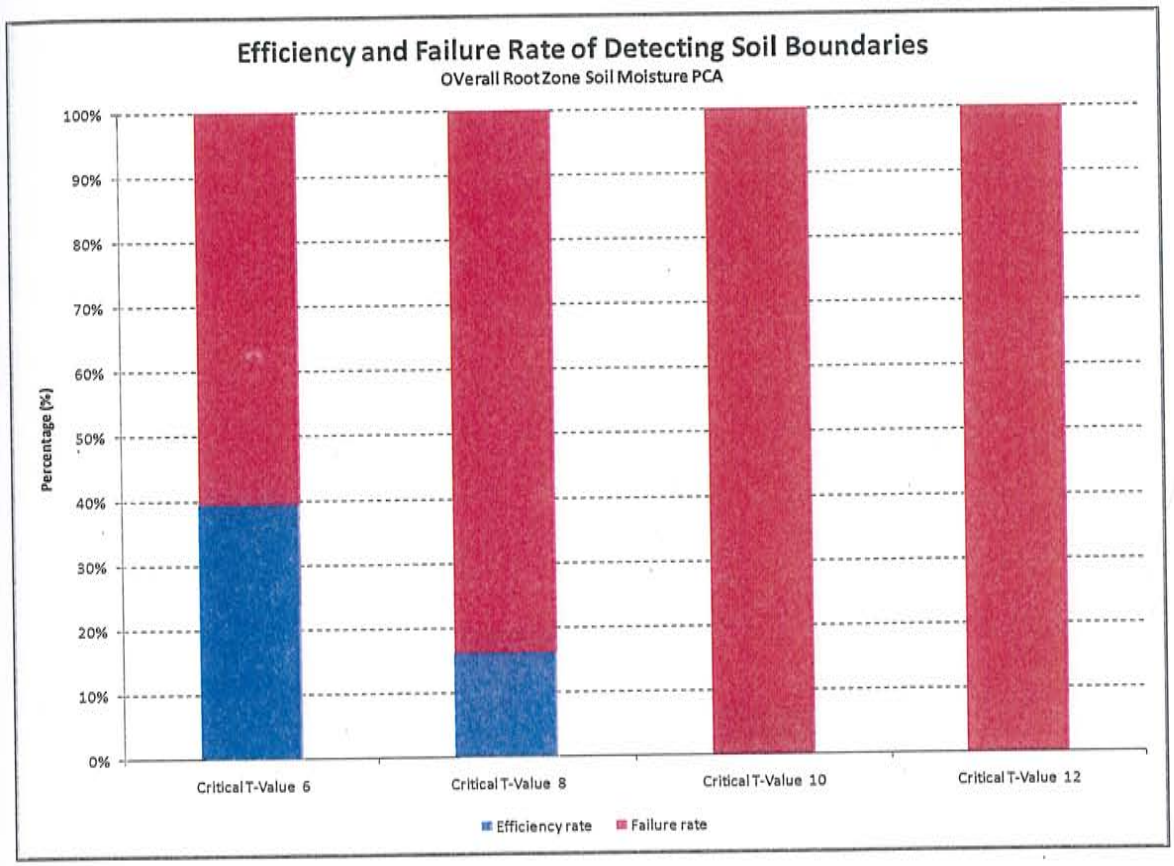

Figure 33: Efficiency and failure rates of detecting soil boundaries using the overall root zone soil moisture PCA at critical t-values of 6, 8, 10 and 12

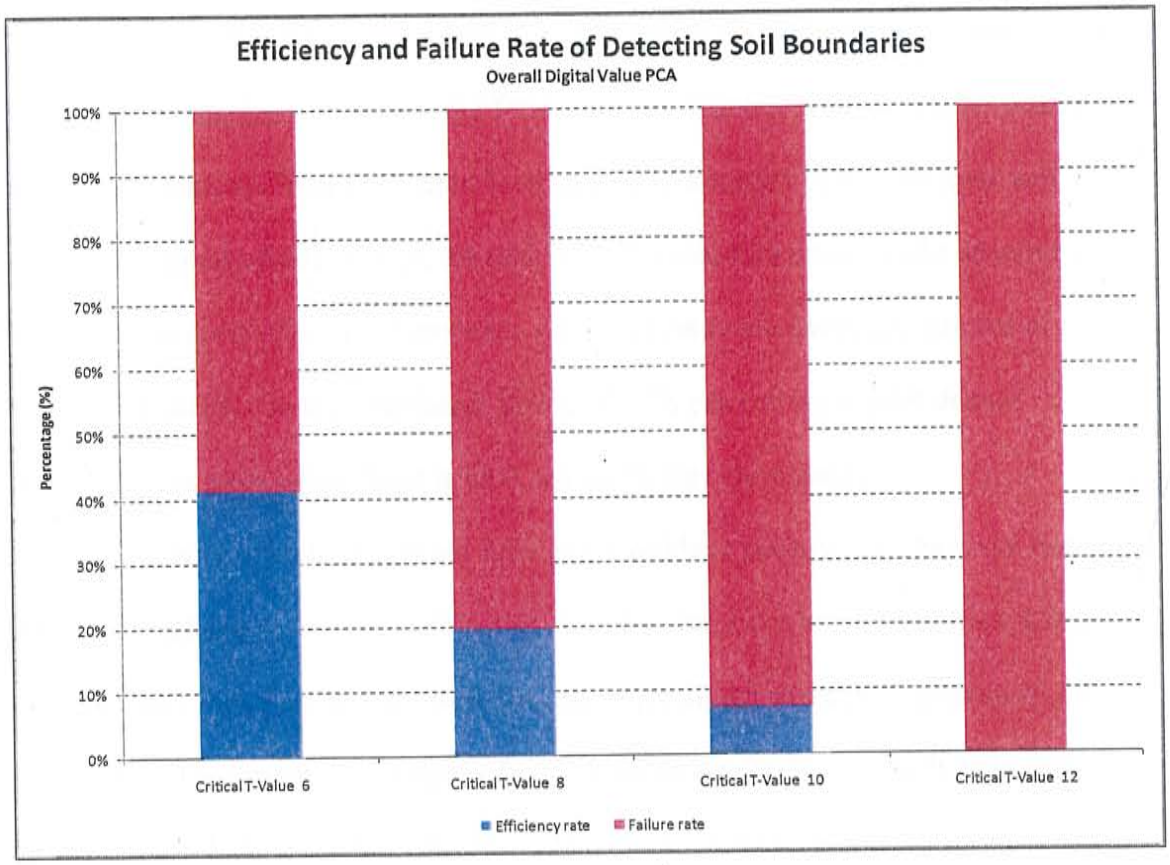

Figure 34: Efficiency and failure rates of detecting soil boundaries using the overall digital value PCA at critical t-value of 6, 8, 10 and 12

Again, when all datasets are combined, the efficiencies are significantly higher (Figure 35). The efficiencies are very similar for detecting either landform or soil boundaries through all datasets. While we often have similar efficiencies in the root zone soil moisture and daily digital values, the root zone soil moisture image might be more useful when used in areas of high soil moisture such as close to the rivers and streams or agricultural areas. On the other hand, the daily PCA can convey a great deal of information in areas where there is little change in the soil moisture.

The extra boundaries are not fully examined here because they have not been formally validated in the field. However, slightly more extra boundaries were detected with the daily root zone soil moisture than the daily digital value PCA (Figure 36 and Figure 37). The largest percentages of extra boundaries detected by both daily datasets are weak boundaries. As the critical t-value increases the number of strong and intermediate extra boundaries decreases to zero.

Georeferencing

Georeferencing is a source of error in our methodology. Because all Landsat images were individually georeferenced by Sung-ho Hong, there can be significant differences from one image to another. It is impossible that multiple georeferenced images lie exactly on top of each other. Five locations near the study areas were selected to analyze the georeferencing error. The UTM coordinates of each location in each image are presented in Table 13. The first date for each location is used as a reference point and each subsequent date is measured to that reference point. The resulting average georeferencing error is 74 m with a standard deviation of 30. There are two dates of images, April 7, 2000 and August 3, 2005, which contribute the most to this error. There

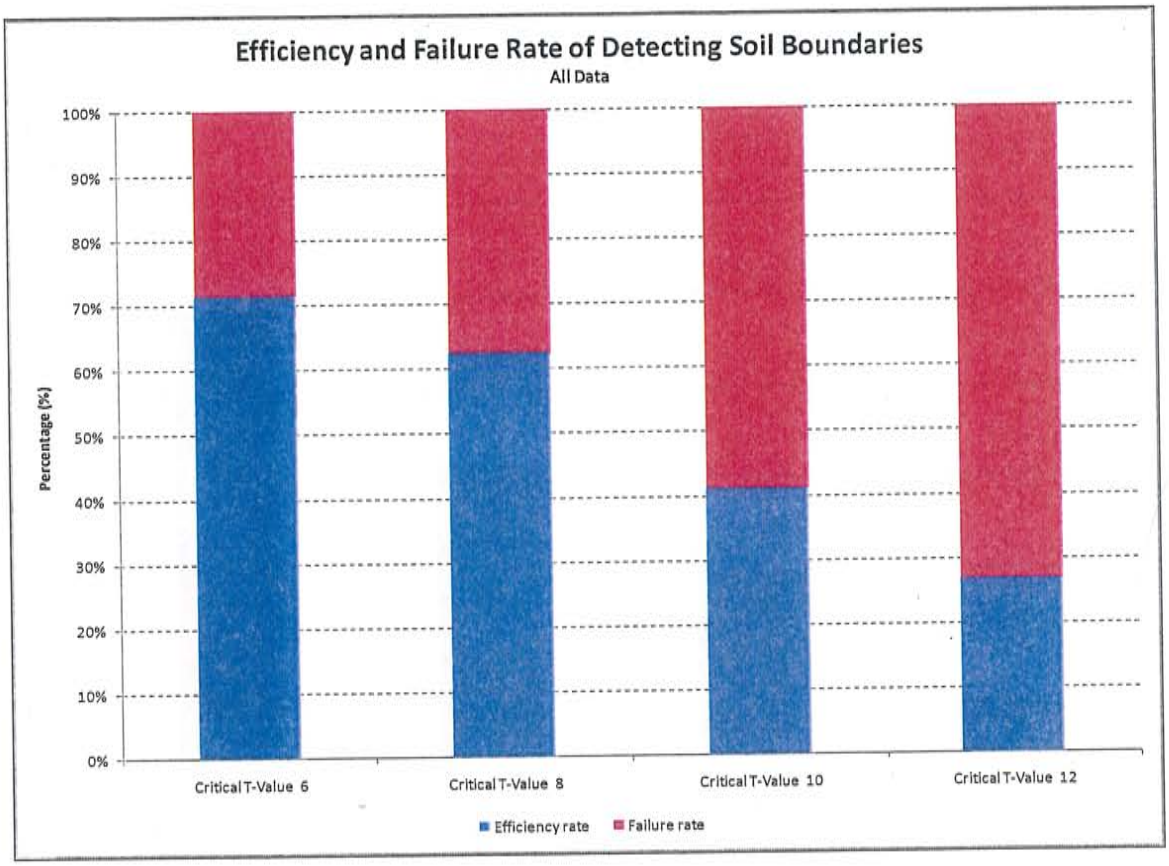

Figure 35: Efficiency and failure rates of detecting soil boundaries using all data combined at critical t-values of 6, 8, 10 and 12

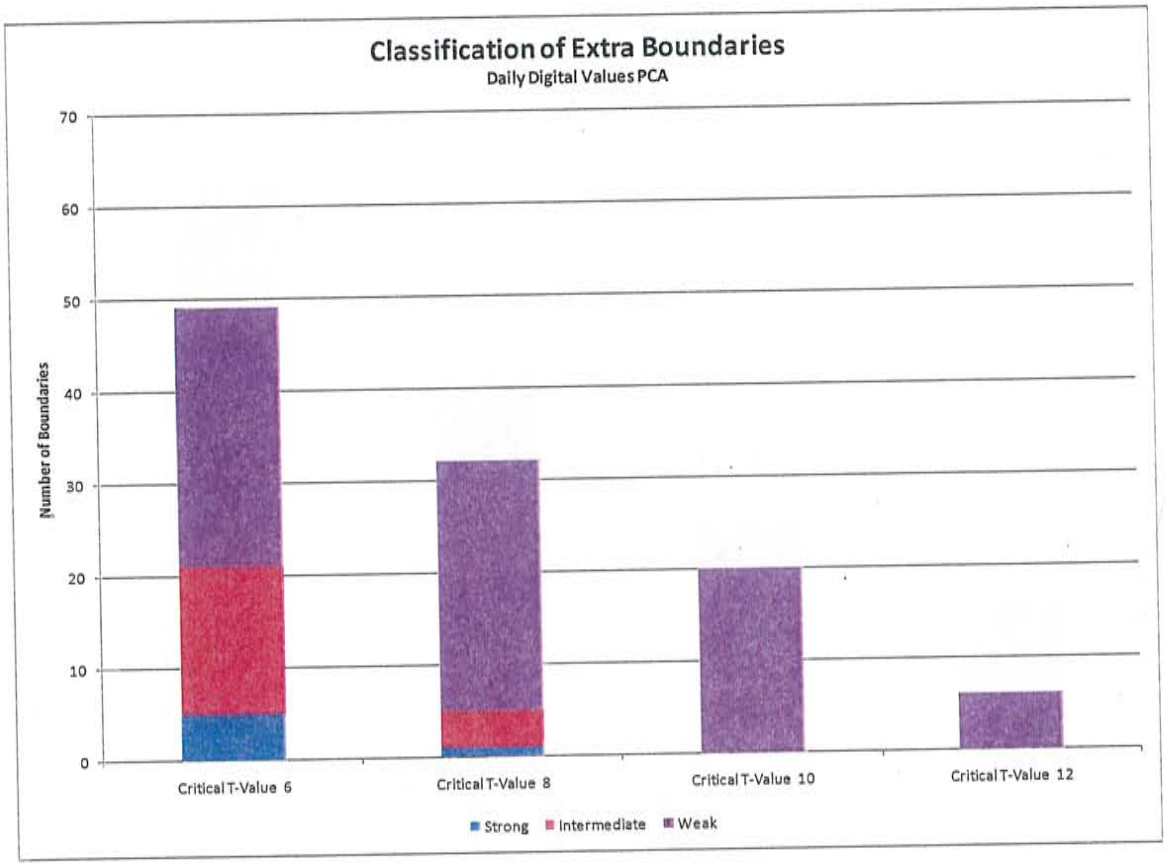

Figure 36: Classification of extra boundaries detected by the daily digital values

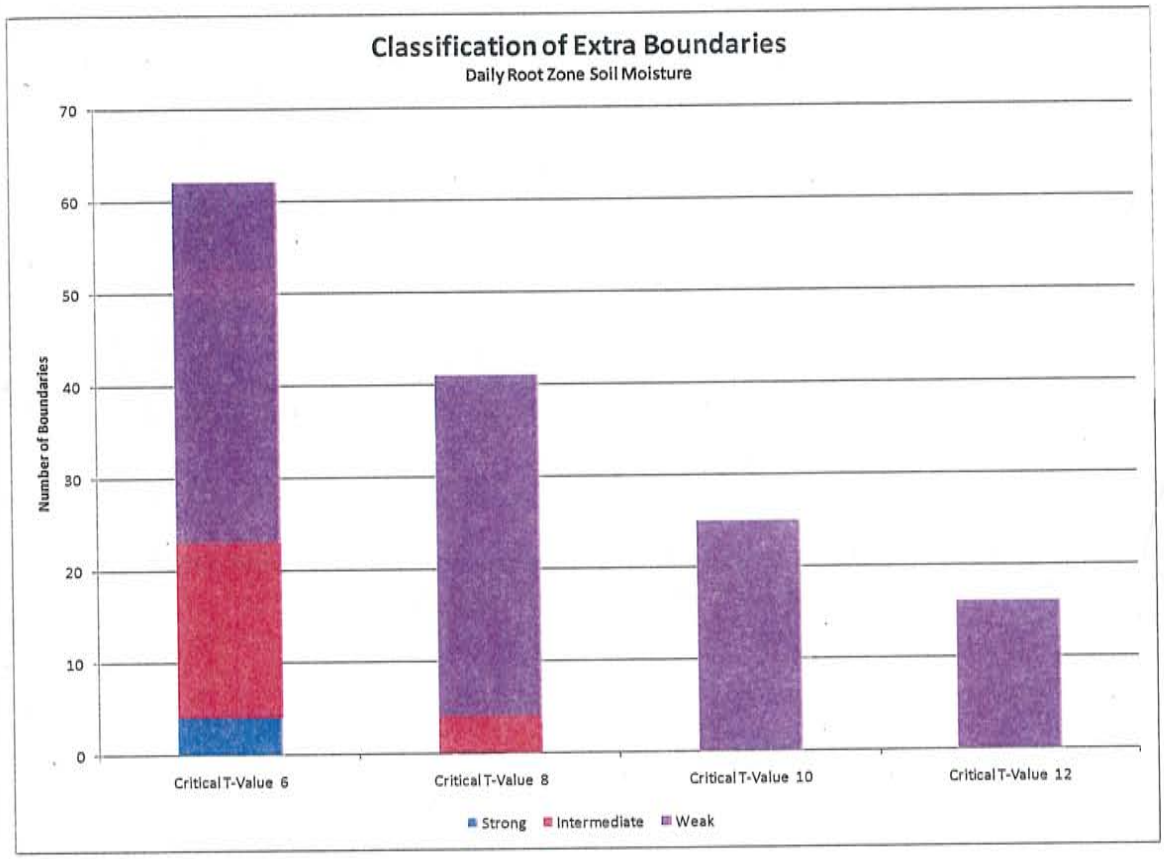

Figure 37: Classification of extra boundaries detected by daily root zone soil moisture

Georeferencing Error

	Socorro Landing Strip			Socorro Drain			Bernardo Exit			Roads near Black Butte			HWY 380 over river		
	Easting	Northing	Distance	Easting	Northing	Distance	Easting	Northing	Distance	Easting	Northing	Distance	Easting	Northing	Distance
4/7/2000	324553.660	3766559.350	Reference	324832.991	3774712.183	Reference	331553.750	3810128.500	Reference	345765.890	3808349.790	Reference	328970.000	3754771.000	Reference
5/6/2002	324470.134	3766517.344	93.494	324775.440	3774662.300	76.160	331512.590	3810091.690	55.219	345746.760	3808354.820	19.780	328880.150	3754715.470	105.625
5/9/2000	324457.535	3766554.302	96.257	324756.420	3774677.530	84.047	331509.770	3810137.950	44.984	345742.320	3808373.110	33.157	328919.440	3754730.610	64.712
5/12/2004	324487.330	3766572.610	67.642	324767.190	3774697.710	67.374	331504.000	3810099.320	57.676	345742.950	3808337.240	26.149	328923.190	3754763.700	47.376
5/22/2005	324439.458	3766554.430	114.308	324746.450	3774677.780	93.128	331500.180	3810112.960	55.778	345749.820	3808331.760	24.152	328895.840	3754720.190	89.896
5/28/2004	324412.450	3766547.176	141.734	324722.820	3774686.740	113.070	331450.720	3810088.350	110.577	345694.130	3808339.620	72.477	328874.360	3754729.960	104.073
5/31/2002	324450.703	3766558.271	102.963	324768.370	3774683.080	70.872	331498.660	3810132.870	55.263	345723.810	3808377.610	50.445	328881.930	3754739.880	93.407
6/4/2001	324452.352	3766546.482	102.122	324777.690	3774651.760	81.909	331510.870	3810114.100	45.233	345741.080	3808345.940	25.107	328922.280	3754735.130	59.698
6/13/2004	324499.836	3766507.432	74.783	324773.620	3774636.260	96.380	331502.000	3810097.570	60.289	345759.770	3808323.930	26.574	328934.640	3754699.590	79.685
6/16/2002	324456.149	3766529.917	101.856	324755.670	3774662.180	92.080	331481.680	3810099.550	77.667	345722.980	3808337.980	44.506	328873.640	3754735.800	102.588
7/2/2005	324454.438	3766564.909	99.378	324753.660	3774694.180	81.348	331489.870	3810122.190	64.191	345712.400	3808315.990	63.274	328903.950	3754752.040	68.717
7/6/2004	324430.289	3766568.909	123.740	324740.900	3774701.510	92.707	331449.560	3810130.090	104.202	345735.180	3808357.770	31.730	328868.390	3754759.920	102.212
7/28/2000	324456.067	3766564.477	97.727	324786.640	3774701.480	47.570	331497.890	3810139.510	56.935	345714.440	3808388.270	64.248	328909.110	3754730.880	72.919
7/31/2002	324432.471	3766575.421	122.250	324751.970	3774686.690	84.937	331483.240	3810119.630	71.066	345745.250	3808323.310	33.574	328897.320	3754749.490	75.796
8/3/2005	324387.000	3766592.300	169.886	324697.060	3774701.316	136.365	331434.851	3810120.820	119.147	345696.603	3808351.222	69.302	328866.420	3754763.530	103.849
8/19/2002	324459.420	3766591.570	99.596	324789.910	3774702.470	44.162	331528.340	3810138.910	27.460	345702.920	3808365.450	72.366	328911.920	3754744.230	63.952
9/14/2000	324439.370	3766551.290	114.574	324779.640	3774689.570	57.945	331500.730	3810147.170	56.211	345686.580	3808365.170	80.788	328904.900	3754722.740	81.037
9/17/2004	324454.680	3766586.150	102.544	324778.660	3774689.910	58.719	331499.260	3810120.500	55.074	345746.260	3808351.050	19.670	328899.080	3754752.410	73.316
9/30/2000	324436.910	3766569.280	117.172	324748.960	3774689.360	87.075	331505.530	3810113.830	50.402	345697.020	3808322.930	73.923	328914.150	3754731.720	68.280
10/14/1999	324488.080	3766587.760	71.469	324802.540	3774719.620	31.346	331530.750	3810144.500	28.018	345755.600	3808372.500	24.932	328913.271	3754783.229	58.032
														Average Georeferencing Error	74
														Standard Deviation	30

Table 13: Georeferencing errors were determined by documenting coordinates in all images at easily identifiable points. Using WGS 1984.

is a second inherent problem even in this type of process. While I have identified these five locations, they are smaller than the pixel size of the Landsat. This means that while we are identifying the UTM coordinates, they are already not completely accurate. There were two transects in particular where the georeferencing error limits our ability to detect boundaries. The data points within transects 13 and 16 are very close together and do not separate into well defined boundaries such as occur in the other transects (Figure 38). In these cases, the boundaries fall within the range of georeferencing error. Along with the georeferencing error, the 30 m^2 Landsat pixel and the split moving window size of five pixels are the greatest limitations of our methodology.

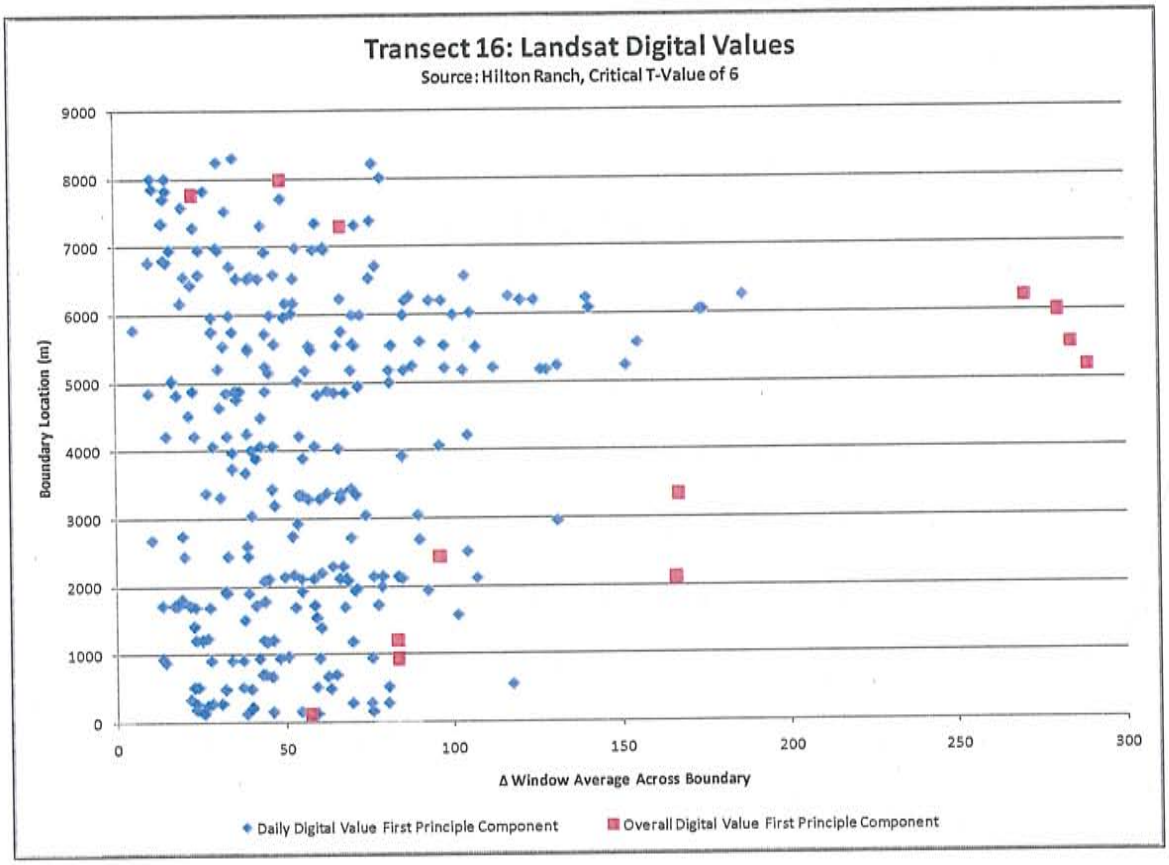

Figure 38: Transect 16; data points occur so close together that boundaries cannot be delineated

CONCLUSIONS

In this study we were investigating three hypotheses. 1) Would more boundaries be detected using the root zone soil moisture than the Landsat digital values? The efficiency and failure rates of the daily data, we determined that they perform almost equally well, with the highest efficiencies of 56.1% for the root zone soil moisture and 53.1% for the digital values. 2) Can we enhance spatial trends and dampen temporal effects by using the split moving window technique on images of root zone soil moisture and the daily first component analysis over multiple days? We discovered that by using multiple images over a period of several years and by using the split moving window technique these effects can be achieved. The compilation of multiple days allows boundaries to be seen that will not be revealed in a single day. 3) Will the compilation of the root zone soil moisture provide more information than a compilation of the daily first principle component? The results reveal that both provide valuable data under different conditions. The root zone soil moisture displays boundaries best under conditions when the moisture content is higher. The daily PCA data tends to exhibit boundaries best when due to topographical change and when the soil moisture content is low. It is our conclusion that in conditions where soil moisture variability is low, calculation using the SEBAL model may be an unnecessary use of time and money. This is supported by a higher efficiency and lower failure rate of the Landsat digital values.

These results suggest that our method is a valuable addition to traditional methods of soil mapping. Most of the preexisting boundaries were detected but the extra boundaries are where the greatest advancement lies. Future work should start in identifying if these boundaries are real and if so why they were not previously mapped.

In this study we have developed tools for digital soil mapping. More field work will be needed, particularly to validate the extra confirmed boundaries. It may be that many of these extra confirmed boundaries are true boundaries. If this is so, it would increase the value of digital soil boundary detection.

The advantage to this method is that unlike traditional soil mapping methods it is not expert knowledge-based. There is little prior knowledge needed to use this method, as we have shown by calculating the efficiency and failure rate of our methodology. Because of this, it can be applied more widely. Also, by analyzing the landscape response over time we can improve greatly on other methods.

BIBLIOGRAPHY

Arnold, R. W., 1983, Concepts of soils and pedology *in* Wilding, L. P., Smeck, N. E., and Hall, G. F., eds., Pedogenesis and Soil Taxonomy: New York, Elsevier, p. 1-21.

Bastiaanssen, W.G.M., M. Menenti, R.A. Feddes, and A.A. M. Holtslag. 1998. A remote sensing surface energy balance algorithm for land (SEBAL). Part 1: Formulation. Journal of Hydrology 212-213:198-212.

Bastiaanssen, W. G. M., 2000, SEBAL-based sensible and latent heat fluxes in the irrigated Gediz Basin, Turkey: Journal of Hydrology, v. 229, no. 1-2, p. 87-100.

Baban, S. M. J., and Yusof, K. W., 2001, Mapping land use/cover distribution on a mountainous tropical island using remote sensing and GIS: International Journal of Remote Sensing, v. 22, no. 10, p. 1909-1918.

Bui, E., 2007, Review of digital soil mapping in Australia, in Lagacherie, P., McBratney, A. B., and Voltz, M., eds., Digital Soil Mapping: An Introductory Perspective: Developments in Soil Science: Amsterdam, Netherlands, Elsevier, p. 25-37.

Burrough, P.A., 1989, Fuzzy mathematical methods for soil survey and land evaluation: Journal of Soil Science, v. 40, p. 477-492.

Burrough, P. A., van Gaans, P. F. M., and Hootsmans, R., 1997, Continuous classification in soil survey: spatial correlation, confusion and boundaries: Geoderma, v. 77, no. 2-4, p. 115-135.

Campbell, J. B., 2007, Introduction to Remote Sensing: New York, The Guilford Press, 626 p.

Cole, N. J., and Boettinger, J. L., 2007, Pedogenic understanding raster classification methodology for mapping soils, Powder River Basin, Wyoming, USA, in Lagacherie, P., McBratney, A. B., and Voltz, M., eds., Digital Soil Mapping: An Introductory Perspective: Developments in Soil Science: Amsterdam, Elsevier, p. 377-388.

Cutler, E. J. B., 1977, Soil Resource Surveys Interpretations and Applications: Canterbury, New Zealand, Lincoln College Press, 272 p.

De Gruijit, J.J., D.J.J. Walvoort, P.F.M. Van Gaans, 1997, Continuous soil-maps - a fuzzy set approach to bridge the gap between aggregation levels of process and distribution models, Geoderma, v. 77, p. 169-195.

Dmitriev, E. A., 1983, Continuity of soils and the problem of soil classification: Moscow University Soil Science Bulletin, v. 38, p. 1-10.

Fortin, M.J., 1997, Effects of data types on vegetation boundary delineation: Canadian Journal of Forest Research, v. 27, no. 11, p. 1851-1858.

Gessler, P. E., Moore, I. D., McKensie, N. J., and Ryan, P. J., 1995, Soil-landscape modelling and spatial prediction of soil attributes: International Journal Geographical Information Science, v. 9, p. 421-432.

Gile, L. H., 1975a, Causes of soil boundaries in an arid region. I. Age and parent materials: Soil Science Society of America Proceedings, v. 39, p. 316-323.

Gile, L. H., 1975b, Causes of soil boundaries in an arid region. II. Dissection, moisture and faunal activity: Soil Science Society of America Proceedings, v. 39, p. 324-330.

Goossens, R., and Van Ranst, E., 1998, The use of remote sensing to map gypsiferous soils in the Ismailia Province (Egypt): Geoderma, v. 87, no. 1-2, p. 47-56.

Greve, M. H., and Greve, M. B., 2004, Determining and representing width of soil boundaries using electrical conductivity and MultiGrid: Computers & Geosciences, v. 30, p. 569-578.

Hendrickx, J. M. H., Wierenga, P. J., Nash, M. S., and Nielson, D. R., 1986, Boundary Location from Texture, Soil Moisture, and Infiltration Data: Soil Science Society of America, v. 50, p. 1515-1520.

Huevelink, G.B.M. and R. Webster, 2001, Modelling soil variation: past, present and future, Geoderma, v. 100, p. 269-301.

Jenny, Hans., 1941 , Factors of Soil Formation, New York, McGraw Hill.

Karale, R. L., Venkataratnam, L., Sehgal, J. L., and Sinha, A. K., 1991, Soil mapping with IRS-1A data in
areas of complex soilscapes. Current Science, Special issue on Remote Sensing for Natural Resources Development, **61**, 198–203.

Kienast-Brown, S., and Boettinger, J. L., 2007, Land-cover classification from Landsat imagery for mapping dynamic wwet and saline soils, in Lagacherie, P., McBratney, A. B., and Voltz, M., eds., Digital Soil Mapping: An Introductory Perspective: Developements in Soil Science: Amsterdam, Elsevier, p. 235-244.

King, G. J., Acton, D. F., and St. Arnaud, R. J., 1983, Soil-landscape analysis in relation to soil distribution and mapping at a site within the Weyburn association: Canadian Journal of Soil Science, v. 45, p. 657-670.

Knox, E.G., 1957, Fragipan horizons in New York soils. III. The basis of rigidity, Soil Science Society of America Process, p. 326-330.

Kruse, F. A., Boardman, J. W., and Farrand, W. H. (1996), Advanced hyperspectral remote sensing analysis workshop. In ERIM Second International Airborne Remote Sensing Conference and Exhibition, San Francisco, CA.

Lagacherie, P., and McBratney, A. B., 2007, Spatial soil information systems and spatial soil inference systems: perspectives for digital soil mapping, in Lagacherie, P., McBratney, A. B., and Voltz, M., eds., Digital Soil Mapping: An Introductory Perspective: Developments in Soil Science: Amsterdam, Elsevier, p. 3-22.

Madiera Netto, J. S., Robbez-Masson, J.-M., and Martins, E., 2007, Visible -NIR hhyperspectral imagery for discrimination soil types in the La Peyne watershed (France), in Lagacherie, P., McBratney, A. B., and Voltz, M., eds., Digital Soil Mapping: An Introductory Perspective: Developments in Soil Science: Amsterdam, Elsevier, p. 219-233.

McBratney, A. B., 1994, On variation, uncertainty and informatics in environmental soil management: Australian Journal of Soil Research, v. 30, p. 913-935.

Oden, N. L., Sokal, R. R., Fortin, M. J., and Goebl, H., 1993, Categorical Wombling: Detecting Regions of Significant Change in Spatially Locaed Categorical Variables: Geographical Analysis, v. 25, no. 4, p. 315-336.

Schaetzl, R., and Anderson, S., 2005, Soils: Genesis and Geomorphology: Cambridge, UK, Cambridge University Press, 817 p.

Sevilleta LTER, 4 December 2008. < http://sev.lternet.edu/>.

Smith, L.I., 2002, 4 December 2008, A Tutorial on Principle Component Analysis, <http://www.cs.otago.ac.nz/cosc453/student_tutorials/principal_components.pdf> , 26 February 2002.

Soil Survey Staff., 1975, Soil taxonomy: a basic system of soil classification for making and interpreting soil surveys, Agriculture loyhandbook 436: Washington DC, Soil Conservation Service, U.S. Department of Agriculture.

Soil Survey Staff, 1984, Soil survey of Socorro County area, New Mexico, Washington DC, Soil Conservation Service, U.S. Department of Agriculture, 328p.

Soil Survey Staff, 1993, Soil survey manual, Washington DC, Soil Conservation Service, U.S. Department of Agriculture.

Soil Survey Staff, 1999, Soil Taxonomy: A basic system of soil classification for making and interpreting soil surveys, U.S Department of Agricultural, 869p.

Webster, R., 1973, Automatic soil-boundary location from transect data: Mathematical Geology, v. 5, p. 27-37.

Webster, R., 1978, Optimally partitioning soil transects: Journal of Soil Science, v. 29, p. 388-402.

Webster, R., and McBratney, A. B., 1981, Soil segment overlap in character space and its implications for soil classification: Journal of Soil Science, no. 32, p. 133-147.

Webster, R., 2000, Is soil variation random?: Geoderma, no. 97, p. 149-163.

Wierenga, P. J., Hendrickx, J. M. H., Nash, M. S., Ludwig, J., and Daughtery, L. A., 1987, Variation of soil and vegetation with distance along a transect in the Chihuahuan Desert: Journal of Arid Environment, v. 13, p. 53-63.

Wilford, J., and Minty, B., 2007, The use of airborne gamma-ray imagery for mapping soils and understanding landscape process, in Lagacherie, P., McBratney, A. B., and Voltz, M., eds., Digital Soil Mapping: An Introductory Perspective: Developments in Soil Science: Amsterdam, Elsevier, p. 207-218.

Womble, W. H., 1951, Differential Systematics: Science, v. 114, p. 315-322.

APPENDIX A

B1

Landform Map Soil Map	Boundary Location (m)								
	270	420	510	600	720	780	840		
Daily DV PCA 6	350						810	990	1200
percentage of days	35.71						78.57	7.14	7.14
range (m)	360						210	0	0
Overall DV PCA 6	330						810		
T-Value	7.7						8		
Daily RZSM 6	325				675				
percentage of days	42.86				42.86				
range (m)	330				90				
Overall RZSM PCA 6	330								
T-Value	7.8								
Daily DV PCA 8							825		
percentage of days							42.8571		
range (m)							150		
Overall DV PCA 8							810		
T-Value							8		
Daily RZSM 8				650					
percentage of days				14.29					
range (m)				30					
Overall RZSM PCA 8									
T-Value									
Daily DV PCA 10						800			
percentage of days						14.2857			
range (m)						90			
Overall DV PCA 10									
T-Value									
Daily RZSM 10				660					
percentage of days				7.14					
range (m)				0					
Overall RZSM PCA 10									
T-Value									
Daily DV PCA 12						780			
percentage of days						7.14			
range (m)						0			
Overall DV PCA 12									
T-Value									
Daily RZSM 12									
percentage of days									
range (m)									
Overall RZSM PCA 12									
T-Value									

A 1: The summary table of transect 1 includes the locations of the soil and landform boundaries along the transect, the locations, percentage of days and range of boundaries detected by the daily digital values, overall digital value PCA, daily root zone soil moisture and overall root zone soil moisture PCA using a critical t-value of 6, 8, 10 and 12

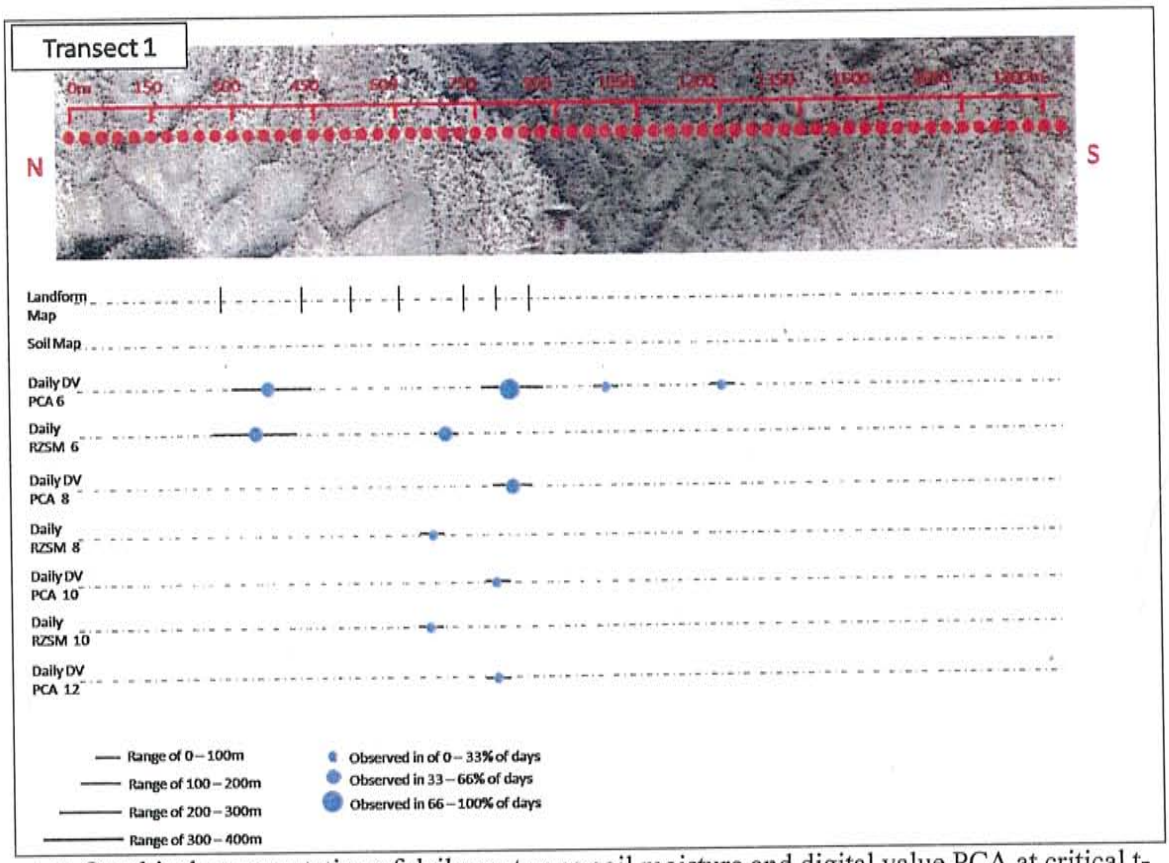

A 2: Graphical representation of daily root zone soil moisture and digital value PCA at critical t-values of 6, 8, 10 and 12 along transect 1. The size of the dot represents the percentage of days the boundary occurs in and the line represents the range over which it occurs. This illustrates how the root zone soil moisture often detects more scatter than the digital values

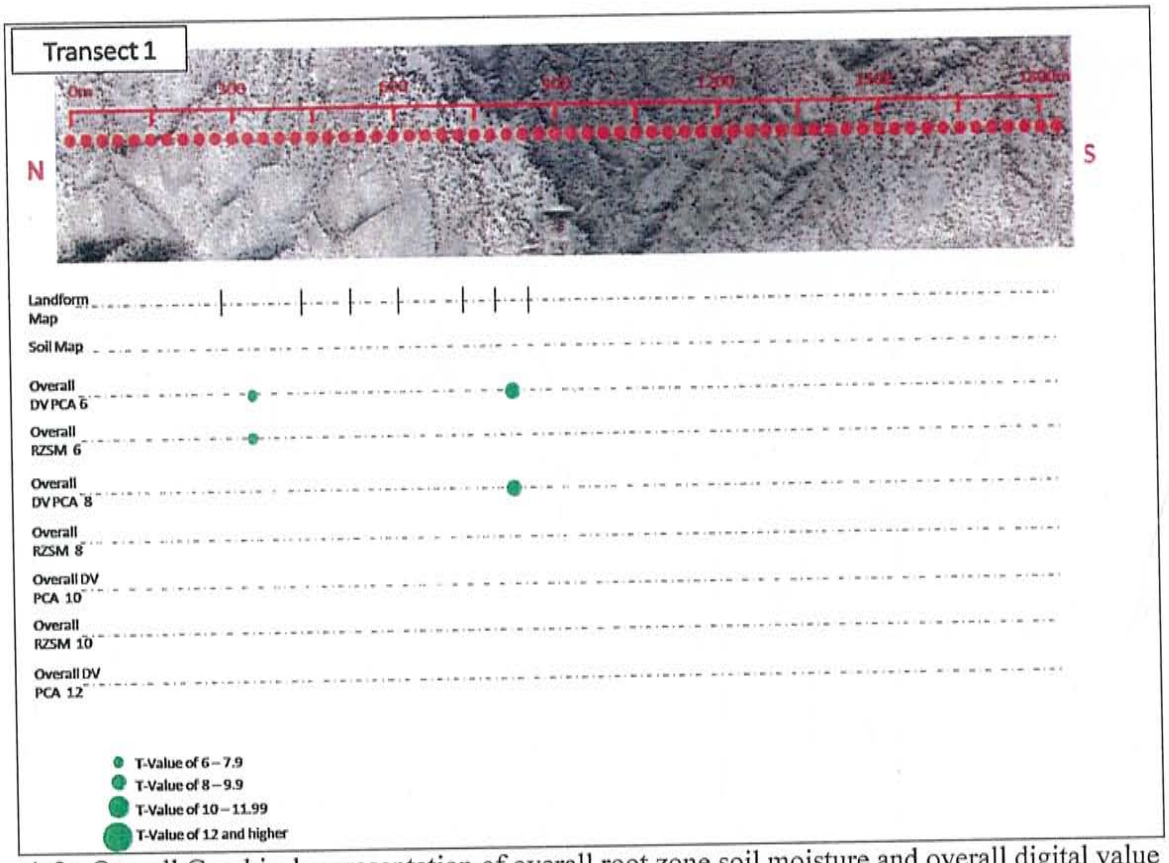

A 3: Overall Graphical representation of overall root zone soil moisture and overall digital value PCA data at critical t-values of 6, 8, 10 and 12 along transect 1. The size of the dot represents the t-value of each boundary

B2

Landform Map Soil Map	Boundary Location (m)									
	330		780	1050 1050	1230					2370
Daily DV PCA 6	350			975	1225	1500		1800	2125	
percentage of days	14.29			35.71	42.86	14.29		7.14	21.43	
range (m)	150			60	180	30		0	30	
Overall DV PCA 6	390				1230	1500	1680		2100	
T-Value	7.2				6.3	6.6	6.3		6.2	
Daily RZSM 6	325	525	800		1300	1530	1680	1860	2025	
percentage of days	28.57	21.43	21.43		42.86	7.14	7.14	7.14	14.29	
range (m)	150	30	90		60	0	0	0	30	
Overall RZSM PCA 6	330	510				1500				
T-Value	6.1	6.3				8.1				
Daily DV PCA 8	240				1100				2100	
percentage of days	14.29				28.57				21.43	
range (m)	0				300				30	
Overall DV PCA 8										
T-Value										
Daily RZSM 8		510	825		1260	1530	1680			
percentage of days		7.14	14.29		7.14	7.14	7.14			
range (m)		0	60		0	0	0			
Overall RZSM PCA 8						1500				
T-Value						8.1				
Daily DV PCA 10									2100	
percentage of days									7.14	
range (m)									0	
Overall DV PCA 10										
T-Value										
Daily RZSM 10			810			1530				
percentage of days			7.14			7.14				
range (m)			0			0				
Overall RZSM PCA 10										
T-Value										
Daily DV PCA 12									2100	
percentage of days									7.14	
range (m)									0	
Overall DV PCA 12										
T-Value										
Daily RZSM 12										
percentage of days										
range (m)										
Overall RZSM PCA 12										
T-Value										

A 4: The summary table of transect 2 includes the locations of the soil and landform boundaries along the transect, the locations, percentage of days and range of boundaries detected by the daily digital values, overall digital value PCA, daily root zone soil moisture and overall root zone soil moisture PCA using a critical t-value of 6, 8, 10 and 12

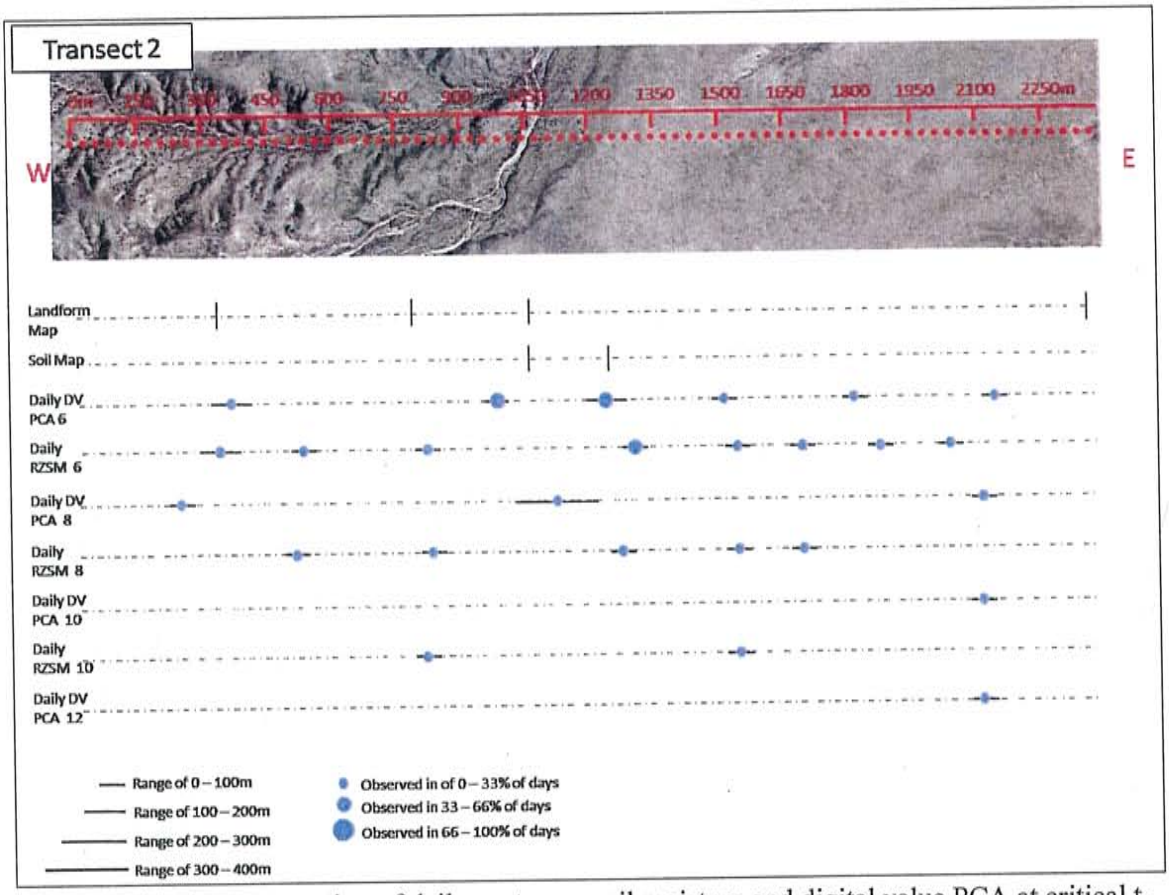

A 5: Graphical representation of daily root zone soil moisture and digital value PCA at critical t-values of 6, 8, 10 and 12 along transect 2. The size of the dot represents the percentage of days the boundary occurs in and the line represents the range over which it occurs.

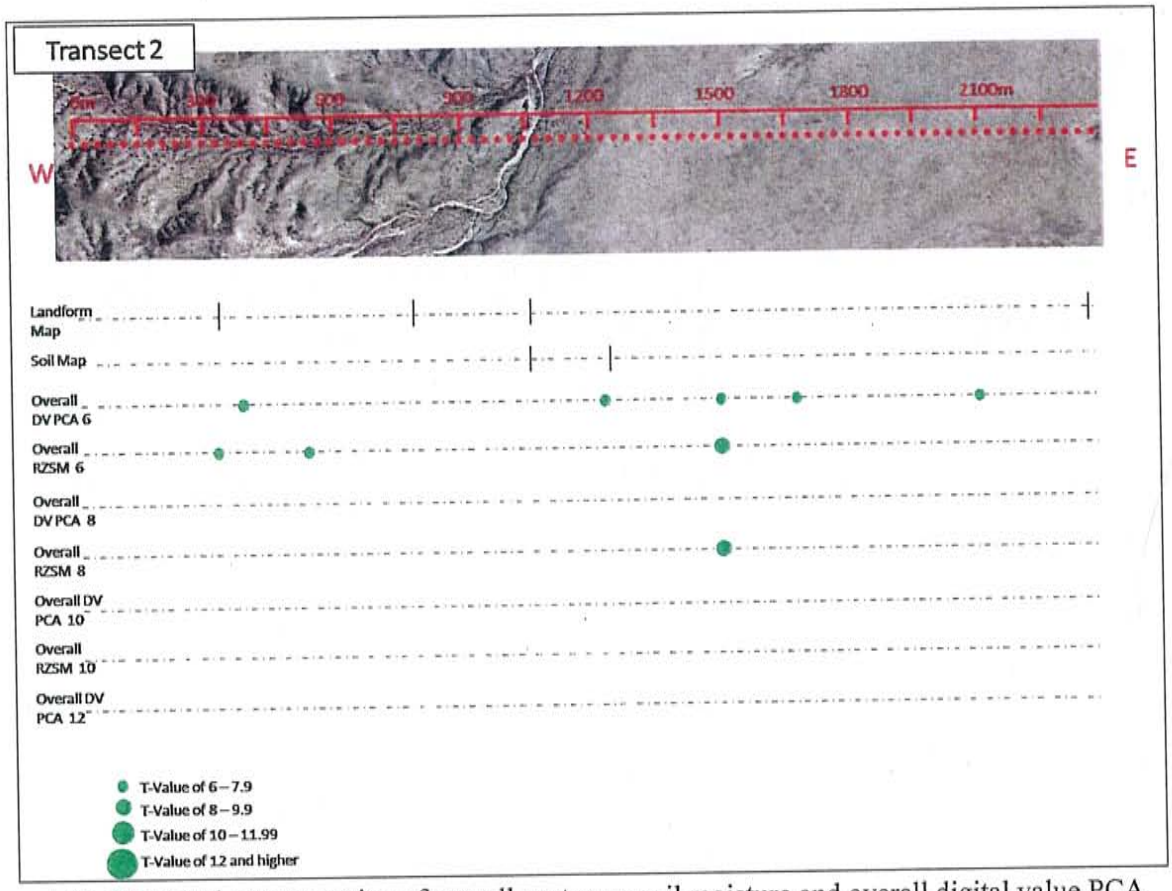

A 6: Graphical representation of overall root zone soil moisture and overall digital value PCA data at critical t-values of 6, 8, 10 and 12 along transect 2. The size of the dot represents the t-value of each boundary

B3

Landform Map / Soil Map	Boundary Location (m)											
	30	120			1200 1230	1620 1560	2010 1950	2310 2310			3240 3240	3450
Daily DV PCA 6 percentage of days range (m)			510 7.14 0	1050 35.71 630		1600 64.29 60	1900 35.71 180	2275 92.86 120	2520 14.29 30	3000 50.00 270		3400 21.43 30
Overall DV PCA 6 T-Value			480 6.4			1590 8.8		2280 7.1	2520 7.3	3000 7.4		3390 9.3
Daily RZSM 6 percentage of days range (m)		125 35.71 0	400 14.29 150	1080 28.57 60	1250 50.00 150	1580 35.71 30		2200 92.86 450	2450 35.71 90	2925 57.14 300	3210 7.14 0	3325 50.00 120
Overall RZSM PCA 6 T-Value		150 7.5	360 6.4	1080 6.8	1260 7.3			2280 6.7	2460 6.1	2970 9.4	3210 7.7	3390 8.7
Daily DV PCA 8 percentage of days range (m)						1550 28.57 30		2250 42.86 330		3000 14.29 60		3360 7.14 0
Overall DV PCA 8 T-Value						1590 8.8						3390 9.3
Daily RZSM 8 percentage of days range (m)		150 7.14 0		1050 7.14 0		1500 28.57 180		2250 57.14 270		2950 28.57 90	3210 7.14 0	3300 21.43 90
Overall RZSM PCA 8 T-Value										2970 9.4		3390 8.7
Daily DV PCA 10 percentage of days range (m)						1590 21.43 30		2280 7.14 0		2970 7.14 0		
Overall DV PCA 10 T-Value												
Daily RZSM 10 percentage of days range (m)						1500 21.43 180		2280 7.14 0		2970 14.29 0		3400 21.43 210
Overall RZSM PCA 10 T-Value												
Daily DV PCA 12 percentage of days range (m)						1560 7.14 0						
Overall DV PCA 12 T-Value												
Daily RZSM 12 percentage of days range (m)						1560 7.14 0		2280 7.14 0		2970 14.29 0		3390 7.14 0
Overall RZSM PCA 12 T-Value												

A 7: The summary table of transect 3 includes the locations of the soil and landform boundaries along the transect, the locations, percentage of days and range of boundaries detected by the daily digital values, overall digital value PCA, daily root zone soil moisture and overall root zone soil moisture PCA using a critical t-value of 6, 8, 10 and 12

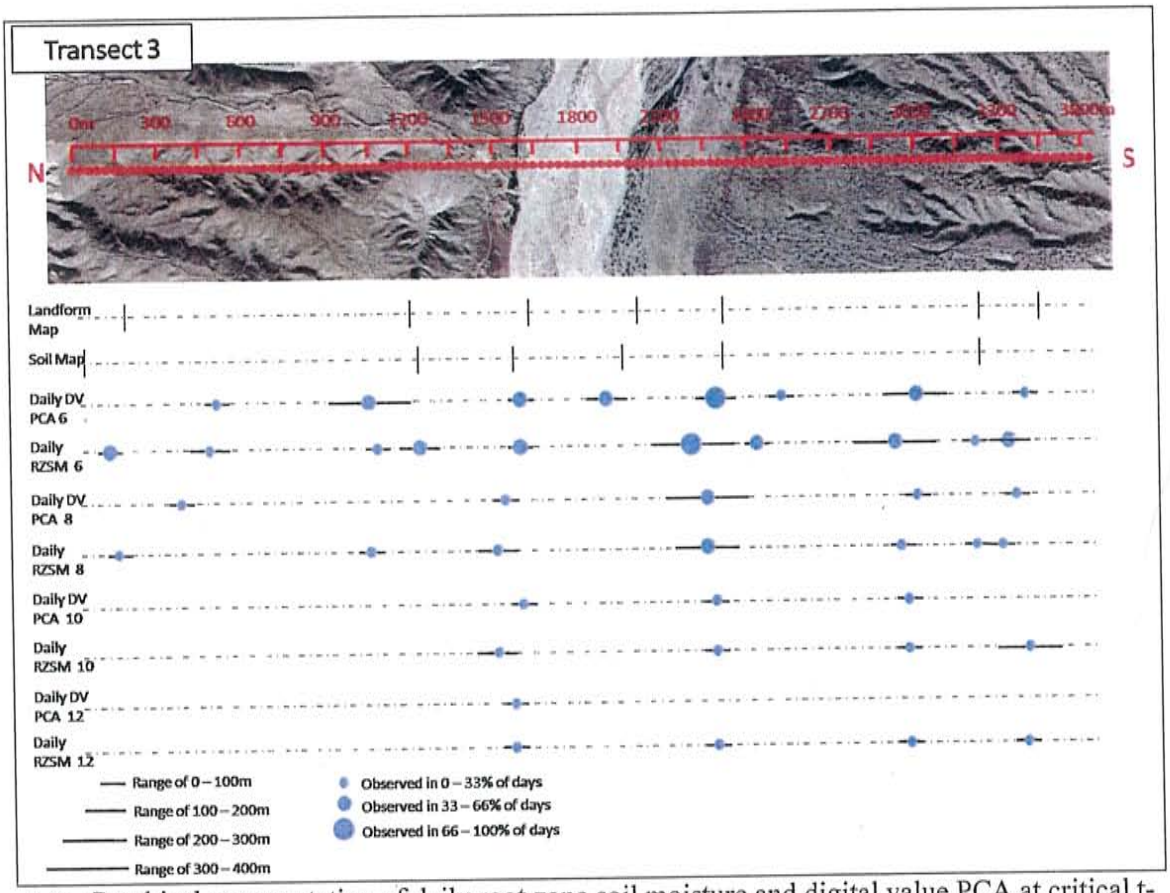

A 8: Graphical representation of daily root zone soil moisture and digital value PCA at critical t-values of 6, 8, 10 and 12 along transect 3. The size of the dot represents the percentage of days the boundary occurs in and the line represents the range over which it occurs.

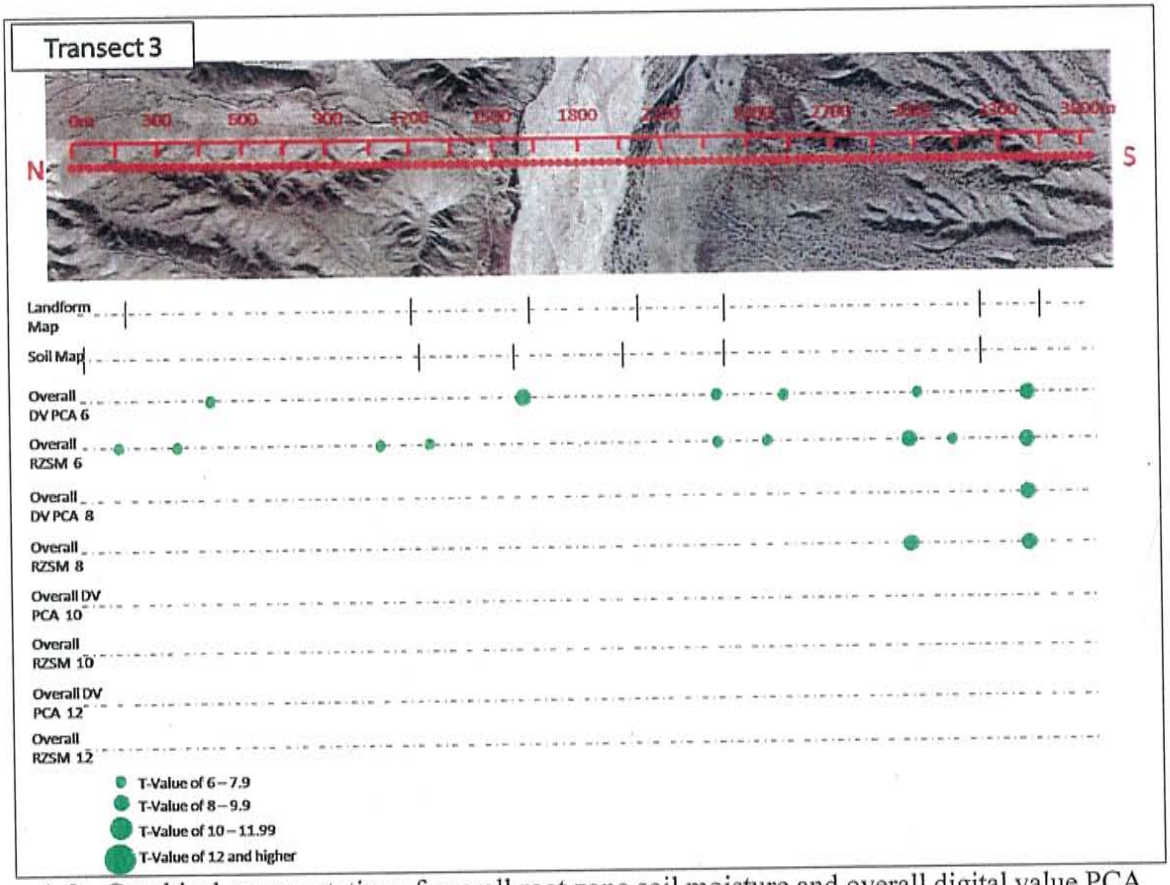

A 9: Graphical representation of overall root zone soil moisture and overall digital value PCA data at critical t-values of 6, 8, 10 and 12 along transect 3. The size of the dot represents the t-value of each boundary

B4

Landform Map / Soil Map	Boundary Location (m)													
	540		1380		1860		2490							
Daily DV PCA 6	300		1290	1650		2100	2340	2640	3060	3400			4600	4980
percentage of days	14.29		50	28.5714		35.7143	7.14286	7.14286	7.14286	21.4286			100	7.14286
range (m)	0		30	60		60	0	0	0	210			270	0
Overall DV PCA 6	300		1290	1680		2130						4500	4650	
T-Value	6		7.1	9.1		9.1						7.7	7.1	
Daily RZSM 6		700	1300	1700		2050		2800	3100	3550	3990	4500		5040
percentage of days		14.2857	42.8571	35.7143		21.4286		28.5714	21.4286	35.7143	7.14286	92.8571		7.14286
range (m)		150	90	180		330		210	180	270	0	540		0
Overall RZSM PCA 6			1290			2100				3270		4500	4680	
T-Value			7.4			7.3				7.1		8	7.2	
Daily DV PCA 8			1290	1650		2130							4700	
percentage of days			7.14286	14.2857		21.4286							21.4286	
range (m)			0	30		30							60	
Overall DV PCA 8				1680		2130								
T-Value				9.1		8.9								
Daily RZSM 8		810	1350	1750				2880	3270	3690		4550		
percentage of days		7.14286	7.14286	21.4286				7.14286	7.14286	7.14286		28.5714		
range (m)		0	0	180				0	0	0		390		
Overall RZSM PCA 8												4500		
T-Value												8		
Daily DV PCA 10				1650										
percentage of days				7.14286										
range (m)				0										
Overall DV PCA 10														
T-Value														
Daily RZSM 10				1770					3270					
percentage of days				7.14286					7.14286					
range (m)				0					0					
Overall RZSM PCA 10														
T-Value														
Daily DV PCA 12														
percentage of days														
range (m)														
Overall DV PCA 12														
T-Value														
Daily RZSM 12														
percentage of days														
range (m)														
Overall RZSM PCA 12														
T-Value														

A 10: The summary table of transect 4 includes the locations of the soil and landform boundaries along the transect, the locations, percentage of days and range of boundaries detected by the daily digital values, overall digital value PCA, daily root zone soil moisture and overall root zone soil moisture PCA using a critical t-value of 6, 8, 10 and 12

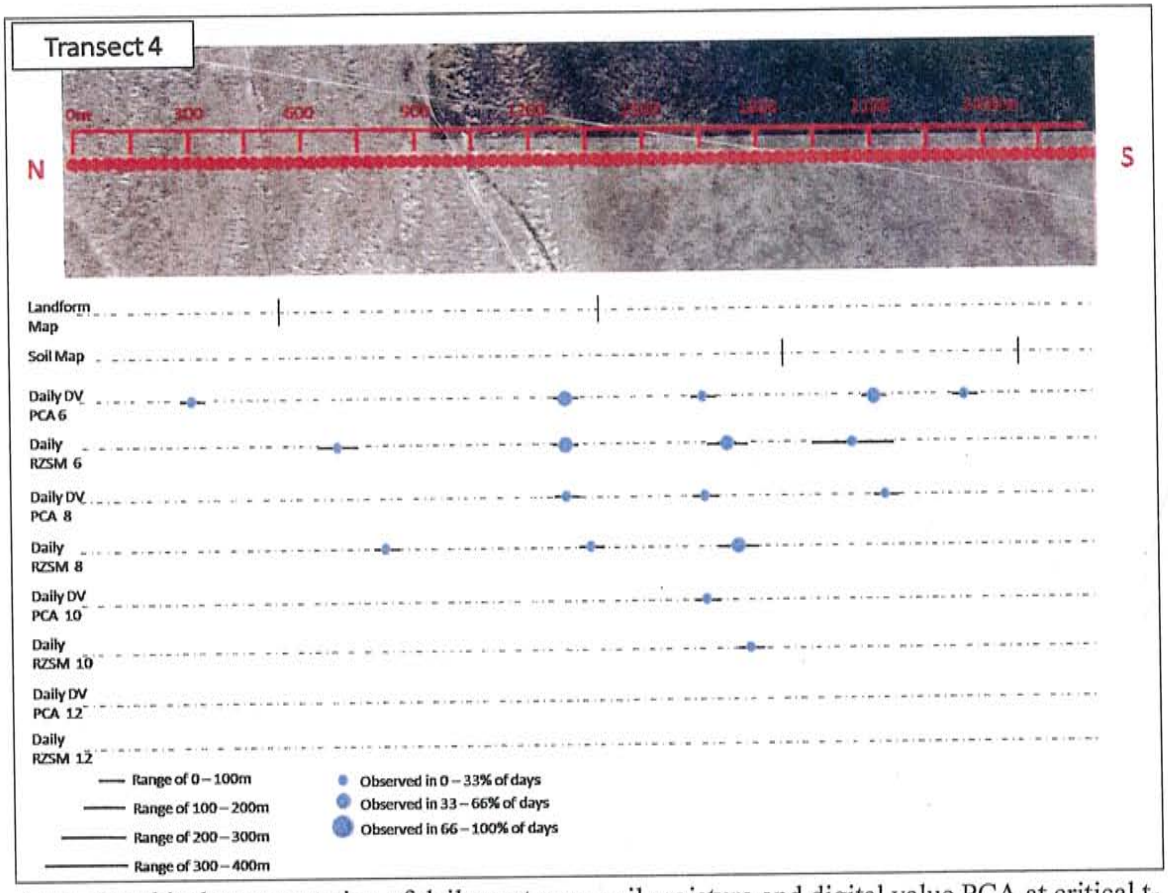

A 11: Graphical representation of daily root zone soil moisture and digital value PCA at critical t-values of 6, 8, 10 and 12 along the first half of transect 4 The size of the dot represents the percentage of days the boundary occurs in and the line represents the range over which it occurs. This illustrates how the root zone soil moisture often detects more scatter than the digital values

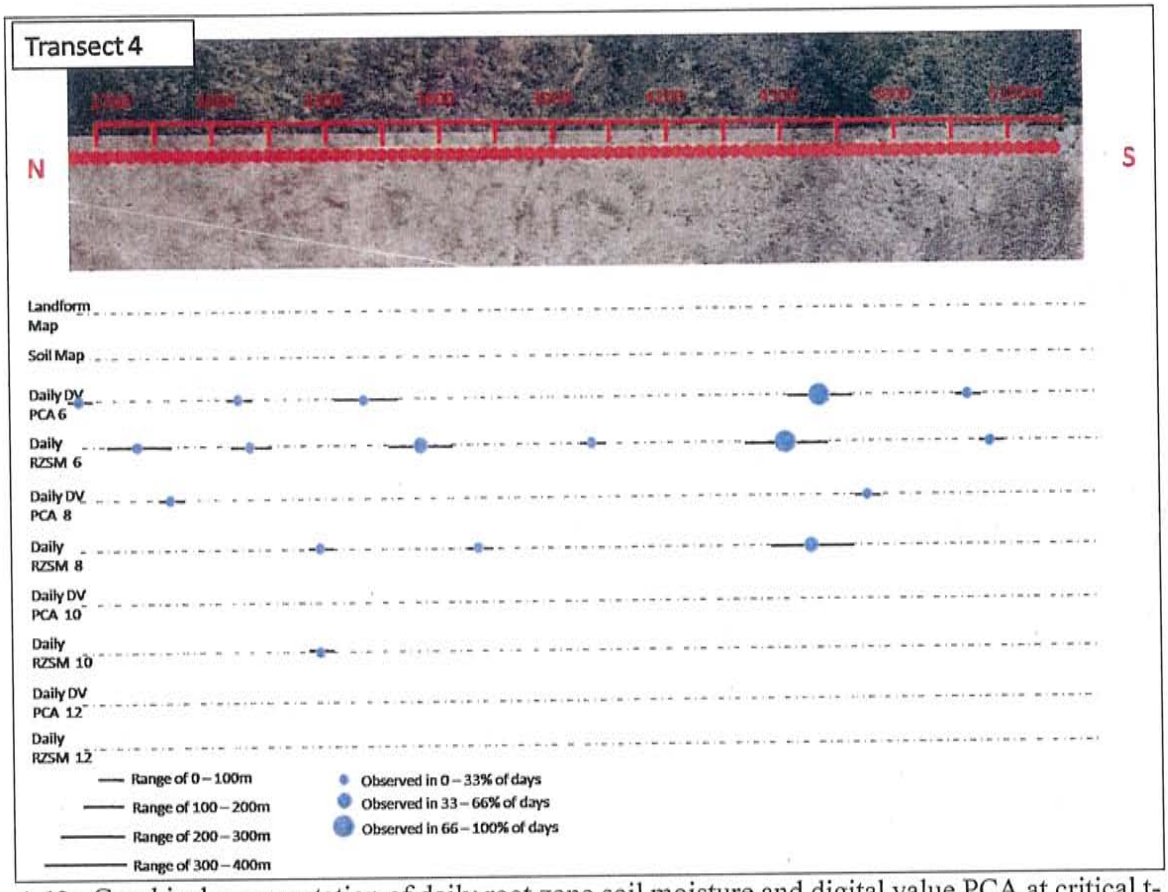

A 12: Graphical representation of daily root zone soil moisture and digital value PCA at critical t-values of 6, 8, 10 and 12 along the second half of transect 4 The size of the dot represents the percentage of days the boundary occurs in and the line represents the range over which it occurs.

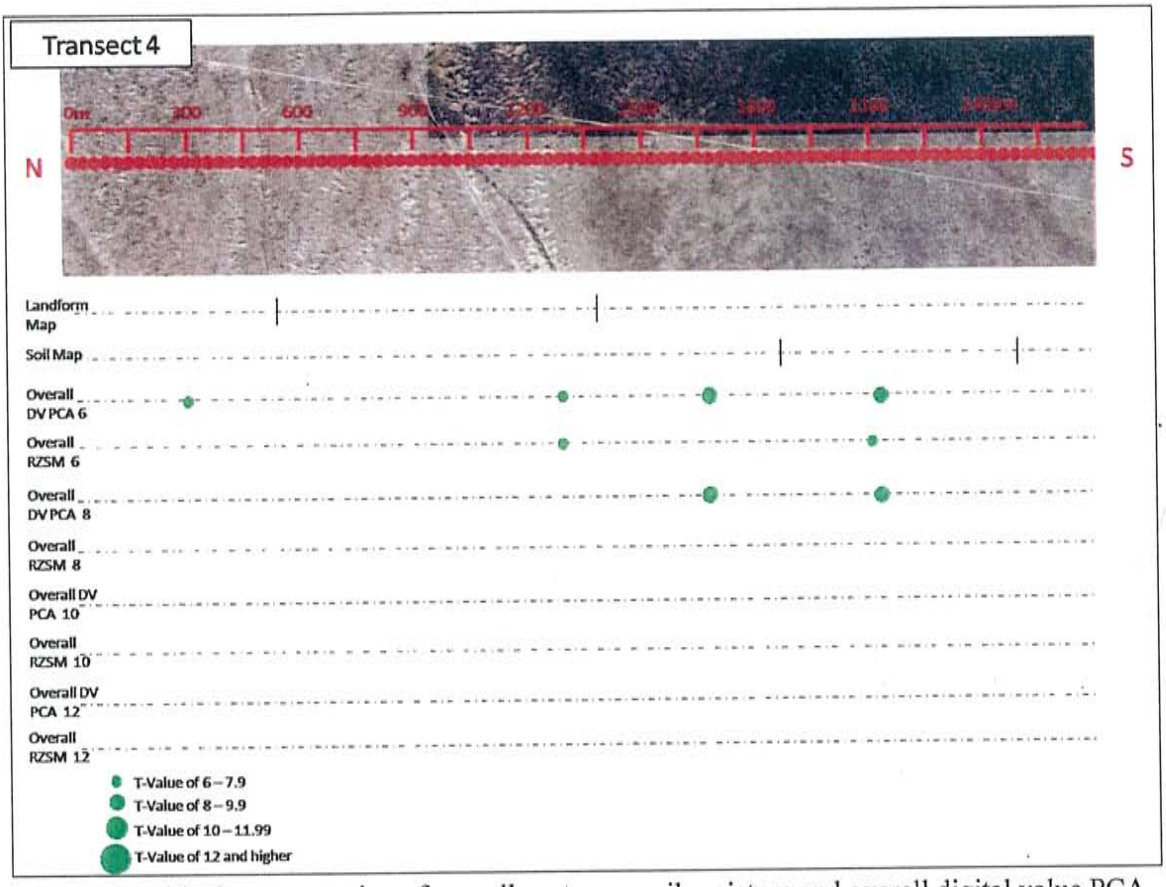

A 13: Graphical representation of overall root zone soil moisture and overall digital value PCA data at critical t-values of 6, 8, 10 and 12 along the first half of transect 4. The size of the dot represents the t-value of each boundary

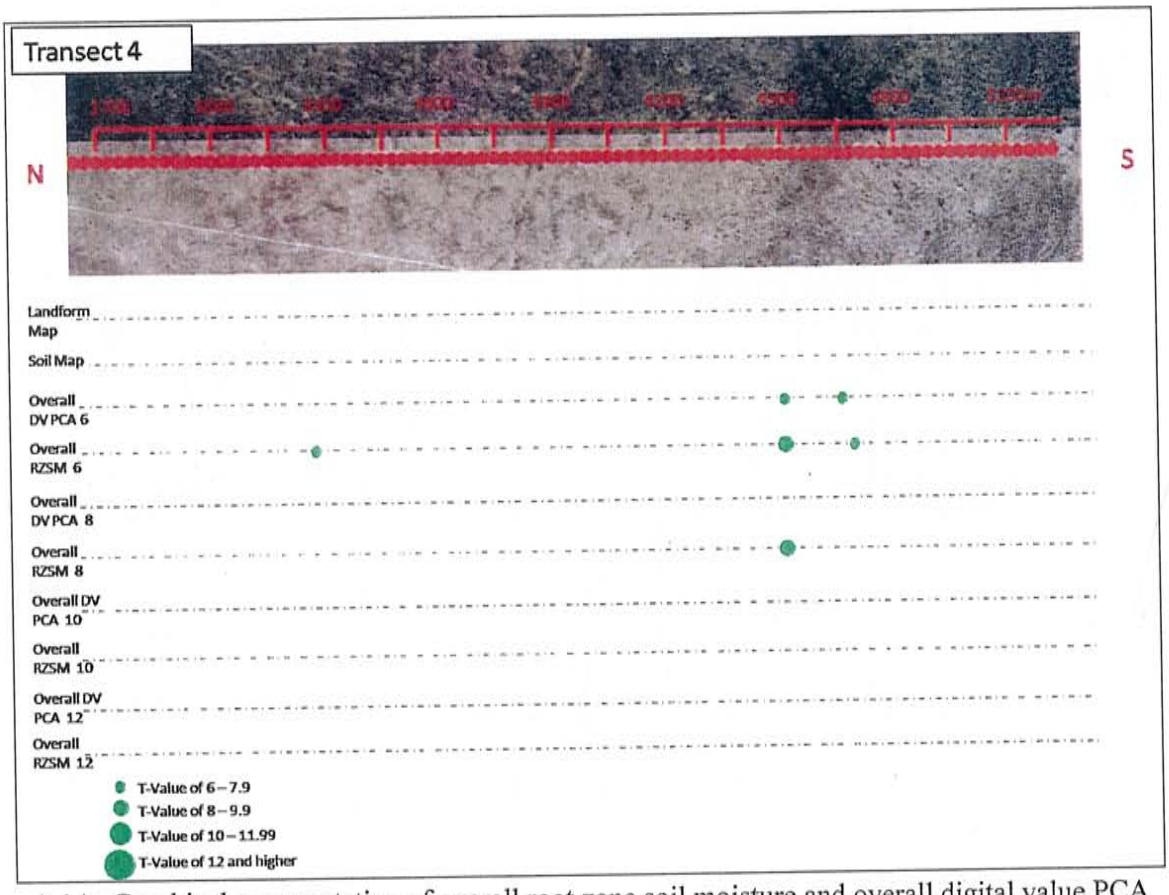

A 14: Graphical representation of overall root zone soil moisture and overall digital value PCA data at critical t-values of 6, 8, 10 and 12 along the second half of transect 4. The size of the dot represents the t-value of each boundary

B5

Landform Map / Soil Map	Boundary Location (m)												
		270				1140				2220	2670 2670		3150 3030
Daily DV PCA 6 percentage of days range (m)	180 14.29 0		500 28.57 60	750 7.14 0	950 28.57 60	1175 28.57 240		1850 21.43 120		2225 50.00 210	2500 42.86 210	2800 28.57 150	3150 85.71 210
Overall DV PCA 6 T-Value	180 9.8		510 7.1		930 6.3								3150 7
Daily RZSM 6 percentage of days range (m)		350 14.29 30	550 14.29 0	800 35.7143 150		1100 28.5714 150		1680 7.14 0	2000 35.7143 180		2450 57.1429 240	2800 35.7143 120	3050 57.1429 60
Overall RZSM PCA 6 T-Value				870 6.1							2520 8.3	2820 8.3	3120 9.2
Daily DV PCA 8 percentage of days range (m)	180 7.14 0		500 21.4286 30				1290 7.14 0	1850 14.29 90		2200 14.29 150	2460 7.14 0	2800 14.29 150	3150 14.29 180
Overall DV PCA 8 T-Value	180 9.8												
Daily RZSM 8 percentage of days range (m)		330 7.14 0	540 7.14 0			1100 14.29 0		1680 7.14 0		2100 7.14 0	2500 14.29 30	2800 14.29 0	3100 35.7143 60
Overall RZSM PCA 8 T-Value											2520 8.3	2820 8.3	3120 9.2
Daily DV PCA 10 percentage of days range (m)	180 7.14 0		510 7.14 0					1800 7.14 0				2790 7.14 0	3120 14.29 0
Overall DV PCA 10 T-Value													
Daily RZSM 10 percentage of days range (m)						1100 7.14 0					2500 14.29 30	2820 7.14 0	3120 7.14 0
Overall RZSM PCA 10 T-Value													
Daily DV PCA 12 percentage of days range (m)													3120 7.14 0
Overall DV PCA 12 T-Value													
Daily RZSM 12 percentage of days range (m)											2490 7.14 0	2820 7.14 0	3120 7.14 0
Overall RZSM PCA 12 T-Value													

A 15: The summary table of transect 5 includes the locations of the soil and landform boundaries along the transect, the locations, percentage of days and range of boundaries detected by the daily digital values, overall digital value PCA, daily root zone soil moisture and overall root zone soil moisture PCA using a critical t-value of 6, 8, 10 and 12

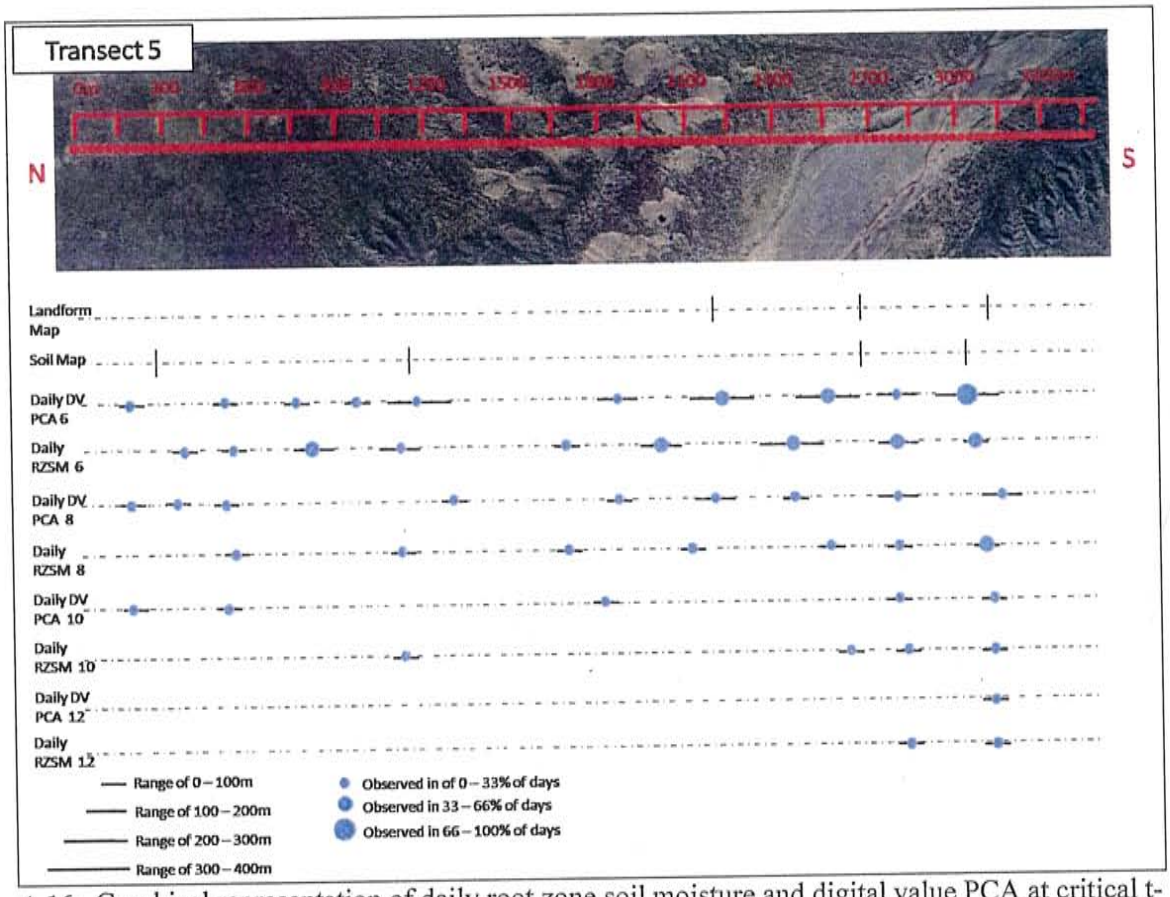

A 16: Graphical representation of daily root zone soil moisture and digital value PCA at critical t-values of 6, 8, 10 and 12 along transect 5 The size of the dot represents the percentage of days the boundary occurs in and the line represents the range over which it occurs.

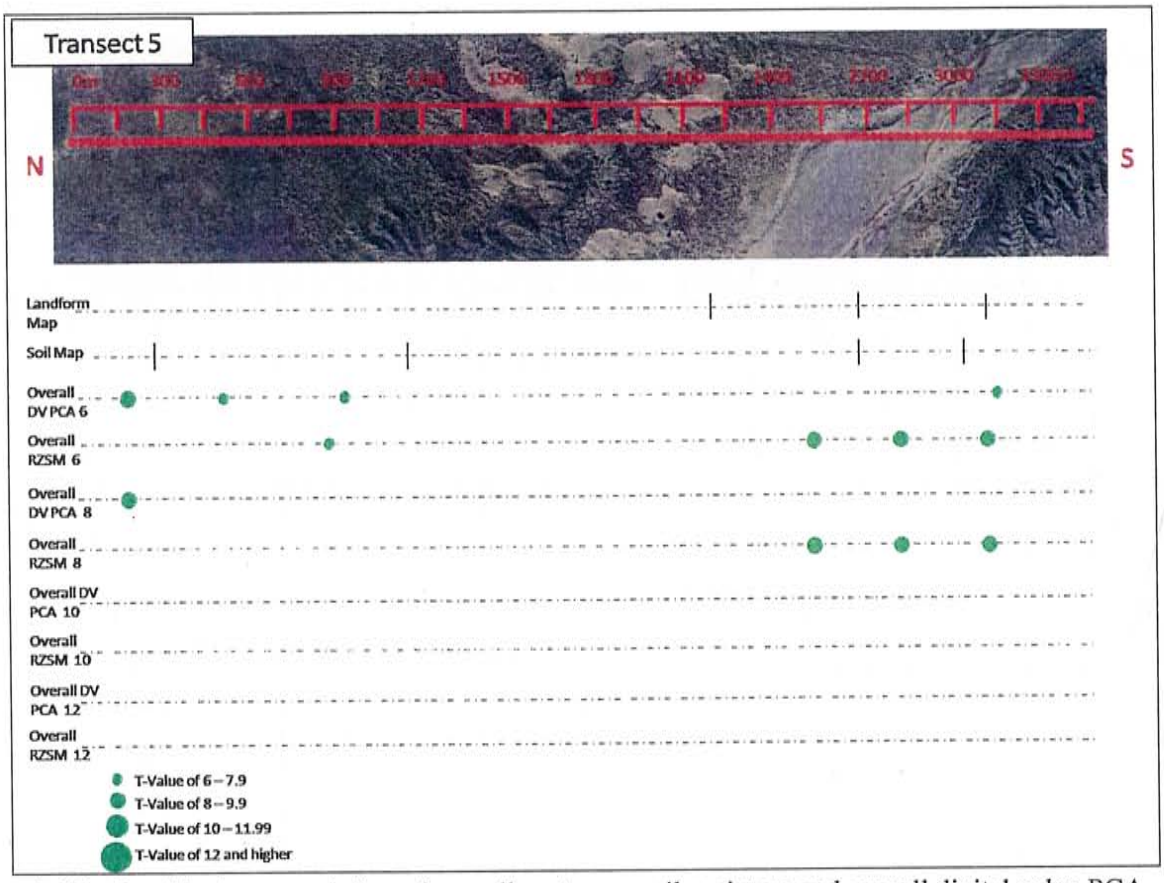

A 17: Graphical representation of overall root zone soil moisture and overall digital value PCA data at critical t-values of 6, 8, 10 and 12 along transect 5. The size of the dot represents the t-value of each boundary

B6

	Boundary Location (m)													
Landform Map Soil Map	150	210		960 930	1200	1500	1680	1800 1800	2100		2850 2070	3030 2970	3060	3120
Daily DV PCA 6 percentage of days range (m)		250 28.57 210	650 35.71 60	950 57.14 180	1300 57.14 180		1700 35.71 210		2150 71.43 180		2750 35.71 90			
Overall DV PCA 6 T-Value	180 6			990 7.9	1290 17.1		1680 6.9		2190 7.9					
Daily RZSM 6 percentage of days range (m)		360 7.14 0	750 28.57 120	950 78.57 300			1600 21.43 30		2050 35.71 180	2250 21.43 60	2750 21.43 210			
Overall RZSM PCA 6 T-Value									2040 6.2					
Daily DV PCA 8 percentage of days range (m)				1000 21.43 180	1300 21.43 30				2100 21.43 90		2760 7.14 0			
Overall DV PCA 8 T-Value					1290 17.1									
Daily RZSM 8 percentage of days range (m)				900 21.43 150					2010 7.14 0	2280 7.14 0				
Overall RZSM PCA 8 T-Value														
Daily DV PCA 10 percentage of days range (m)					1290 7.14 0									
Overall DV PCA 10 T-Value					1290 17.1									
Daily RZSM 10 percentage of days range (m)				1050 7.14 0										
Overall RZSM PCA 10 T-Value														
Daily DV PCA 12 percentage of days range (m)														
Overall DV PCA 12 T-Value					1290 17.1									
Daily RZSM 12 percentage of days range (m)														
Overall RZSM PCA 12 T-Value														

A 18: The summary table of transect 6 includes the locations of the soil and landform boundaries along the transect, the locations, percentage of days and range of boundaries detected by the daily digital values, overall digital value PCA, daily root zone soil moisture and overall root zone soil moisture PCA using a critical t-value of 6, 8, 10 and 12

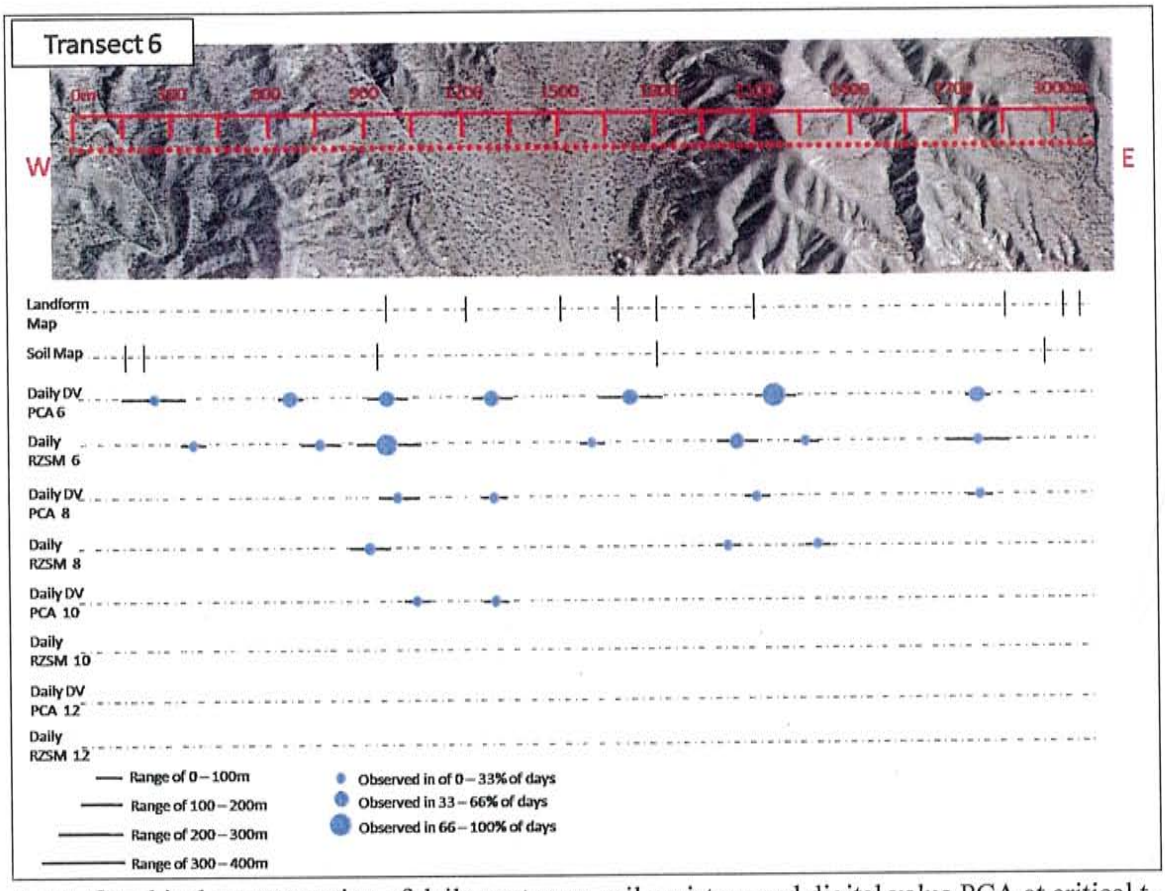

A 19: Graphical representation of daily root zone soil moisture and digital value PCA at critical t-values of 6, 8, 10 and 12 along transect 6 The size of the dot represents the percentage of days the boundary occurs in and the line represents the range over which it occurs.

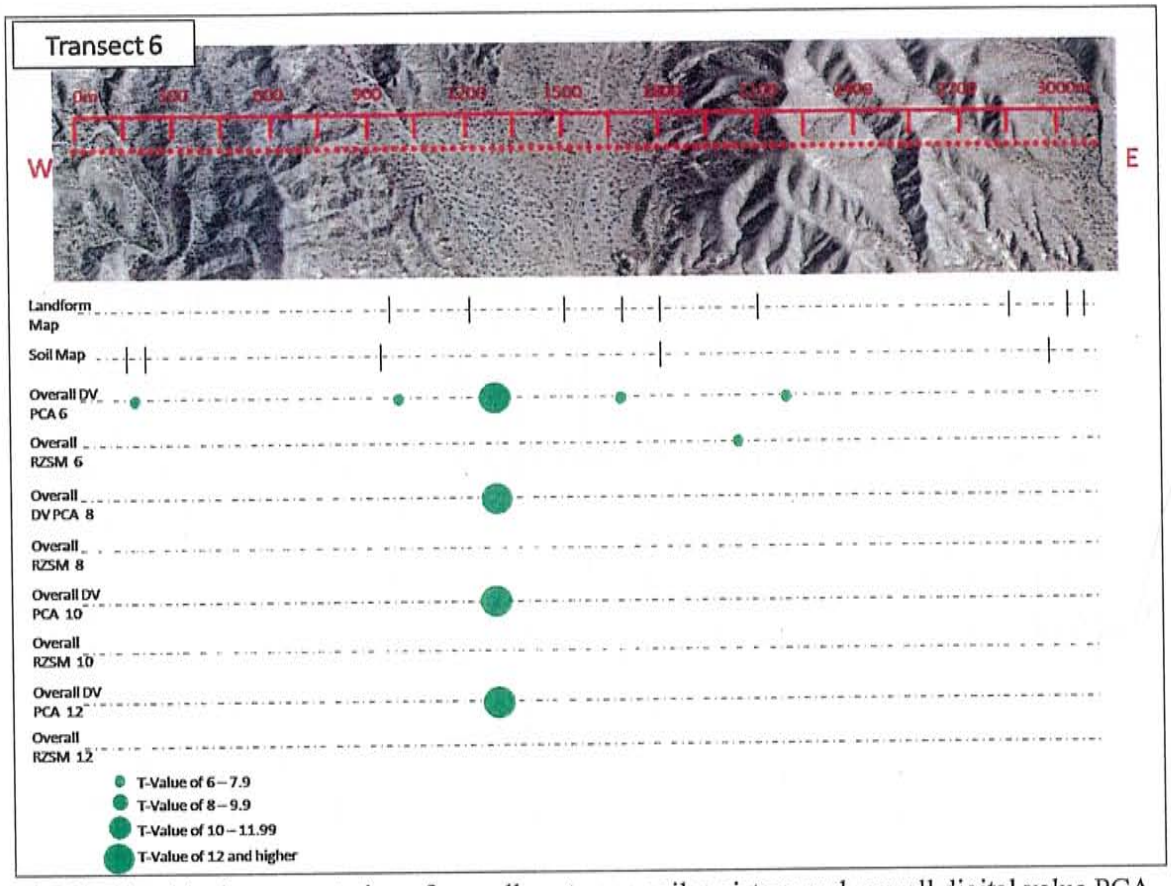

A 20: Graphical representation of overall root zone soil moisture and overall digital value PCA data at critical t-values of 6, 8, 10 and 12 along transect 6. The size of the dot represents the t-value of each boundary

B7

Landform Map / Soil Map	Boundary Location (m)														
	180	390		870	1170 990				2400			3180 3210		3600
Daily DV PCA 6 percentage of days range (m)		350 35.71 210		600 85.71 210	1000 92.86 270		1550 21.43 60		2000 14.29 90	2300 71.43 270			3200 35.71 90		
Overall DV PCA 6 T-Value		330 7.7	480 6.3	690 6.4			1530 6.2			2280 6.4		3090 6.1			
Daily RZSM 6 percentage of days range (m)		350 28.57 0		675 50.00 90	925 78.57 150	1250 21.43 60	1500 14.29 30	1650 35.71 300	2175 14.29 60	2375 57.14 90	2650 14.29 0	2940 7.14 0	3120 28.57 0	3300 85.71 60	
Overall RZSM PCA 6 T-Value		360 7.1			1020 8.3		1500 6.7			2340 7.6		2940 6.5	3150 6.6	3300 9.1	
Daily DV PCA 8 percentage of days range (m)				650 14.29 30	1050 42.86 270		1560 7.14 0		1950 7.14 0	2450 21.43 180				3300 21.43 450	
Overall DV PCA 8 T-Value															
Daily RZSM 8 percentage of days range (m)		350 21.43 0		700 14.29 30	950 50.00 90	1230 7.14 0	1500 14.29 90		2200 14.29 60	2400 28.57 60		2940 7.14 0	3120 7.14 0	3300 50.00 30	
Overall RZSM PCA 8 T-Value					1020 8.3									3300 9.1	
Daily DV PCA 10 percentage of days range (m)					1000 14.29 60				1950 7.14 0	2400 7.14 0		2970 7.14 0		3420 7.14 0	
Overall DV PCA 10 T-Value															
Daily RZSM 10 percentage of days range (m)				720 7.14 0	1050 28.57 90		1590 7.14 0							3300 14.29 0	
Overall RZSM PCA 10 T-Value															
Daily DV PCA 12 percentage of days range (m)										2400 7.14 0					
Overall DV PCA 12 T-Value															
Daily RZSM 12 percentage of days range (m)				720 7.14 0	1020 14.29 0									3300 7.14 0	
Overall RZSM PCA 12 T-Value															

A 21: The summary table of transect 7 includes the locations of the soil and landform boundaries along the transect, the locations, percentage of days and range of boundaries detected by the daily digital values, overall digital value PCA, daily root zone soil moisture and overall root zone soil moisture PCA using a critical t-value of 6, 8, 10 and 12

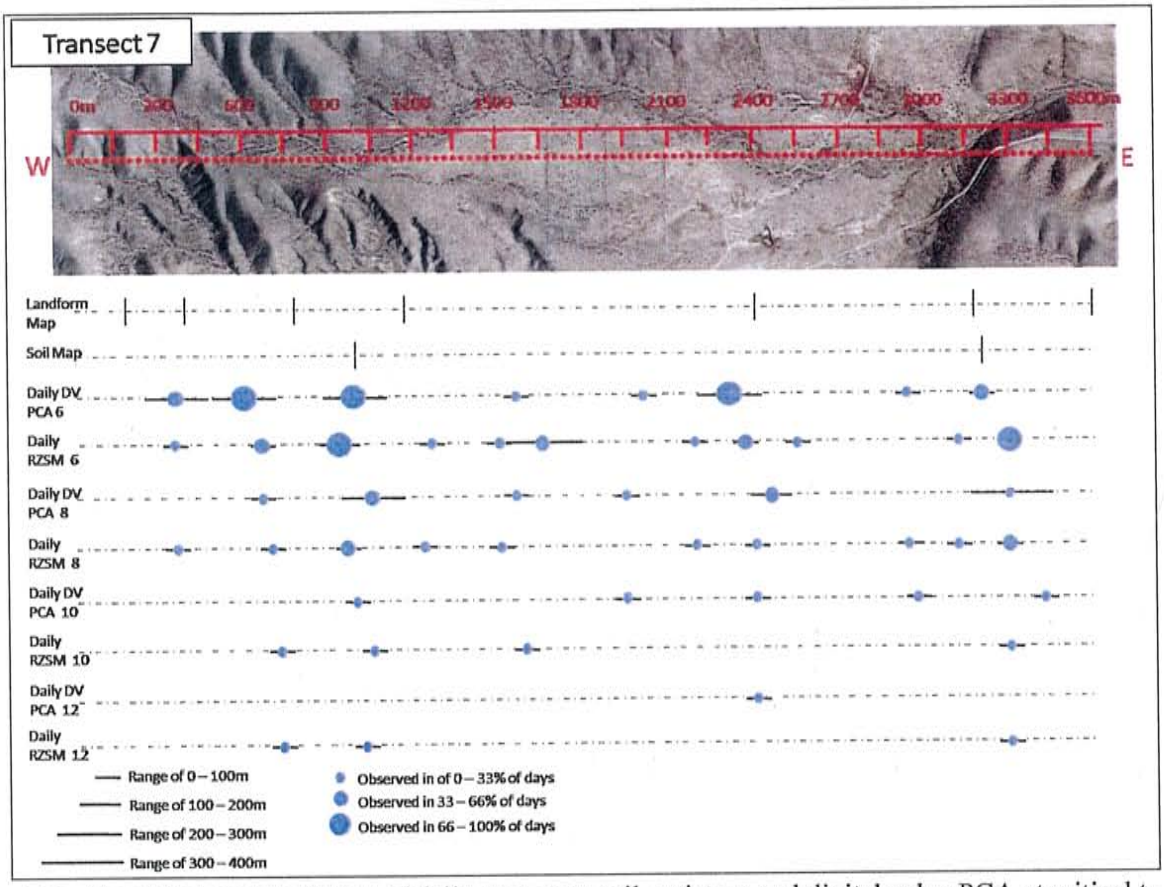

A 22: Graphical representation of daily root zone soil moisture and digital value PCA at critical t-values of 6, 8, 10 and 12 along transect 7 The size of the dot represents the percentage of days the boundary occurs in and the line represents the range over which it occurs

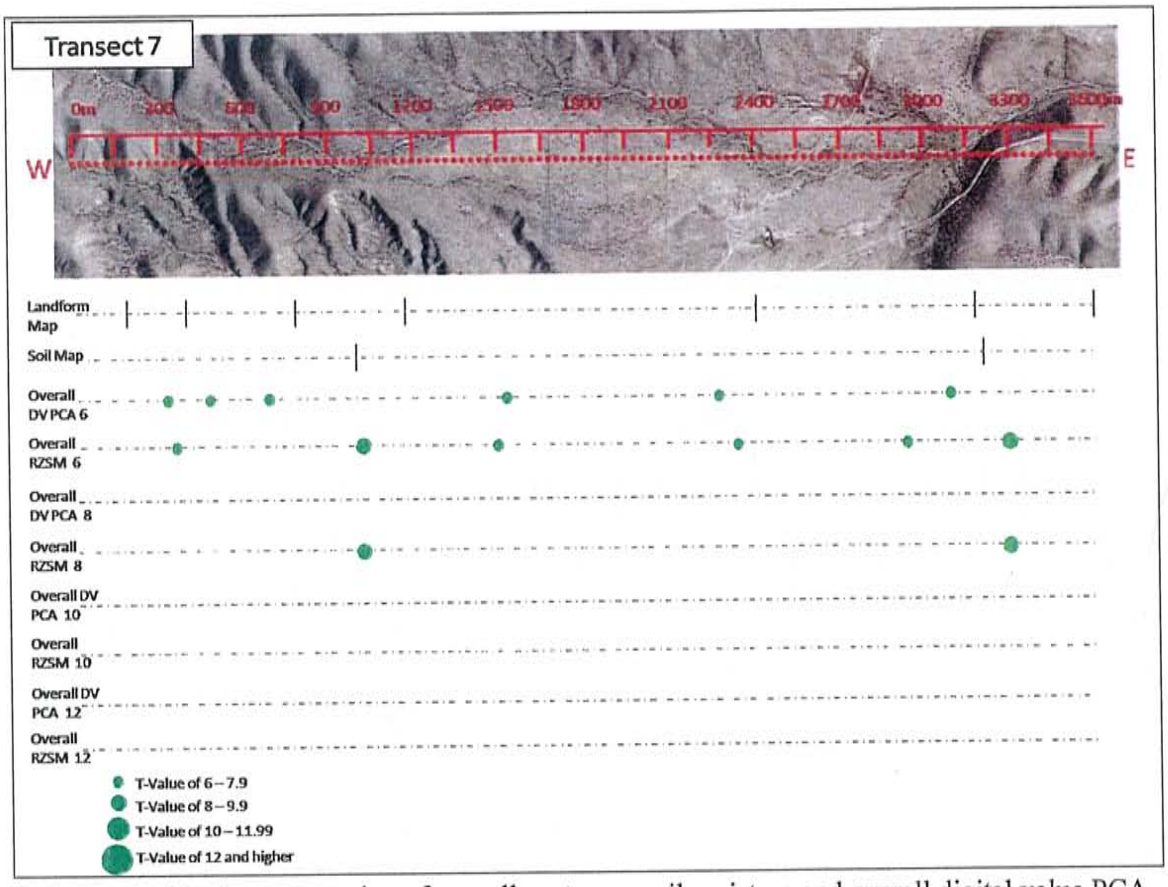

A 23: Graphical representation of overall root zone soil moisture and overall digital value PCA data at critical t-values of 6, 8, 10 and 12 along transect 7. The size of the dot represents the t-value of each boundary

B8

Landform Map Soil Map	Boundary Location (m)														
				1950 1860	2190				3240 3120	3420		3870	3990 3990	4200	
Daily DV PCA 6	200		1530	1825	2100	2300	2600	2900		3400	3600	3725	3950	4300	
percentage of days	71.43		7.14	50.00	50.00	21.43	21.43	100.00		35.71	28.57	71.43	50.00	50.00	
range (m)	810		0	90	120	240	30	360		180	60	90	120	60	
Overall DV PCA 6	420			1860	2100	2280	2610	3060		3360	3660	3780	3990	4230	
T-Value	7.9			6.9	6.3	6.2	15	9.3		6.8	6.8	7.2	6.3	8.2	
Daily RZSM 6	225	1000		1800	2250		2700	2940		3375	3570	3775	4050	4200	
percentage of days	21.43	35.71		57.14	35.71		21.43	7.14		57.14	7.14	21.43	14.29	35.71	
range (m)	180	420		330	120		120	0		300	0	60	120	30	
Overall RZSM PCA 6	270			1860						3360	3540	3780		4230	
T-Value	7.3			6.6						6.2	6.8	7.3		8.6	
Daily DV PCA 8	400		1530		2100		2640		3100	3400		3750		4230	
percentage of days	28.57		7.14		14.29		7.14		28.57	14.29		14.29		7.14	
range (m)	210		0		120		0		0	30		30		0	
Overall DV PCA 8							2610	3060						4230	
T-Value							15	9.3						8.2	
Daily RZSM 8				1860		2300	2700	2940	3200			3780	4020	4225	
percentage of days				7.14		14.29	7.14	7.14	14.29			7.14	7.14	21.43	
range (m)				0		60	0	0	240			0	0	0	
Overall RZSM PCA 8														4230	
T-Value														8.6	
Daily DV PCA 10	450						2640			3390		3720			
percentage of days	7.14						7.14			7.14		7.14			
range (m)	0						0			0		0			
Overall DV PCA 10							2610								
T-Value							15								
Daily RZSM 10						2310	2700	2940		3330		3780			
percentage of days						7.14	7.14	7.14		7.14		7.14			
range (m)						0	0	0		0		0			
Overall RZSM PCA 10															
T-Value															
Daily DV PCA 12	450						2640			3390		3720			
percentage of days	7.14						7.14			7.14		7.14			
range (m)	0						0			0		0			
Overall DV PCA 12							2620								
T-Value							15								
Daily RZSM 12						2310				3330		3780			
percentage of days						7.14				7.14		7.14			
range (m)						0				0		0			
Overall RZSM PCA 12															
T-Value															

A 24: The summary table of transect 8 includes that locations of the soil and landform boundaries along the transect, the locations, percentage of days and range of boundaries detected by the daily digital values, overall digital value PCA, daily root zone soil moisture and overall root zone soil moisture PCA using a critical t-value of 6, 8, 10 and 12

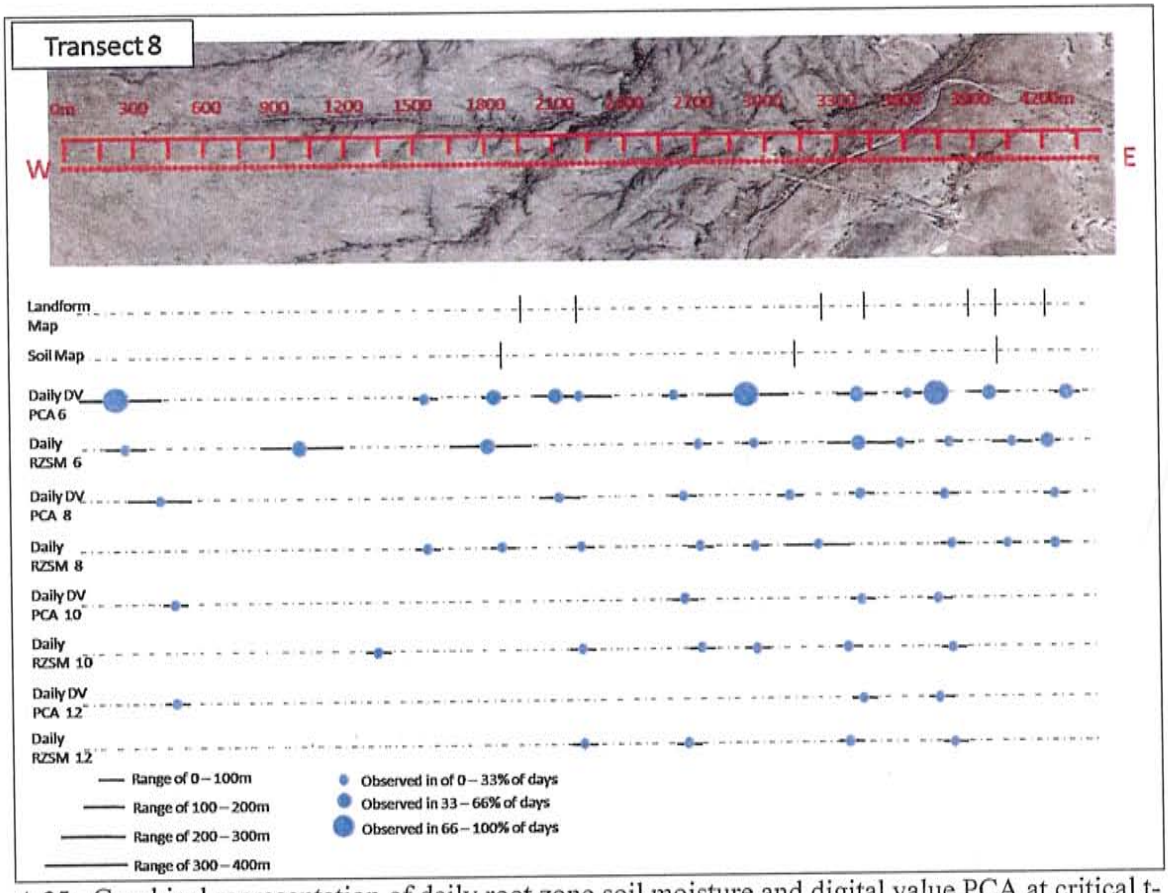

A 25: Graphical representation of daily root zone soil moisture and digital value PCA at critical t-values of 6, 8, 10 and 12 along transect 8 The size of the dot represents the percentage of days the boundary occurs in and the line represents the range over which it occurs.

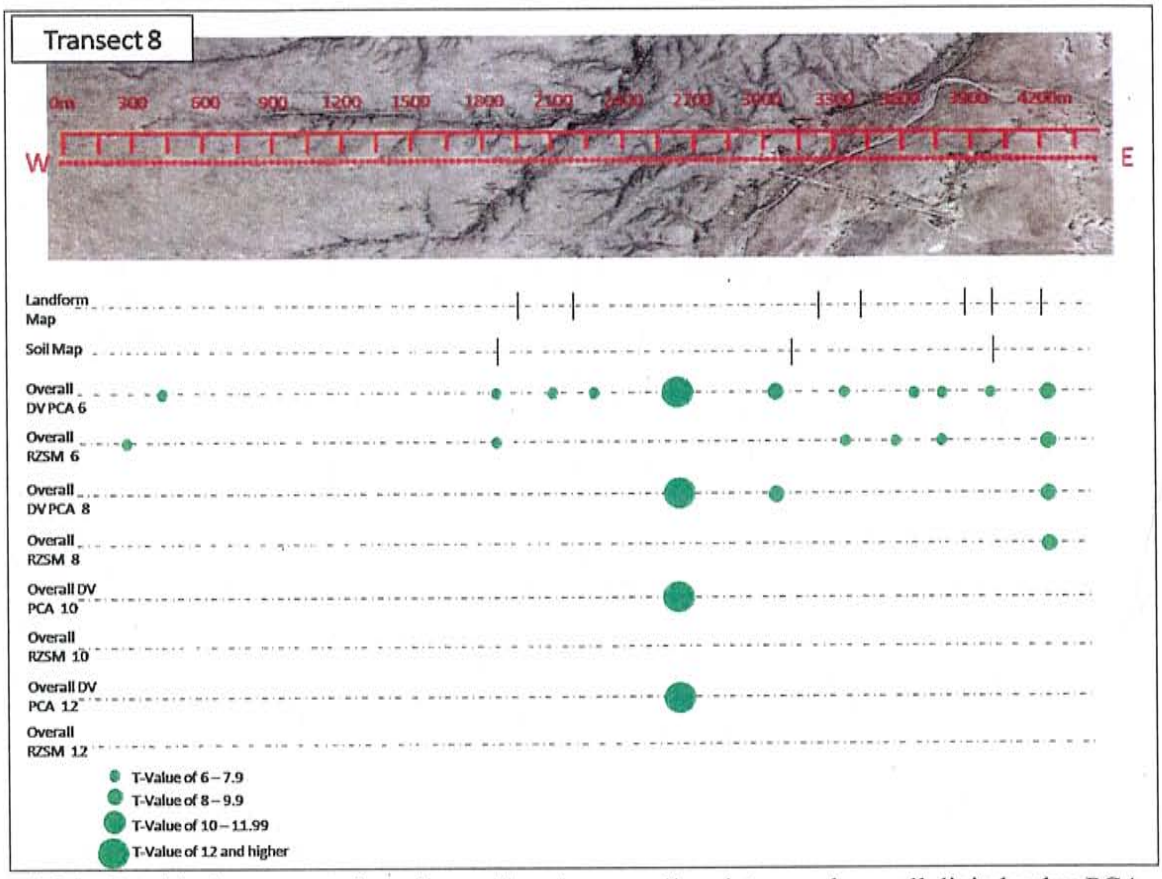

A 26: Graphical representation of overall root zone soil moisture and overall digital value PCA data at critical t-values of 6, 8, 10 and 12 along transect 8. The size of the dot represents the t-value of each boundary

B9

Landform Map Soil Map	Boundary Location (m)										
	120		810		1410	1530	1800 1980			3090	3540
Daily DV PCA 6 percentage of days range (m)	210 7.14 0	650 50.00 180		1020 7.14 0	1450 71.43 150		1850 35.71 210	2100 42.86 240	2600 71.43 210	3000 85.71 240	3500 14.29 90
Overall DV PCA 6 T-Value		510 6.9	780 6.6		1470 7.6		1770 7.6		2580 6.5	3000 6.6	3510 11
Daily RZSM 6 percentage of days range (m)		660 7.14 0		1020 7.14 0		1500 14.29 0		2075 35.71 330	2600 42.86 240	3125 35.71 300	3600 21.43 300
Overall RZSM PCA 6 T-Value							1920 8.1		2610 7.8	3030 6.3	3690 6
Daily DV PCA 8 percentage of days range (m)			750 7.14 0			1500 28.57 150	1800 28.57 120		2600 28.57 210	3030 14.29 0	3600 7.14 0
Overall DV PCA 8 T-Value											3510 11.2
Daily RZSM 8 percentage of days range (m)								2150 21.43 240	2600 14.29 240	3180 7.14 0	
Overall RZSM PCA 8 T-Value							1920 8.1				
Daily DV PCA 10 percentage of days range (m)			750 7.14 0			1500 7.14 0	1740 7.14 0		2580 7.14 0	3030 7.14 0	
Overall DV PCA 10 T-Value											3510 11.2
Daily RZSM 10 percentage of days range (m)								2220 7.14 0			
Overall RZSM PCA 10 T-Value											
Daily DV PCA 12 percentage of days range (m)							1740 7.14 0			3030 7.14 0	
Overall DV PCA 12 T-Value											
Daily RZSM 12 percentage of days range (m)											
Overall RZSM PCA 12 T-Value											

A 27: The summary table of transect 9 includes the locations of the soil and landform boundaries along the transect, the locations, percentage of days and range of boundaries detected by the daily digital values, overall digital value PCA, daily root zone soil moisture and overall root zone soil moisture PCA using a critical t-value of 6, 8, 10 and 12

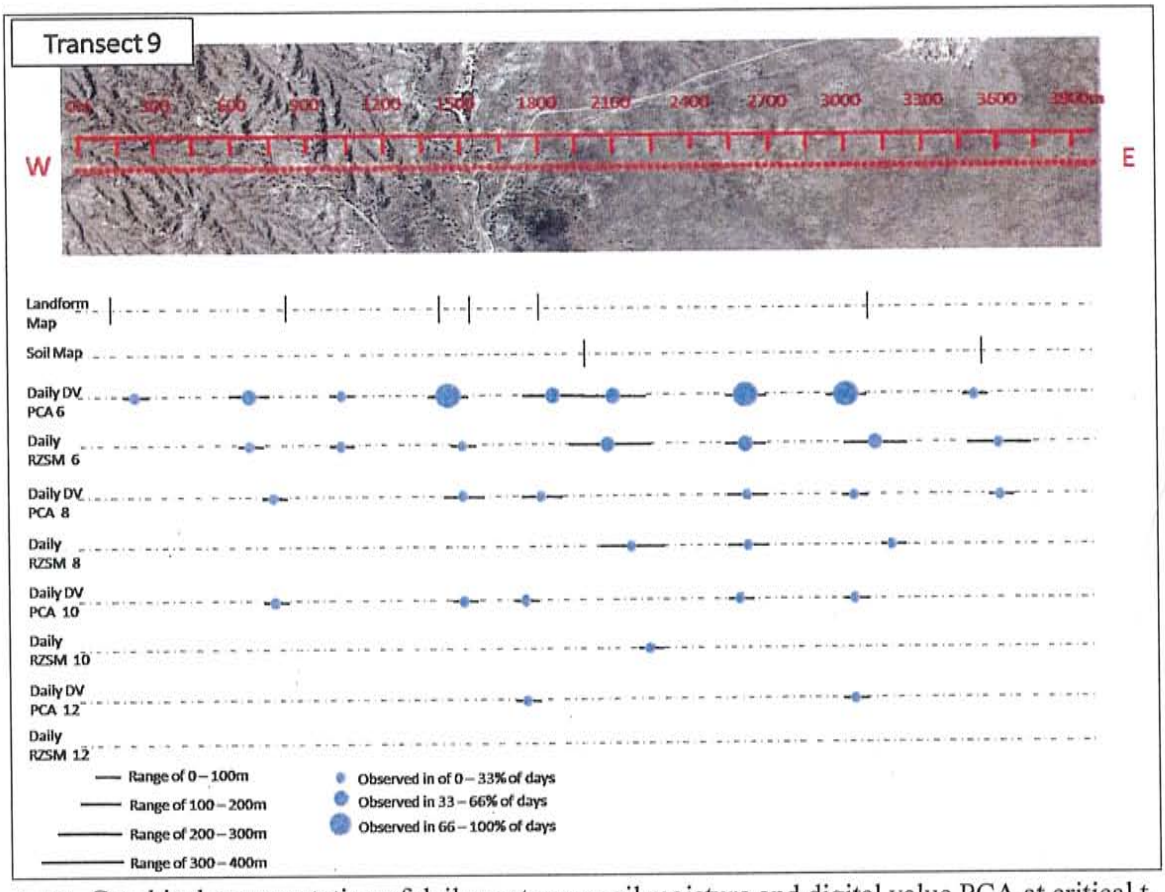

A 28: Graphical representation of daily root zone soil moisture and digital value PCA at critical t-values of 6, 8, 10 and 12 along transect 9 The size of the dot represents the percentage of days the boundary occurs in and the line represents the range over which it occurs.

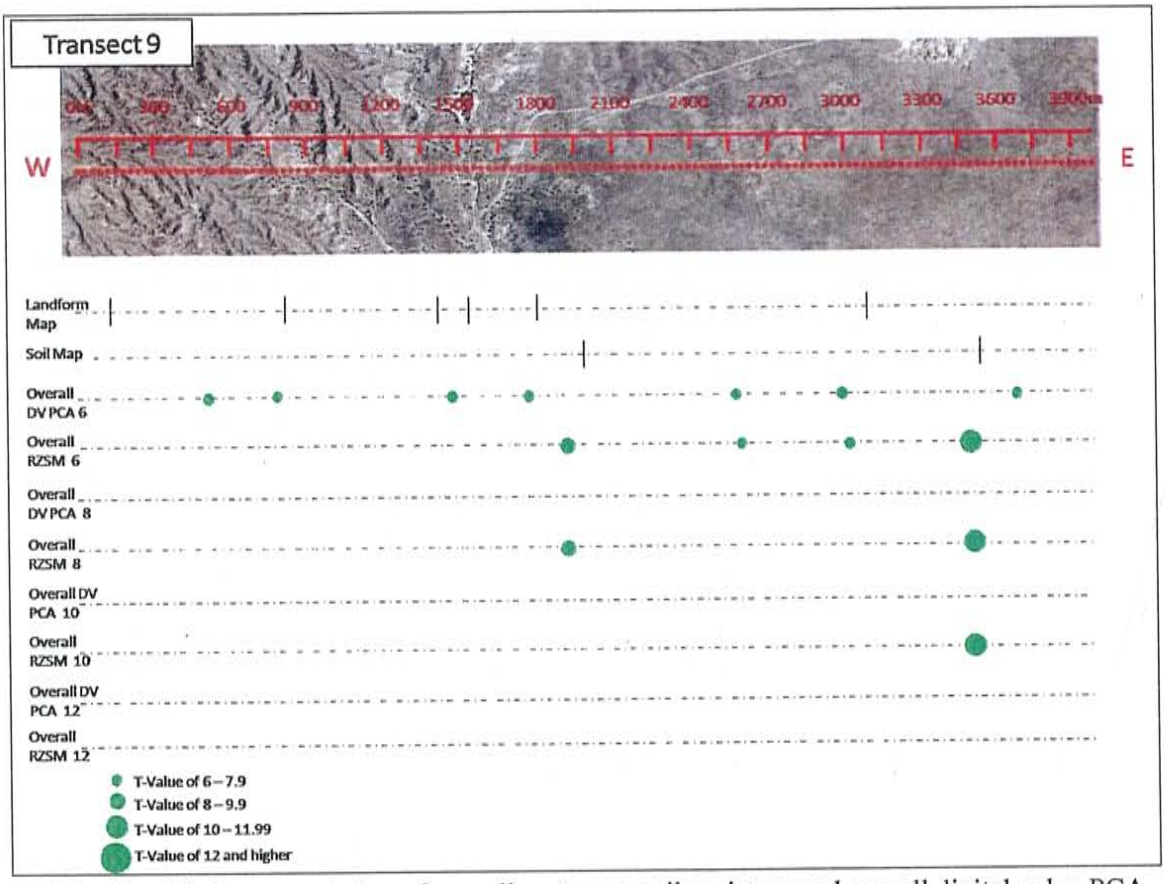

A 29: Graphical representation of overall root zone soil moisture and overall digital value PCA data at critical t-values of 6, 8, 10 and 12 along transect 9. The size of the dot represents the t-value of each boundary

B10

Landform Map / Soil Map	Boundary Location (m)													
	270 270					1830 1830	2160 2160	2400 2400		2700 2730				3660
Daily DV PCA 6	275	650	1075	1400		1750	2200			2725	2850		3250	
percentage of days	60.00	60.00	50.00	60.00		30.00	75.00			65.00	50.00		65.00	
range (m)	180	180	180	300		210	60			120	270		120	
Overall DV PCA 6	270		1080	1410		1830	2130			2730	2970		3300	
T-Value	8.2		7.2	9.3		7.6	7.1			11.8	7.7		9.1	
Daily RZSM 6	300	700	1100	1400	1650	1825	2175	2400	2580	2700		3000	3250	
percentage of days	70.00	80.00	75.00	50.00	60.00	10.00	70.00	30.00	5.00	95.00		25.00	50.00	
range (m)	150	270	240	120	150	30	300	120	0	210		150	210	
Overall RZSM PCA 6	270		1080	1440		1740	2160			2730	2940		3300	
T-Value	6.9		7.6	6.5		6	6.5			8.5	6.7		6.7	
Daily DV PCA 8	250	650	1050	1350			2150			2700	2850	3090	3300	
percentage of days	35.00	40.00	25.00	35.00			10.00			35.00	10.00	5.00	40.00	
range (m)	150	120	120	150			120			30	60	0	30	
Overall DV PCA 8	270			1410						2730			3300	
T-Value	8.2			9.3						11.8			9.1	
Daily RZSM 8	300	650	1100	1400		1750	2250			2700		3000	3350	
percentage of days	45.00	35.00	40.00	30.00		20.00	30.00			45.00		10.00	40.00	
range (m)	120	240	150	120		270	390			270		30	150	
Overall RZSM PCA 8										2730				
T-Value										8.5				
Daily DV PCA 10	250	700	1050	1350			2200			2730			3300	
percentage of days	20.00	15.00	5.00	15.00			10.00			5.00			5.00	
range (m)	30	60	0	150			120			0			0	
Overall DV PCA 10										2730				
T-Value										11.8				
Daily RZSM 10	300	650	1100	1350		1700	2040			2700		3000	3300	
percentage of days	30.00	15.00	15.00	20.00		15.00	5.00			20.00		5.00	25.00	
range (m)	120	180	150	90		270	0			240		0	120	
Overall RZSM PCA 10														
T-Value														
Daily DV PCA 12	270	690					2280							
percentage of days	5.00	5.00					5.00							
range (m)	0	0					0							
Overall DV PCA 12														
T-Value														
Daily RZSM 12	300	650	1100	1400	1560					2700		3000	3300	
percentage of days	25.00	15.00	10.00	15.00	5.00					15.00		5.00	5.00	
range (m)	90	180	90	90	0					150		0	0	
Overall RZSM PCA 12														
T-Value														

A 30: The summary table of transect 10 includes the locations of the soil and landform boundaries along the transect, the locations, percentage of days and range of boundaries detected by the daily digital values, overall digital value PCA, daily root zone soil moisture and overall root zone soil moisture PCA using a critical t-value of 6, 8, 10 and 12

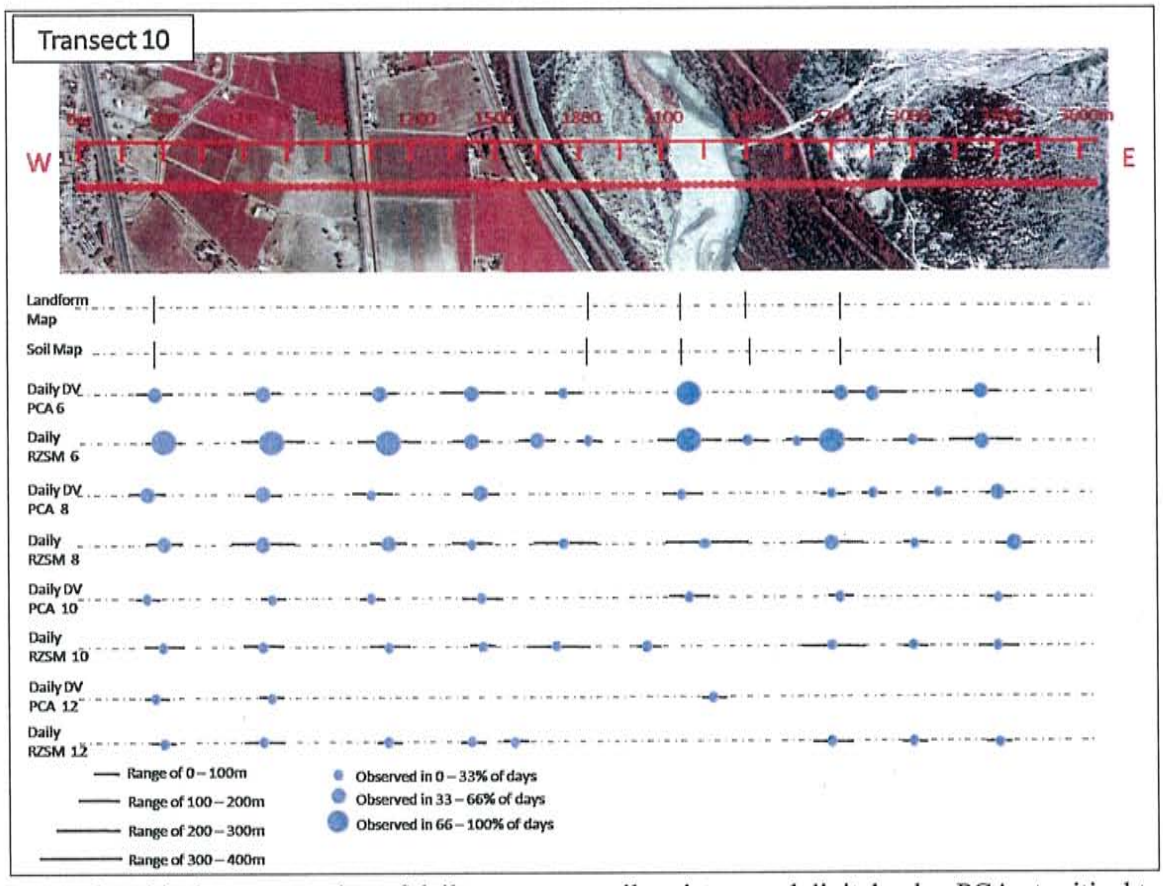

A 31: Graphical representation of daily root zone soil moisture and digital value PCA at critical t-values of 6, 8, 10 and 12 along transect 10 The size of the dot represents the percentage of days the boundary occurs in and the line represents the range over which it occurs.

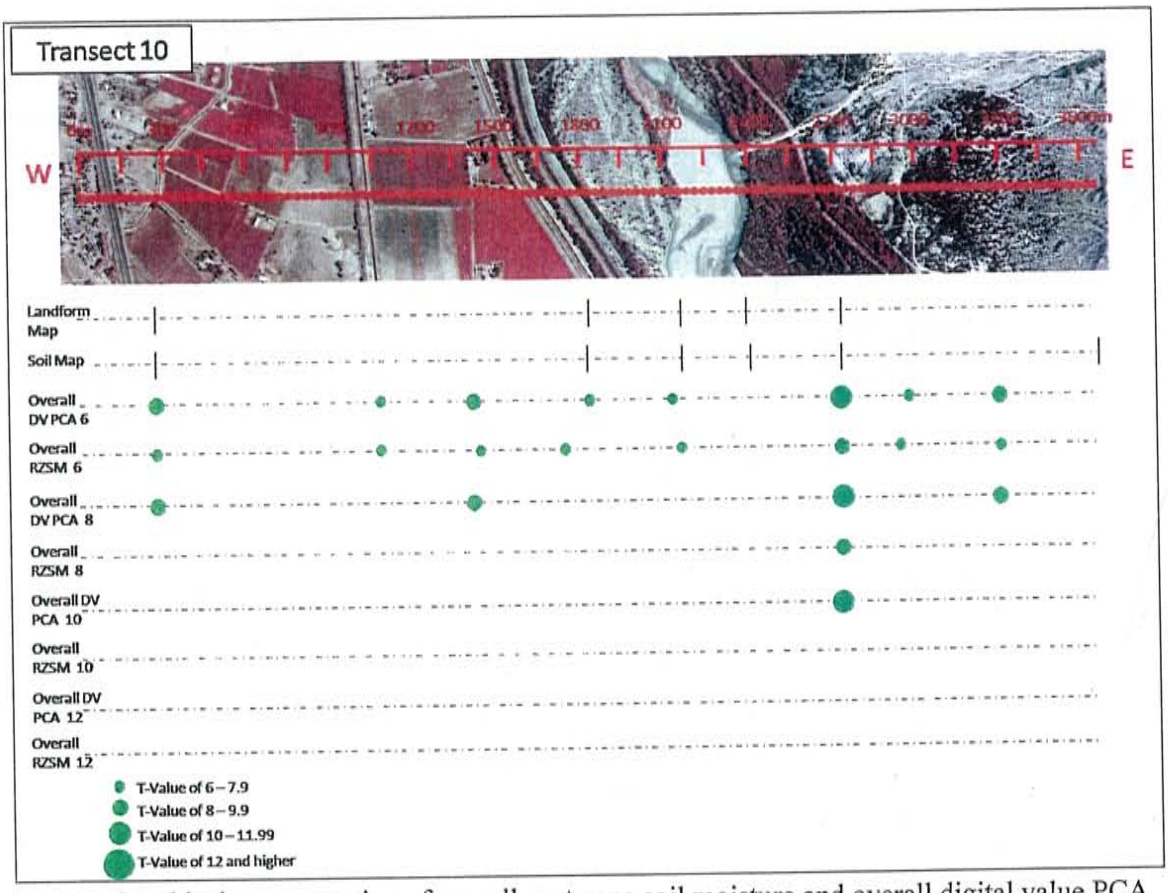

A 32: Graphical representation of overall root zone soil moisture and overall digital value PCA data at critical t-values of 6, 8, 10 and 12 along transect 10. The size of the dot represents the t-value of each boundary

B11

Landform Map Soil Map	Boundary Location (m)										
	300	360	510 510	720 750	900	1050	1140 1200	1245 1245	1440	1515	1590
Daily DV PCA 6 percentage of days range (m)	250 90.00 120		500 60.00 60	625 50.00 150				1300 45.00 60			
Overall DV PCA 6 T-Value	210 9.4		510 9	720 6.6				1260 10.7			
Daily RZSM 6 percentage of days range (m)	200 25.00 60	450 60.00 150		700 50.00 90			1100 25.00 180				
Overall RZSM PCA 6 T-Value	210 8.8	420 8.6		690 8							
Daily DV PCA 8 percentage of days range (m)	200 50.00 90	475 30.00 30						1250 25.00 30			
Overall DV PCA 8 T-Value	210 9.4		510 9					1260 10.7			
Daily RZSM 8 percentage of days range (m)	225 10.00 30	450 20.00 60		725 30.00 60				1290 5.00 0			
Overall RZSM PCA 8 T-Value	210 8.8	420 8.6		690 8							
Daily DV PCA 10 percentage of days range (m)	200 20.00 60		500 10.00 30					1260 5.00 0			
Overall DV PCA 10 T-Value								1260 10.7			
Daily RZSM 10 percentage of days range (m)	240 5.00 0										
Overall RZSM PCA 10 T-Value											
Daily DV PCA 12 percentage of days range (m)											
Overall DV PCA 12 T-Value											
Daily RZSM 12 percentage of days range (m)											
Overall RZSM PCA 12 T-Value											

A 33: The summary table of transect 11 includes the locations of the soil and landform boundaries along the transect, the locations, percentage of days and range of boundaries detected by the daily digital values, overall digital value PCA, daily root zone soil moisture and overall root zone soil moisture PCA using a critical t-value of 6, 8, 10 and 12

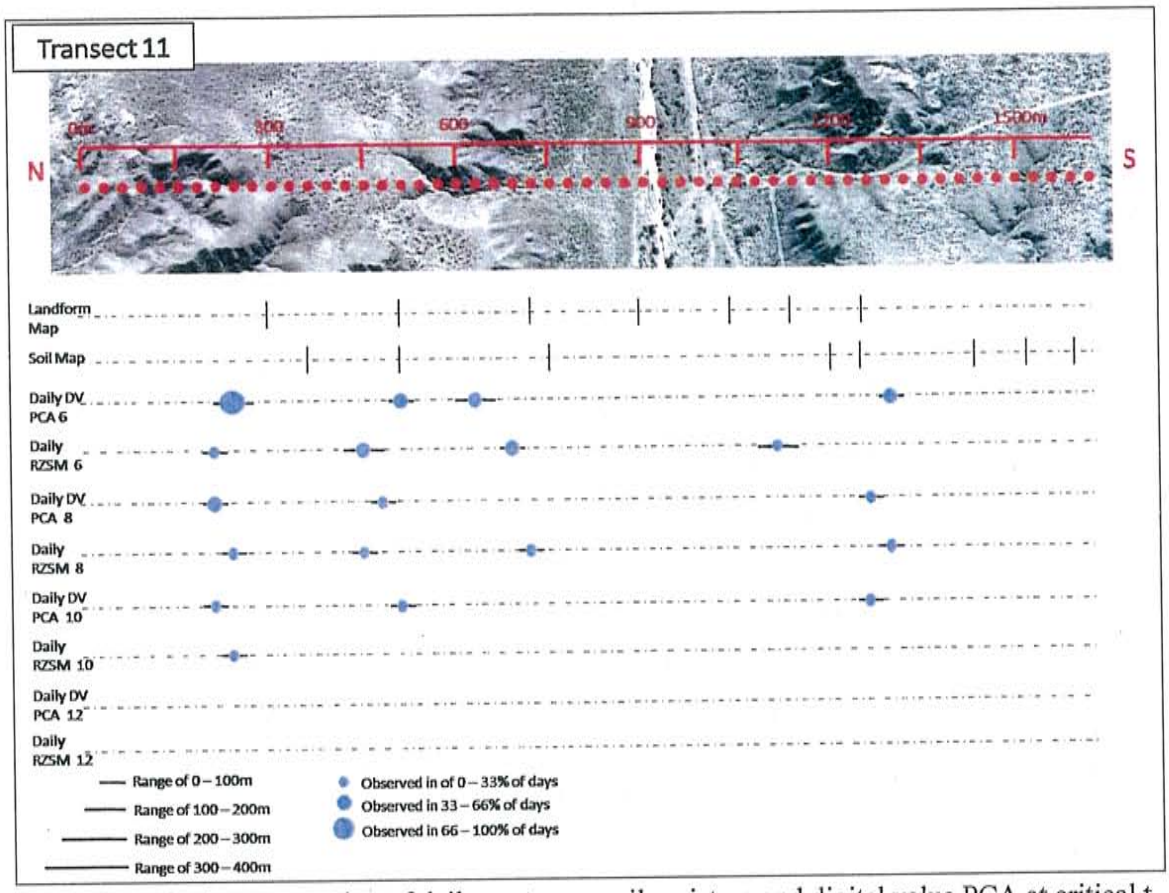

A 34: Graphical representation of daily root zone soil moisture and digital value PCA at critical t-values of 6, 8, 10 and 12 along transect 11 The size of the dot represents the percentage of days the boundary occurs in and the line represents the range over which it occurs.

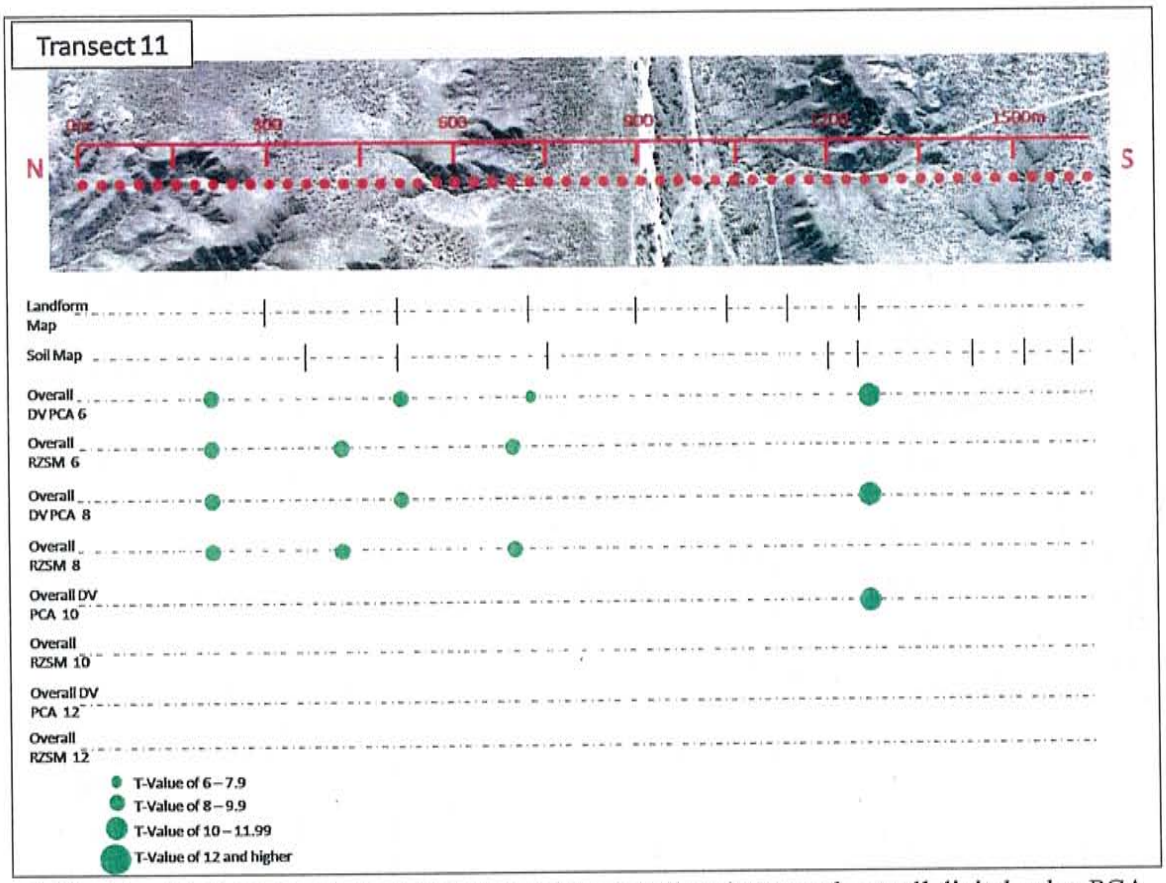

A 35: Graphical representation of overall root zone soil moisture and overall digital value PCA data at critical t-values of 6, 8, 10 and 12 along transect 11. The size of the dot represents the t-value of each boundary

B12

Landform Map Soil Map	Boundary Location (m)								
		390 390	570 570		1050 1080				
Daily DV PCA 6 percentage of days range (m)	200 15.00 60	375 90.00 120			1025 75.00 150	1170 5.00 0	1500 65.00 270		1775 60.00 150
Overall DV PCA 6 T-Value		360 8.5			990 10	1170 6.8	1440 7.5		1800 6.6
Daily RZSM 6 percentage of days range (m)	175 30.00 150	425 70.00 90	550 7.00 30	690 5.00 90	1000 20.00 120		1450 20.00 90	1650 20.00 30	1825 15.00 90
Overall RZSM PCA 6 T-Value	390 6.1							1650 7.6	
Daily DV PCA 8 percentage of days range (m)		350 60.00 120			1000 45.00 90		1500 10.00 150		1800 10.00 0
Overall DV PCA 8 T-Value		360 8.5			990 10				
Daily RZSM 8 percentage of days range (m)	270 5.00 0	400 30.00 90		690 5.00 0	960 5.00 0		1500 10.00 0		1825 10.00 90
Overall RZSM PCA 8 T-Value									
Daily DV PCA 10 percentage of days range (m)		350 25.00 30			1000 20.00 90				
Overall DV PCA 10 T-Value					990 10				
Daily RZSM 10 percentage of days range (m)		400 10.00 30					1500 5.00 0		1800 10.00 90
Overall RZSM PCA 10 T-Value									
Daily DV PCA 12 percentage of days range (m)		380 10.00 30			1020 5.00 0				
Overall DV PCA 12 T-Value									
Daily RZSM 12 percentage of days range (m)		400 10.00 30							1860 5.00 0
Overall RZSM PCA 12 T-Value									

A 36: The summary table of transect 12 includes the locations of the soil and landform boundaries along the transect, the locations, percentage of days and range of boundaries detected by the daily digital values, overall digital value PCA, daily root zone soil moisture and overall root zone soil moisture PCA using a critical t-value of 6, 8, 10 and 12

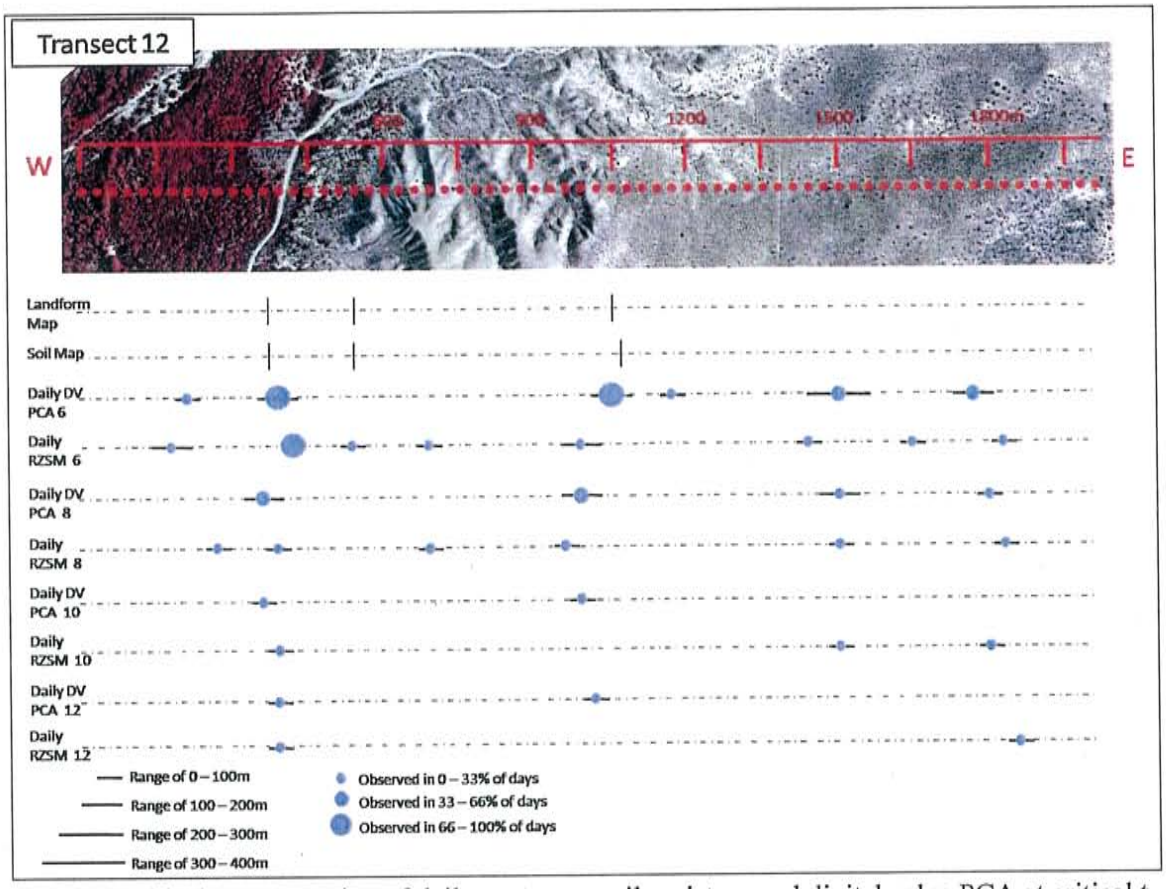

A 37: Graphical representation of daily root zone soil moisture and digital value PCA at critical t-values of 6, 8, 10 and 12 along transect 12 The size of the dot represents the percentage of days the boundary occurs in and the line represents the range over which it occurs.

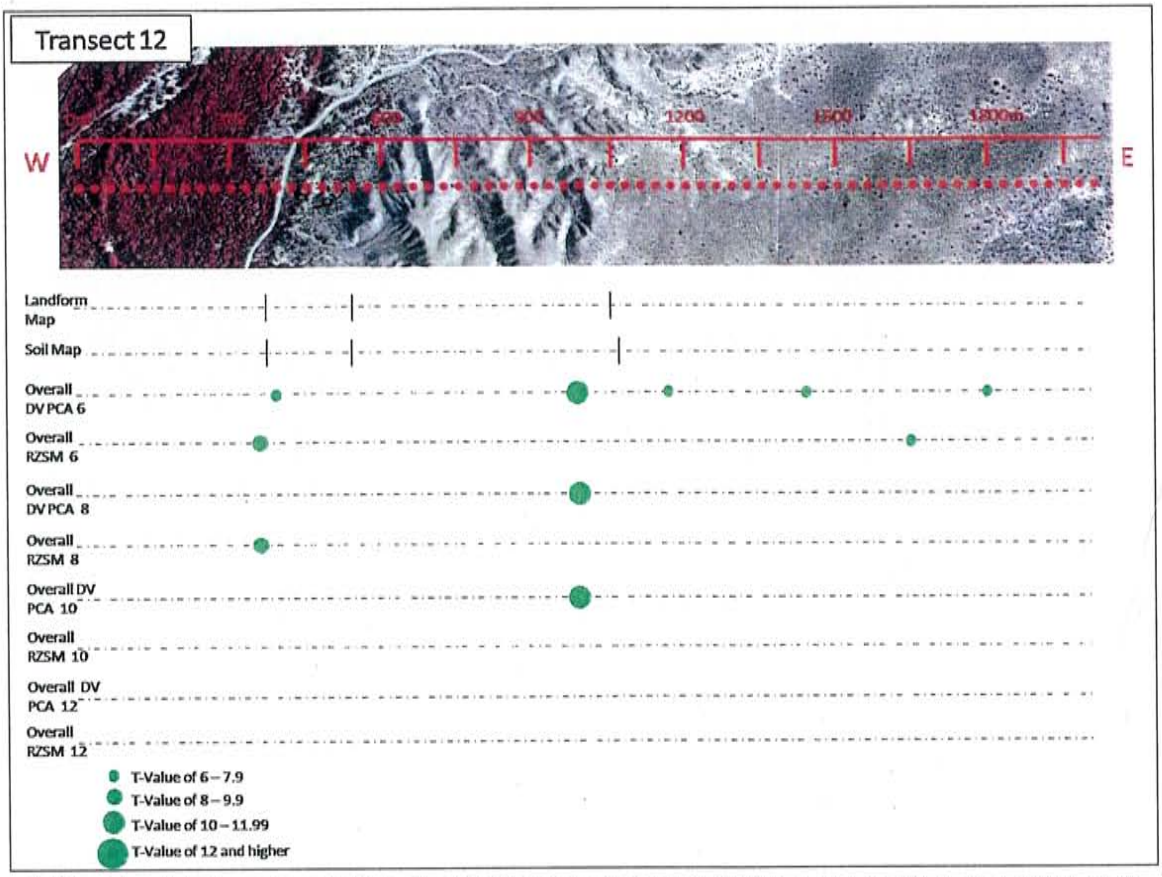

A 38: Graphical representation of overall root zone soil moisture and overall digital value PCA data at critical t-values of 6, 8, 10 and 12 along transect 12. The size of the dot represents the t-value of each boundary

B14

Landform Map / Soil Map	Boundary Location (m)														
	450		1050 / 1050	1310	1590				2730 / 2730	3030 / 3030	3240 / 3240		3630 / 3630	4110 / 4230	4530
Daily DV PCA 6		850				1800	2200	2350			3100		3600		
percentage of days		55.00				70.00	40.00	25.00			55.00		95.00		
range (m)		660				480	240	60			570		510		
Overall DV PCA 6		840			1590		2190	2340			3120		3600		
T-Value		6.7			9		7.8	9.1			8.1		6.4		
Daily RZSM 6		900			1600	1850	2150	2350	2750		3200		3600	4000	
percentage of days		45.00			85.00	65.00	40.00	35.00	65.00		65.00		95.00	30.00	
range (m)		360			300	180	120	150	150		330		300	570	
Overall RZSM PCA 6		960			1560	1860	2190	2340	2700		3120		3600	3990	
T-Value		6.6			9.2	8.4	6.9	18.6	9.5		7		7.1	7.3	
Daily DV PCA 8		850			1600	1975		2300	2700		3150		3660		
percentage of days		25.00			15.00	15.00		30.00	5.00		15.00		5.00		
range (m)		240			60	120		210	0		210		0		
Overall DV PCA 8					1590			2340			3120				
T-Value					9			9			8				
Daily RZSM 8		1000			1525	1900	2200	2350	2700		3150		3600	4150	
percentage of days		15.00			55.00	20.00	15.00	15.00	45.00		30.00		65.00	15.00	
range (m)		120			120	60	30	60	90		330		360	480	
Overall RZSM PCA 8					1560			2340	2700						
T-Value					9.2			18.6	9.5						
Daily DV PCA 10		875			1600			2300			3120				
percentage of days		10.00			10.00			25.00			5.00				
range (m)		30			60			360			0				
Overall DV PCA 10															
T-Value															
Daily RZSM 10		960			1550	1800	2200	2400	2750			3300	3600		
percentage of days		5.00			35.00	10.00	15.00	10.00	30.00			20.00	30.00		
range (m)		0			60	0	30	60	90			240	240		
Overall RZSM PCA 10								2340							
T-Value								18.6							
Daily DV PCA 12					1530	1980		2340							
percentage of days					5.00	5.00		5.00							
range (m)					0	0		0							
Overall DV PCA 12															
T-Value															
Daily RZSM 12					1550		2200	2340	2750			3300	3650		
percentage of days					10.00		10.00	5.00	10.00			15.00	25.00		
range (m)					30		30	0	30			240	180		
Overall RZSM PCA 12								2340							
T-Value								18.6							

A 39: The summary table of transect 14 includes that locations of the soil and landform boundaries along the transect, the locations, percentage of days and range of boundaries detected by the daily digital values, overall digital value PCA, daily root zone soil moisture and overall root zone soil moisture PCA using a critical t-value of 6, 8, 10 and 12

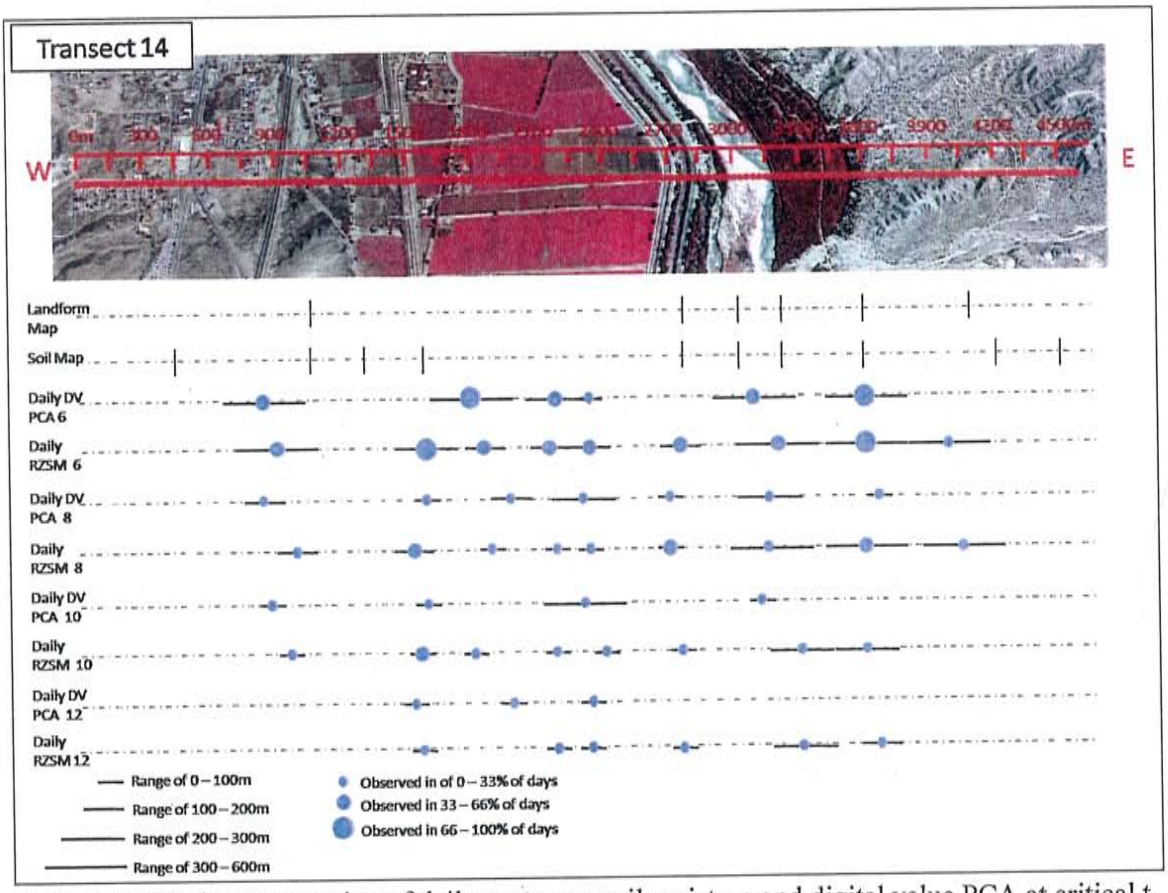

A 40: Graphical representation of daily root zone soil moisture and digital value PCA at critical t-values of 6, 8, 10 and 12 along transect 14 The size of the dot represents the percentage of days the boundary occurs in and the line represents the range over which it occurs.

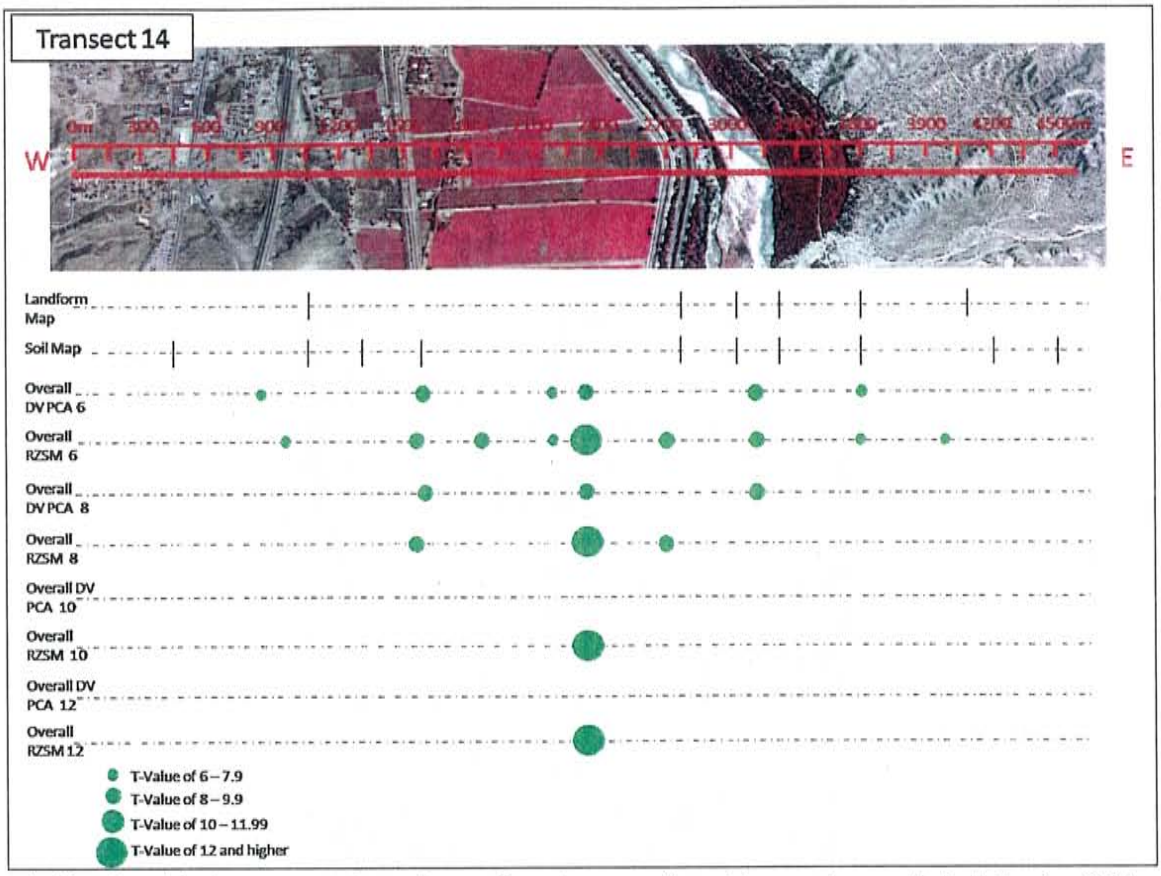

A 41: Graphical representation of overall root zone soil moisture and overall digital value PCA data at critical t-values of 6, 8, 10 and 12 along transect 14. The size of the dot represents the t-value of each boundary

APPENDIX B: GEOREFERENCING

B 1: Five locations identified to determine georeferencing error

B 2: First georeferencing location at the Socorro airport

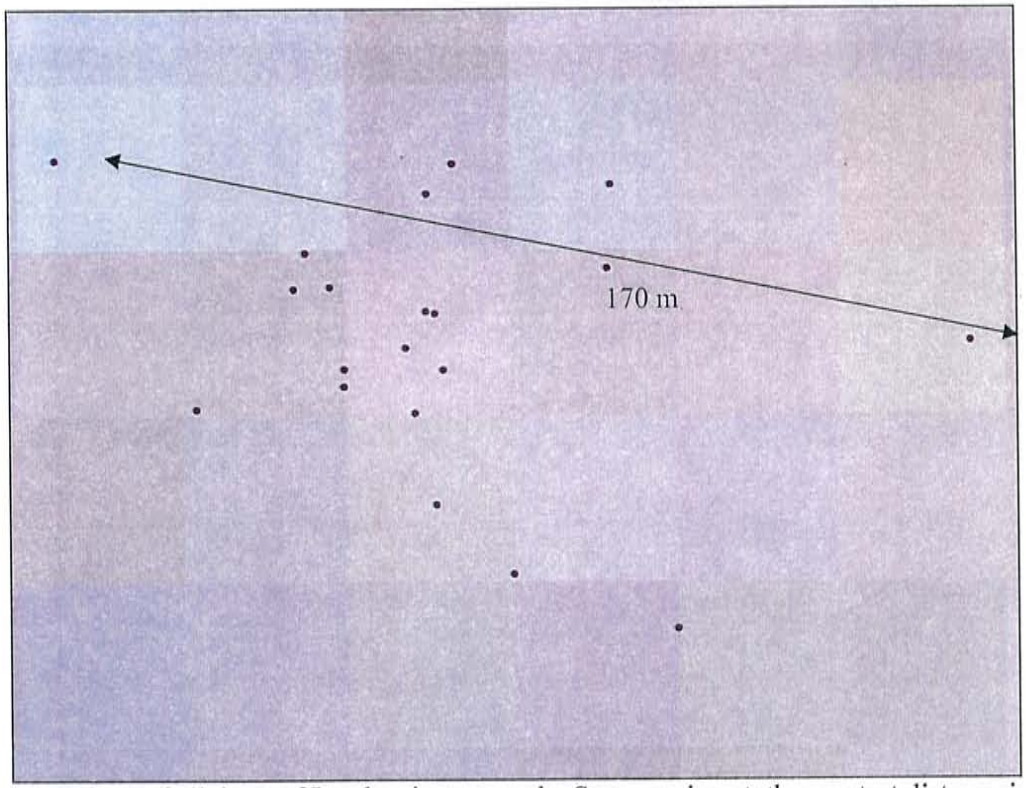

B 3: Locations of all dates of Landsat images at the Socorro airport, the greatest distance is 170 m

B 4: Second georeferencing location at the drain north of Socorro

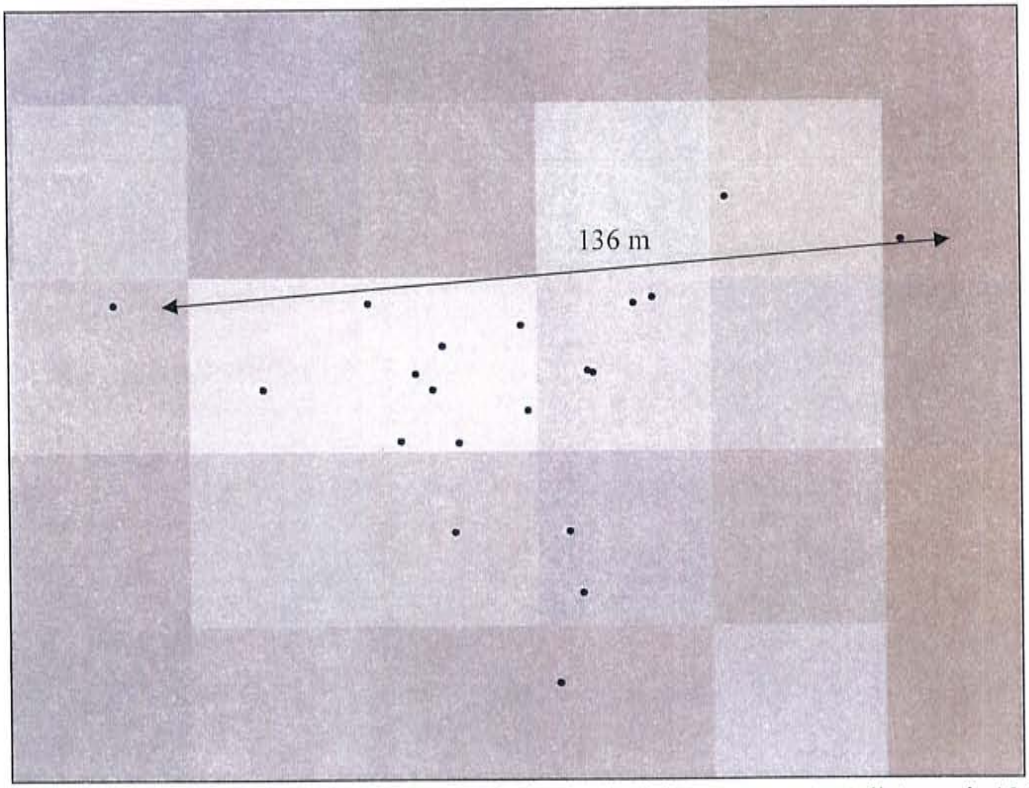

B 5: Locations of all dates of images at the drain north of Socorro, greatest distance is 136 m

B 6: Third georeferencing location at the Bernardo exit on I-25

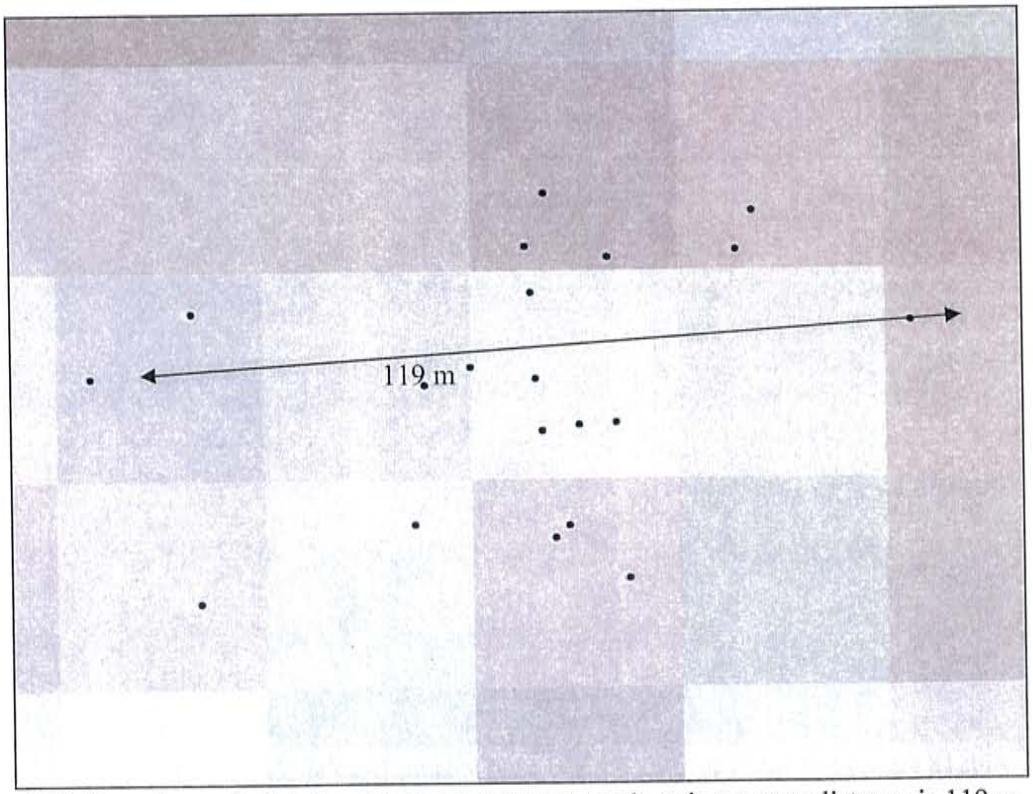

B 7: Locations of all dates of images at the Bernardo exit, greatest distance is 119 m

B 8: Third georeferencing location near Black Butte in the Sevilleta NWR

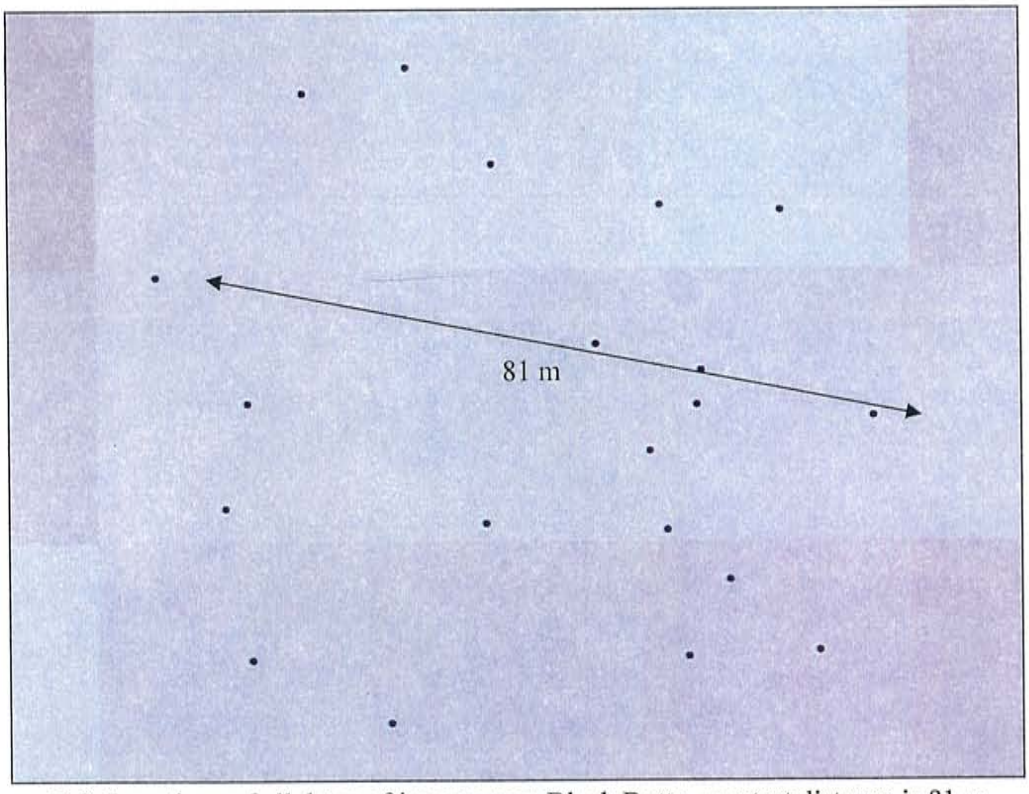

B 9: Locations of all dates of images near Black Butte, greatest distance is 81 m

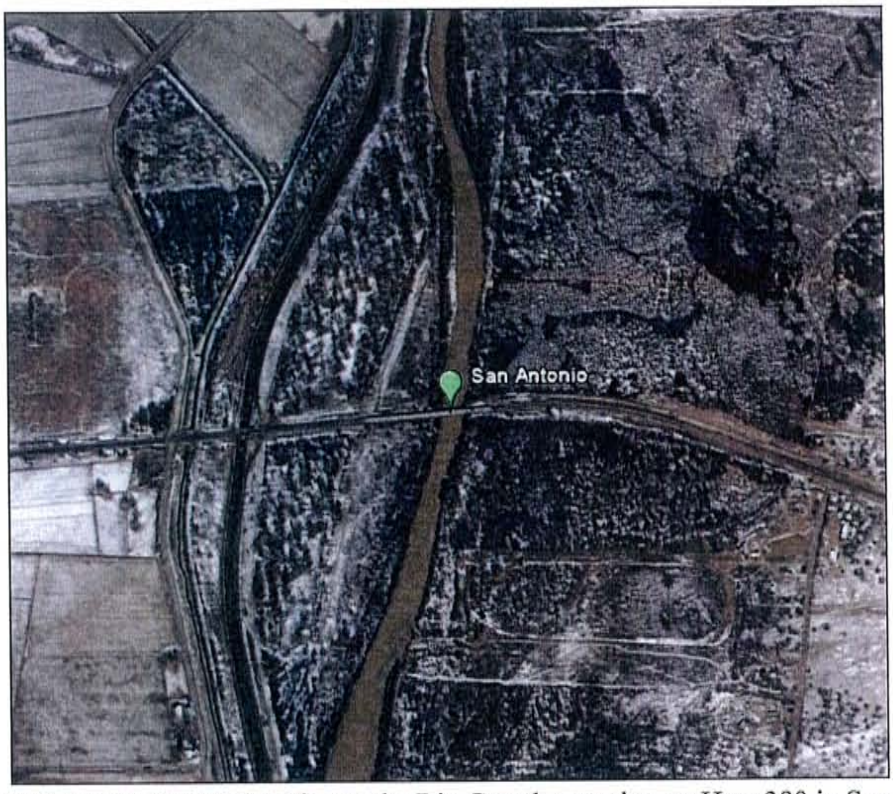

B 10: Third georeferencing location at the Rio Grande crossing on Hwy 380 in San Antonio

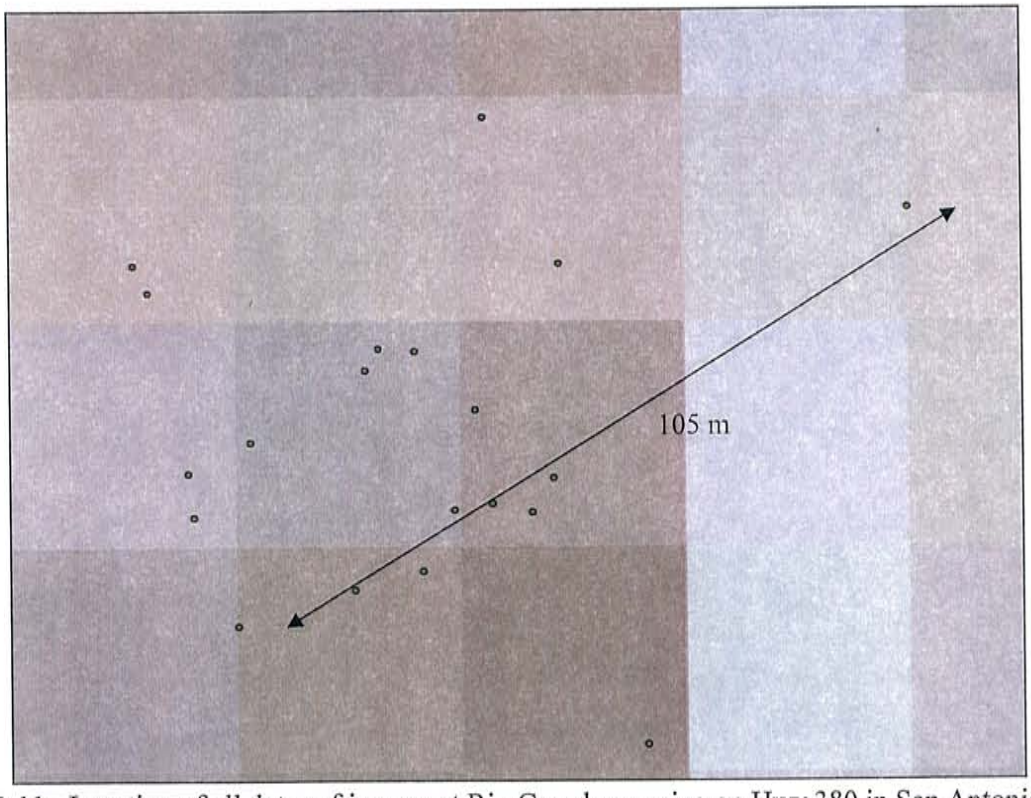

B 11: Location of all dates of images at Rio Grande crossing on Hwy 380 in San Antonio, greatest distance is 105